AN ABSTRACT OF THE DISSERTATION OF

Nitzan Soffer for the degree of Doctor of Philosophy in Microbiology presented on November, 27, 2013.

Title: What is Killing the Corals? Viral and Bacterial Interrogations Using Metagenomics and Microscopy

Abstract approved:

_____

Rebecca L. Vega Thurber

Corals have multiple roles in maintaining ocean health and are some of the world's most diverse ecosystems. The coral animal is host to a multitude of taxa, including symbiotic dinoflagellate algae, fungi, bacteria, protists, and viruses. Environmental stressors and disease agents can perturb the delicate balance of the coral host and its microbiota, which can lead to disease. This ultimately results in reduced fitness and/or mortality. There are over 30 described coral disease signs, but with a few exceptions, little is known about their potential etiological agents. Without knowledge on the causes of these diseases, little can be done to mitigate future outbreaks. Chapter 1 of this dissertation provides examples for studying novel diseases in difficult to study organisms with the use of metagenomic tools. Armed with these metagenomic tools and electron microscopy, this dissertation aimed to determine potential pathogens in two coral diseases, White Plague disease (WP), and Growth Anomalies (GAs). First, I set to determine whether viruses may be involved in WP disease from a 2010 outbreak in the US Virgin Islands (USVI). In chapter 2, I

compared viromes from 21 *Montastraea annularis* samples (7= Diseased, 7= Diseased=Bleached, 5= Bleached, 2= Healthy) and surrounding seawater (n=2). After comparing the viromes, I found that small circular REP- encoding eukaryotic ssDNA viruses (SCSDv) similar to circo and nano viruses were associated with WP diseased tissue, and thus potential pathogens. Electron microscopy confirmed the presence of viral particles, and absence of bacterial infection in WP diseased tissue. Even though it was likely that viruses are involved with WP it was still important to understand the changes in bacterial community and the roles of bacteriophages during WP coral infection to characterize opportunistic microbes. These questions were addressed in Chapter 3 where I described the bacterial communities and bacteriophage consortia associated with the USVI corals. I also constructed phage-bacteria networks to understand which phages may interact with bacteria of interest (those shown to be differentially abundant in *Montastraea annularis* of different health states). I determined that there was a range of interaction specificity across the different phages and bacteria. Chapter 4 aimed to elucidate a potential pathogen responsible for Growth Anomalies, a chronic disease resulting in skeletal deformities, loss of symbiotic algae and reduction of fitness in Hawaiin *Porites lobata*. By comparing microbial and viral metagenomes across health states I was able to determine any changes in composition from healthy and diseased corals. Overall, microbial communities and viral consortia did not vary across health states. The hypothesized *Porites spp*. symbiont *Oceanspirillales* was dominant in all libraries. However, relative abundances of taxa in the orders *Vibrionales* and *Verrucomicrobiales* were elevated in diseased compared to healthy corals and healthy appearing tissue of GA

infected corals. In addition, bacterial functional pathways remained stable across

health states, while signatures of virulence factors were elevated in diseased viromes

from healthy. Lastly, chapter 5 summarized overall trends of microbes and viruses

determined through the studies. In addition, suggestions for future studies were

outlined. Overall, this dissertation revealed a potential viral pathogenic group for

white plague disease, explored how phages can influence bacterial opportunists in

corals of different health states, and determined bacterial orders and virulence factors

that are associated with Growth Anomalies. This dissertation includes the first study

to find an association between a viral group and coral disease. In addition, this

dissertation contains the first (to date) phage-bacterial inferred network constructed

from paired phage-bacteria metagenomes.

What is Killing the Corals? Viral and Bacterial Interrogations Using Metagenomics
and Microscopy

by
Nitzan Soffer

A DISSERTATION

submitted to

Oregon State University

in partial fulfillment of
the requirements for the
degree of

Doctor of Philosophy

Presented November 27, 2013
Commencement June 2014

Doctor of Philosophy dissertation of Nitzan Soffer presented on November, 27, 2013

APPROVED:

_____

Major Professor, representing Microbiology

_____

Chair of the Department of Microbiology

_____

Dean of the Graduate School

I understand that my dissertation will become part of the permanent collection of
Oregon State University libraries. My signature below authorizes release of my
dissertation to any reader upon request.

_____

Nitzan Soffer, Author

ACKNOWLEDGEMENTS

To those who helped me on my PhD journey, I acknowledge thee from now till eternity. This poem may be cheesy, but this is the product of being busy

First and foremost, my advisor, Dr. Vega Thurber, who gave me a chance for a degree do over.

Herpes, we both love, but not on our faces or other places,

Only in corals they belong, where we can study them all day long!

Becky taught me how to write, even though it's something that gave me a massive fright

She taught me metagenomics and a bevy of lab techniques, giving me her time during her busy weeks

I am her first, and will always be, so in a way it's special to me

Because of her I am getting this PhD, thanks for investing in me

So to Becky, thanks for the tough love, now I am ready to rise above

To the members of my committee, both those who were at FIU and OSU currently

I thank you all for your time and wit, Drs. Jerri Bartholomew, Virginia Weis, Steve Giovannoni, Roger Ely, Giri N. Deron Burkepile, Lauren Richardson, Josh Voss, and well I guess that is it.

Next comes Jerome, and Jesse my postdoc heros, who encouraged me even when I felt like lots of zeros and everyday I wanted to quit, they convinced me to stick with it

Ryan and Rory, the Irish dudes, thanks for humoring me during my grad school moods.

Thanks for Adrienne, Marilyn, and Tyler the friendly scuba divers, making sure I didn't die during my crazy field work at the USVI.

My Hawaii collaborator, Courtney Couch, for my work she did vouch, thanks for the comments on the paper, it went all that much better

NSF we had a good 5 years, you gave me money and squashed my financial fears.

My friends from OSU, Jamie, Aimee, Charlene aka Chinkooki, Lauren, Estefania Gema, Julie, Justin, Prabhat, Zach, Carole, Michelle, Meagan, Lauren, and Amy I honestly don't know what I would do without you!

Especially Lmar, you saved my life my first week here, you will always be to my heart near

Also, the Trashy Nashys, you guys are awesome, I hope you let the group blossom.

To the 5th floor people, you adopted me as your own, cause of you I never felt alone

And of course my friends from Florida, Zack, Cindy, Robin, Xaymara, Maria, Kristen, and Laura, even though far away, you are important to me in every way.

To the support from Microbio, Sally, Mary, and Bonnie, Theo, Cindy, Linda and Tasha, you were all lots of help, I'd give you 5 stars if you were on Yelp.

To my friends from back in the day, here is what I want to say: Tina, Misung, Fran, Bethany, Vinny, Alex, Shirley, Natty and Reichan, I am glad we still talk, and always will, you're definitely worth the phone bill!

To Rachel and Oded, thanks for the encouragement you said

Of course to my family, especially my mother, I could not ask for any other. She is the best mom one can find, and would do anything to help me out of a bind.

To my brother, thanks for the cheese, you helped me when I say please

To my grandparents, cousins, uncles and aunts, I can't wait to see you soon, and enjoy some crembos with you in the afternoon

Anyways, I'm running out of time to make things rhyme, but I just wanted to say, you are all important to me in some way, and even those I didn't name, you were important just the same.

CONTRIBUTIONS OF AUTHORS

Chapter 2: Marilyn Brandt provided expertise in identifying diseased white plague corals, was involved in field work, coral collections, and manuscript editing. Adrienne Correa and Tyler Smith provided field support and manuscript editing. Rebecca Vega Thurber was the PI on the grant supporting this research, and helped with manuscript editing and guidance on analysis.

Chapter 3. Jesse Zaneveld helped construct the network, manuscript editing and guidance using QIIME. Rebecca Vega Thurber was the PI on the grant supporting this research, and helped with manuscript editing and guidance on analysis.

Chapter 4. Courtney Couch collected and processed samples, aided with statistical analysis methods, edited manuscript and provided expertise on GA ecology. Jesse Zaneveld provided QIIME and PICRUSt guidance and manuscript editing. Drew Harvell was a PI on one of the grants supporting this research. Rebecca Vega Thurber was the PI on the grant supporting this research, and helped with manuscript editing and guidance on analysis.

TABLE OF CONTENTS

LIST OF FIGURES

LIST OF FIGURES (Continued)

LIST OF TABLES

1 Introduction

1.1 Challenges in emerging disease discovery

The numbers of emerging novel diseases have been increasing in both human and non-human populations the last few decades (Harvell et al., 1999, Ward and Lafferty 2004; Burge et al., 2013; Chiu, 2013). For example, two new coronaviruses causing acute respiratory distress in humans have appeared the last few years; Severe Acute Respiratory Syndrome (SARS) and Middle East Respiratory Syndrome (MERS-CoV)(Rota et al., 2003; Bermingham et al., 2012). Climate change, anthropogenic inputs and increased human populations are associated with emergence of diseases (Harvell et al., 1999; Daszak et al., 2000; Johnson et al., 2010). Marine organisms have also been facing an onslaught of new diseases/conditions; coral reefs alone include over 30 described diseases (Sutherland et al., 2004; Ward and Lafferty 2004; Sokolow, 2009; Bourne et al., 2009; Rosenberg and Kushmaro, 2011), and new ones are being discovered to date, such as "multifocal lesion event" which is characterized by patches of bleached tissue (Paramasivam et al., 2013). The alarming spike in detection of novel diseases showcases the need to identify and characterize disease agents with no *a priori* knowledge.

Traditionally, fulfillment of Koch's postulates was necessary to establish the etiological agent of a disease. Koch's postulates require that before a disease agent is considered a cause, the following criteria be met:
 1. A microorganism must be found in all diseased, but not in any healthy organisms;
 2. This microorganism must be isolated from the diseased organism and cultured;

3. The cultured microorganism should be able to cause the disease in healthy organisms; and

4. The microorganism should then be re-isolated from those diseased organisms.

There are cases where a pathogen has been shown to cause disease, but Koch's postulates have not been fulfilled. For example, the pathogen that causes leprosy, *Mycobacterium leprae,* could never be cultured (Monot et al., 2005). Some diseases are caused by more than one microorganism and most microbes that have been characterized from the environment could not be cultured in laboratory conditions (Rappe and Giovanoni, 2003; Angly et al. 2006). Thus Koch's postulates are not always a feasible approach for determining the causative agent of disease.

Despite these challenges, new pathogens can be discovered and characterized with modern techniques. Metagenomics, the direct analysis of genes and/or genomes from the environment (Handelsman et al., 1998), is one way to circumvent the issue of culturing, isolating and avoiding reinfections of healthy individuals. Metagenomics can be either shotgun or amplicon based. Shotgun metagenomics is the sequencing of all genes/genomes directly from the environment, without targeting any specific genes/markers. Amplicon based metagenomics is sequencing targeted genes/markers (such as 16S rDNA) directly from the environment. Since there is no universal genetic marker (such as ribosomal RNA) for viruses, shotgun metagenomics has opened the door for efficient discovery of novel viruses (Rohwer and Edwards, 2002; Mokili et al., 2012; Chiu, 2013; Belak et al., 2013). Given that a majority of new diseases are caused by viruses (Woolhouse and Gaunt, 2007, Radford et al., 2012), shotgun metagenomic tools have been very important in

disease etiological studies since many pathogens of emerging diseases have little homology to known pathogens making detection with standard tests such as PCR inadequate (Chiu, 2013).

The original metagenomic study used cloning and sanger sequencing to produce libraries (Handelsman et al., 1998), but the advancement of next generation sequencing (NGS) platforms, which are continually improving, has increased the output of sequencing by reducing costs and labor intensity. Some current technologies include 454 pyrosequcing , Illumina Miseq/Hiseq and Ion Torrent. A majority of metagenomic studies to determine disease agents have used either the 454 or Illumina platform (reviewed in Mokili et al., 2012; Chiu et al., 201; Belak et al., 2013). The general pipeline of shotgun metagenomics includes:

 1. Isolating size fraction of interest (optional)

 2. DNA/RNA extraction,

 3. Amplification (optional)

4. Sequencing, typically using next generation technologies,

5. Assembly (this step is commonly skipped in 454 produced viral libraries)

6. Annotations (e.g. tBLASTx to database)

7. Bioinformatic analysis/comparisons of metagenomes.

Each of these steps must usually be optimized for the environment, host, microbe (bacterial, viral), and hypothesis tested.

1.2 Is there a bias towards Multiple Displacement Amplification (MDA) bias?

One issue prevalent in metagenomic studies is obtaining enough DNA/RNA from samples. Viruses have small genomes and host, bacterial or other genetic material may overwhelm any resulting metagenome. One way to circumvent this issue is amplification of DNA. Amplification of DNA from known samples can be achieved with the Polymerase Chain Reaction (PCR) using primers specified for genes/sequences of interest. When exploring environmental samples where no specific sequences are known, these methods are impractical.

A few methods exist for overcoming specified amplification such as Linker Amplified Shotgun Library (LASL) and Multiple Displacement Amplification (MDA) (Breitbart et al., 2002; Dean et al., 2001). All amplification processes come with a suite of biases, however MDA, which is one of the most permissive tools has received a majority of the criticism. MDA works with random hexamer primers and the phi-29 DNA polymerase which uses a rolling circle amplification method (Dean et al., 2001). Some criticisms of this technique include bias towards ssDNA sequence amplification, skewing metagenomes to overestimate ssDNA genomes, and stochastic amplification (Kim, et al. 2008; Abulencia et al., 2006; Yilmaz et al., 2010; Kim and Bae, 2011). After using this technique for two viral metagenomic studies and reviewing literature based on this technique, it appears that criticism of MDA amplification biases are ironically biased themselves.

The literature on MDA conflicts about whether the nature of the bias is stochastic or linear. Yilmaz et al., (2010) show that there is excellent technical replication (~98% similarity) among samples processed with the same MDA amplification technique,

demonstrating lack of stochastic bias. Yet, differences do occur in operational taxonomic units (OTU) composition between unamplified and amplified metagenomes, ultimately confirming that MDA does bias a sample, but that this bias is reproducible. Therefore, although there might be slight skewdness, MDA amplification is a reliable technique for comparing metagenomes if samples are treated consistently. In Abulencia et al., (2006), which claims that MDA has stochastic biases, authors compared different communities after applying MDA to varying quantities of starting DNA and did not include technical replicates. Therefore, one cannot determine if the differences in metagenomes were a result of samples being diluted or if this was the result of a stochastic bias (unlikely given Yilmaz et al., 2010).

Lastly, the two papers that demonstrated higher abundance of ssDNA viruses in MDA amplified libraries were either artificially enriched for ssDNA viruses by removing a denaturation step, which increased ssDNA viral similarities from 40-90% (Kim et al., 2008), or MDA amplification was compared to Linker Amplified Shotgun Libraries (LASLs) (Kim and Bae, 2011). However, LASLs should be avoided for anyone interested in all DNA viruses of a virome, because only dsDNA virus similarities would be found. If there is still debate as to whether MDA can be used for quantitative comparisons of dsDNA and ssDNA viromes, one can test this by: creating ssDNA and dsDNA phage consortia in culture (i.e. *Myoviridae, Microviride*), amplify with MDA using known starting ratios and quantities of the viruses, and then comparing multiple technical replicates of MDA amplified viromes with each other. Ultimately metagenomes processed with consistent MDA methods can be used to make quantitative comparisons.

The following sections highlight some examples of metagenomic studies from clinical diagnoses, discovery of disease agents in non-human diseases, and testing for microbial diseases in coral reefs.

1.3 Clinical diagnosis using metagenomics

The study by Breitbart et al., 2003 on the viral metagenome from human feces propelled the use of metagenomics in a clinical setting. This was the first viral metagenome from a human sample and led to the discovery of 1,200 viral operational taxonomic units (OTU). Since then, hundreds of metagenomic studies involving human gut and diseases have been carried (Pub med search). In addition to describing microbial assemblages, metagenomics is a useful method for discovering and diagnosing new diseases. In 2009, RNA samples from humans that died of an unknown hemorrhagic fever in South Africa, were shotgun pyrosequenced, ascertaining the probable cause of disease within 72 hours. The resulting viromes included a new arenavirus, the first "old world" virus discovered in over 30 years. By comparison, it took almost a month to determine that SARS was caused by a novel coronavirus using microscopy and degenerate PCR reactions (Rota et al., 2003; Bermingham et al., 2012). NGS tools are useful for studying hemorrhagic fevers, which usually onset sporadically and have a quick (within a few days) and high mortality rate (up to 100%, Bray et al., 2003). Without the use of non-specific techniques that can be conducted rapidly, such as shotgun sequencing, the etiological agent can disappear in the subject before discovery, slowing down mitigation efforts.

Another hemorrhagic fever detected with NGS was a novel Rhabdovirus

from central Africa. Grard et al. (2012) originally attempted to identify the virus

using a Taqman qPCR assay of all currently known hemorrhagic viruses, but these

methods failed. Consequently, unbiased shotgun 454 pyrosequencing was used to

detect virus sequences approximately 40% similar to Rhadboviridae. Although this

study was based on 1 blood sample, they were able to find this virus at >1 million

copies/mL, and found no other candidate pathogen viruses. Additionally, the nurse

attending to this patient carried this virus, although at a 1000-fold lower titer and

asymptomatically. Thus, it was concluded that this novel Rhabdovirus was the cause

of this hemorrhagic fever. These case studies demonstrate the potential, and need for

unbiased sequencing methods for detecting emerging diseases in humans.

1.4 Metagenomic discoveries in non-human animals

Domesticated and wild organisms that are difficult to sample and/or protected

and therefore cannot be sampled, make typical clinical diagnostics such as those

used in human medicine impractical. In addition, in some cases where techniques

such as PCR or culturing are already developed, these techniques can still fail to

provide a clear diagnosis if there is enough genomic divergence. Metagenomic

analyses provide an alternative that circumvents these issues, and potential disease

agents from sea lions to mink have been discovered (Blomström et al., 2010; Ng et

al., 2009). For example, in the study by Ng et al. (2009) the cause of mortality in sea

lions which were living in an aquarium facility was determined using viral

metagenomics when chemical toxicity assays, culturing of bacteria/fungi, and

histopathology all failed to explain the deaths. With shotgun sequencing and

BLAST searches, researchers found that 10% of the viromes were similar to anneloviruses. Using a PCR specific for this novel annelovirus, they were able to confirm the presence of this virus in all 3 dead, but no healthy sea lions from the facility. A survey wild sea lions for the annelovirus determined that 11% of wild sea lions were asymptomatic carriers of the virus. Researchers concluded that the annelovirus may lead to secondary opportunist pathogens leading to mortality, or that the disease was not progressed enough in the wild sea lions to cause mortality. In the event of another sea lion mortality event, this annelovirus can now be quickly tested for because of metagenomics.

Back on land, mink in Denmark were suffering from "shaking mink syndrome," and intense efforts to determine the etiological agent were carried out unsuccessfully. Known bacteria and viruses were not determined to be the cause. However, the viral metagenomic study by Blomström et al., 2010 determined a strong association of a novel astrovirus and shaking mink syndrome. This study compared the viral metagenomes of 3 experimentally infected, 3 naturally infected and 6 healthy minks and found that a novel astrovirus was only found in shaking mink. Given that this virus was absent from any healthy mink, and that transfer of brain material from a diseased mink to a healthy one led to disease onset, it is very likely that this virus is the cause.

1.5 Coral reef metagenomics- wading through the coral-microbiome

The previous examples highlight the use of metagenomics as a method for determining associations of disease and an etiological agent. However, these examples use samples of tissues/serum that are contained within the body of an animal and have

relatively little contact with environmental microbes compared to tissues such as skin or gut. In some biological systems that involve multi-partner symbioses and complicated microbial interactions, metagenomic studies may not provide as straightforward a diagnosis. For example, shallow water reef building corals, scleractinians, contain symbiotic algae within their tissues. In addition, a highly diverse community of bacteria and viruses lives within the tissue and on the mucosal surface layer of the coral (bacteria reviewed in Krediet et al., 2013; viruses in Vega-Thurber and Correa 2011). Corals are also hosts to fungi, endolithic algae, and protists, all potential carriers of their own microbiomes (Knowlton and Rohwer, 2003; Johnston and Rohwer, 2007; Rosenberg et al., 2007)

The role of many members of the coral microbiome are still unknown, although some bacterial types such as those similar to *Photobactrium spp.* (Ritchie , 2006) have been shown to produce antibiotics, while *Vibrio spp*. tend to be pathogenic (Kushmaro et al., 2001; Haim and Rosenberg, 2002; Cervino et al., 2004). Interestingly, *Vibrio spp.* are found in both healthy and diseased corals making determining the causes of coral disease difficult (Chimetto et al., 2008; Krediet et al., 2013). In addition, signs of disease can be more ambiguous in corals than for example a person suffering from hemorrhagic fever. Signs of coral disease are typically described during environmental monitoring and thus rely on macro visual signs such as color (e.g. white, yellow, black), pattern (e.g. band, splotches) and progression speed (e.g. white plague I, II, III).

White plague is a major coral disease focused on in this dissertation, and is characterized by: a white band of necrotic tissue arising from the base of the colony, progressing upwards at a rate of 1-3mm/day (type I), 3mm-2cm/day (type II) or greater

than 2cm per day (type III). Although the first few studies to examine white plague (type II) determined that a bacterial pathogen, *Aurantimonas coralicida* was responsible using Koch's postulates (Richardson et al, 1998; Denner et al, 2003), subsequent experiments and microbial surveys were not able to isolate this bacterial pathogen from corals with signs of white plague (Pantos et al., 2003; Sunagawa et al., 2009; Cardenas et al., 2012; Kellogg et al., 2012; Roder et al., 2013; Garcia et al., 2013; Cook et al., 2013). The most recent study by Cook et al., (2013) concluded that bacteria communities were similar across healthy, diseased and healthy areas from white plague diseased corals.

These unsuccessful attempts to identify a bacterial pathogen have led to three hypotheses about potential disease agents in white plague; 1) white plague is a manifestation of stress (environmental or otherwise) and not caused by any particular pathogen. 2) that multiple/non-specific bacteria are causing this disease and 3) a non-bacterial pathogen may be causing this disease, such as a virus. Since white plague has been shown to progress quickly within a host (0.3 to 2cm per day), resulting in complete tissue mortality, and quickly spreads throughout reefs, it is plausible that it is caused by a virus (Dustan, 1977; Richardson et al, 1998; Richardson et al, 2001; Sokolow et al., 2009).

Another coral disease of unknown cause is Growth Anomalies (GA). These are chronic, slow progressing tissue malformations that continue to survive despite the tissues losing their symbiotic algae (*Symbiodinium*) and exhibiting decreased fitness. A study has shown that GAs are transmissible to healthy corals in aquarium experiments (Kaczmarsky and Richardson, 2007), but the etiological agent has not been determined and the results of this study have been questioned by the community.

This dissertation will explore potential pathogens for WP and GA disease using metagenomics and address the hypotheses that viruses have roles in white plague disease (both eukaryotic and bacteriophages), and that either virus or microbes are involved in GAs.

1.6 Chapter introductions

Chapter 2: This chapter of the dissertation describes the viral metagenome of *Montastraea annularis* corals during a 2010 USVI white plague outbreak and bleaching event. In this combined metagenomic and microscopy investigation, I demonstrate that small circular ssDNA eukaryotic (similar to nanoviruses, circoviruses and satellite DNAs) viruses have the potential to cause white plague. In addition, I confirm previous studies that bleached corals host Nucelocytoplasmic large DNA viruses (such as *Phycodnaviridae*, *Poxviridae* and *Mimiviridae*) while healthy corals are dominated by viruses similar to herpes viruses. This chapter was published in the ISME Journal (doi:10.1038/ismej.2013.137).

Chapter 3: This chapter further explores microbes in white plague diseased corals, but examines the bacterial community from a bacteriophage perspective. This chapter describes the bacterial community of white plague infected, bleached and healthy corals, as well as the bacteriophage communities associated with each bacterial library. A phage-bacteria network was constructed to provide potential mechanisms for bacterial community dynamics, as well as show the potential for phage-bacteria networks in phage-therapy development. This chapter was submitted to Environmental Microbiology.

Chapter 4: This chapter compares viral and bacterial communities of mucus of Growth Anomalies (GA) affected corals from Hawaii to determine whether a microbe has the potential of causing this disease. In addition, functional analysis of the virome and bacterial communities were analyzed. Bacterial community members were mostly similar across health states and transect location, with *Oceanspirillales* being the dominant bacterial order in all libraries. Members in the order *Vibrionales* and *Verrucomicrobiales* were more relativity abundant in GA infected tissue than either healthy appearing tissue from GA corals, or healthy corals. However, these were at low abundances. Viral consortia were highly variable within and among health states. Lastly, virulence genes were found significantly more abundant in diseased (GA) than healthy corals from the viral metagenomes, and no differences were found in the bacterial community functional pathways. This chapter will be submitted PLoS One.

POTENTIAL ROLE OF VIRUSES IN WHITE PLAGUE CORAL DISEASE

Nitzan Soffer, Marilyn E. Brandt, Adrienne M.S. Correa, Tyler B. Smith,

and Rebecca Vega Thurber

CHAPTER 2: POTENTIAL ROLE OF VIRUSES IN WHITE PLAGUE CORAL DISEASE

2.1 Abstract

White plague-like diseases of tropical corals are implicated in reef decline worldwide, although their etiological cause is generally unknown. Studies thus far have focused on bacterial or eukaryotic pathogens as the source of these diseases; no studies have examined the role of viruses. Using a combination of transmission electron microscopy (TEM) and 454 pyrosequencing, we compared 24 viral metagenomes generated from *Montastraea annularis* corals showing signs of white plague-like disease (WP) and/or bleaching, control conspecific corals, and adjacent seawater. TEM was used for visual inspection of diseased coral tissue. No bacteria were visually identified within diseased coral tissues, but viral particles and sequence similarities to eukaryotic circular Rep-encoding ssDNA (CRESS-DNA) viruses and their associated satellites (SCSDVs) were abundant in WP Diseased tissues. In contrast, sequence similarities to SCSDVs were not found in any healthy coral tissues, suggesting SCSDVs might play a role in WP disease. Furthermore, *Herpesviridae* gene signatures dominated healthy tissues, corroborating reports that herpes-like viruses infect all corals. Nucleocytoplasmic large DNA virus (NCLDV) sequences, similar to those recently identified in cultures of *Symbiodinium* (the algal symbionts of corals), were most common in bleached corals. This finding further implicates that these NCLDV viruses may play a role in bleaching, as suggested in previous studies. This study determined that a specific group of viruses is associated with diseased Caribbean corals and highlights the potential for viral disease in regional coral reef decline.

2.2 Introduction

Difficulties associated with isolating, culturing, and manipulating potential pathogens as well as in quantitatively and temporally connecting the prevalence of a given microbe or virus to specific signs of infection have limited our understanding of the etiology of many wildlife diseases. Given these challenges, non-culture-based methods are increasingly used in research to characterize disease in novel environments or organisms. For example, surveys such as amplicon-based 16S rDNA profiling, can compare whole microbial assemblages from organisms of different health states, but to comprehensively survey viruses, shotgun-based metagenomic sequencing approaches are often required (Mokili et al, 2012). This is because viruses lack a common phylogenetic marker, and therefore marker-based amplicon sequencing (e.g., 16S or 18S rRNA surveys) cannot necessarily be applied to diverse viral consortia. Some examples of the successful application of viral metagenomics to elucidate the pathogens associated with a disease include the identification of: an astrovirus as the probable cause for shaking mink syndrome (Blomstrom et al, 2010), an anellovirus associated with a California sea lion mortality event (Ng et al, 2009), and a coronavirus that causes human respiratory disease (Bermingham et al, 2012).

Marine wildlife diseases are increasing in prevalence and incidence (Ward & Lafferty, 2004; Harvell et al, 2004). Reports of non-bleaching coral diseases have increased over 50-fold from 1965 to 2005 (Sokolow, 2009). Such epizootics are of concern because they have contributed to declines in coral abundance and cover (Gardener et al, 2003; Rogers, 2009). However, of the more than 20 described global coral diseases, only 6-8 have pathogens ascribed to their etiology (Green & Bruckner,

2000; Sutherland et al, 2004; Rosenberg et al., 2007; Bourne et al, 2009; Pollack et al, 2011). One coral disease of particular ecological importance is white plague (WP), a rapid tissue loss disease that affects multiple species of Caribbean corals, including dominant reef-building *Montastraea* species. Caribbean WP is characterized by lesions that begin basally or peripherally on a colony, and then progress rapidly (mm to cm day^{-1}) across the colony surface resulting in partial to total colony mortality (Miller et al, 2006; Weil et al, 2006; Richardson et al, 2001). Three types of WP (I, II, III) are differentiated based on tissue loss progression rates, with type I progressing the slowest (a few mm/day), type II progressing at a maximum rate of 2 cm/day, and type III progressing the fastest (> 2 cm/day) (Dustan, 1977; Richardson et al, 1998; Richardson et al, 2001). Although an infectious agent, the bacterium *Aurantimonas coralicida*, was hypothesized to be the cause of WP type II in the coral *Dichocoenia stokesii* (Richardson et al, 1998; Denner et al, 2003), *A. coralicida* is not always associated with WP- infected coral colonies. For example, this bacterium was associated with healthy but not WP-infected *Montastraea annularis* colonies (Pantos et al, 2003) or WP-infected colonies from different geographic regions and/or host species (*Siderastrea*, *Diploria*) (Cardenas et al, 2012; Sunagawa et al, 2009).

Given the limited success in identifying the causative agents of WP diseases, controversy exists as to whether similar disease signs represent unique etiologies. It is possible that the different WP types are either the same disease variably manifested or alternatively, white plague signs may represent a variety of different diseases, even in cases where progression rates are similar (Pollock et al, 2011). For example, a WP-like disease of corals in the Red Sea has been shown to be caused by the bacterial pathogen,

Thalassomonas loyana, and not *A. coralicida*. Phage therapy reduces signs of this disease *in situ* and in aquaria, confirming the bacterial nature of the pathogen (Thompson et al, 2006; Efrony et al, 2007; Atad et al, 2012). Alternatively, an additional hypothesis is that a virus and not a bacterium might be the cause of some of these WP signs. To test this hypothesis, we determined if various viral types are differentially associated with a WP type I-like outbreak that occurred in the US Virgin Islands in 2010.

Currently little is known about viral disease in corals. Studies have characterized the viruses associated with bleached and healthy corals, corals exposed to different environmental stressors, and within the algal symbionts (*Symbiodinium* spp.) of corals (Wegley et al, 2007; Marhaver et al, 2008; Vega Thurber et al, 2008; Wilson et al, 2004; Correa et al, 2013). Based on these works, four major groups of viruses are predicted to infect corals and their associated microbes: bacteriophages, enveloped herpes-like viruses, nucleocytoplasmic large DNA viruses (NCLDVs, including members of the *Phycodnaviridae, Mimiviridae,* and *Iridoviridae*), and small circular ssDNA viruses (for a review, see Vega & Correa, 2011). For example, herpes-like sequences were found in stressed *Porites compressa* corals as well as in other cnidarians such as the starlet anemone, *Nematostella*, and the medusozoan, *Hydra* (Vega Thurber et al, 2008). Genomic and microscopic evidence indicate that phycodnavirus-like particles can be present within bleached and/or heat-stressed corals, and these VLPs have been suggested to target *Symbiodinium* (Wilson et al, 2009; Patten et al, 2008; Correa et al, 2013). Active infection of *Symbiodinium* by members of the *Phycodnaviridae* was indirectly demonstrated based on the identification of phycodnavirus-like cDNAs in cultures of two different clades of *Symbiodinium* (Correa et al, 2013). Lastly, sequence similarities to and

viral-like particles reminiscent of nano-, circo- and gemini- viruses, all of which are eukaryotic circular Rep-encoding ssDNA (CRESS-DNA) viruses and their associated satellites (collectively referred to "SCSDVs" in this paper) also have been found in corals (Rosario et el, 2012; Wegley et al, 2007; Vega Thurber et al, 2008; Marhaver et al, 2008; Littman et al, 2011; Davy & Patten, 2007; Patten et al, 2008).

Although these previous works laid the foundation for our understanding of viruses associated with diseased corals, the potential contribution of these viruses to colony WP-disease signs is unknown, and their role in bleaching is poorly understood. Henceforth, we refer to coral colonies exhibiting signs of WP as "diseased" while colonies showing signs of symbiont loss, which may or may not be due to a pathogen, are described as "bleached." To determine if viruses contribute to either bleaching and/or WP signs, we applied transmission electron microscopy and replicated metagenomics to characterize viruses from Caribbean *M. annularis* corals that appeared healthy, bleached, and/or affected by a white plague-like disease. Here, we present evidence that (1) the viral consortia among Healthy (H), Bleached (B), WP Diseased (D), and WP Diseased-Bleached (BD) coral tissues are significantly different, and (2) SCSDVs dominate WP Diseased corals but are absent from healthy corals. These data suggest SCSDVs may play a role in some manifestations of white plague-like disease in corals.

2.3 Materials and methods

Reef site and specimen collection

Sampling of the scleractinian coral, *Montastraea annularis*, was conducted at Brewers Bay, in St. Thomas, US Virgin Islands, during a concurrent white plague outbreak and bleaching event in September 2010. During this event, up to 90% of corals

on the examined reef were bleached, while a maximum of 7% showed signs of WP and bleaching (Brandt et al, 2013). Collections took place over two days at depths of 5.5-7.6 m. Temperature at depth was ~29.0°C. All *M. annularis* colonies used in this study were located within ~75 m of each other. In addition to being affected with WP Disease signs, all WP Diseased colonies showed signs of bleaching (Figure 2.1). Therefore, bleached coral colonies closest to WP Diseased colonies were selected as controls. All apparently healthy *M. annularis* colonies (N = 2) that could be located during specimen collection dives were sampled.

White plague infections were defined using the following signs: 1) lesions consisted of an area of recent tissue loss where denuded skeleton with little to no algal colonization was delineated from living tissue by a smooth, undulating margin, 2) lesions were located peripherally or basally on the colony, and 3) lesions expanded at an mean rate of 0.23 ± 0.12 cm/day (Figure 2.1). These disease signs and epidemiological properties are consistent with those previously reported for WP (reviewed in Sutherland et al, 2004; Bythell et al, 2004; Brandt et al, 2013), and tissue loss rates were most similar to reports of WP type I disease (Dustan, 1977; Sutherland et al, 2004).

Coral tissue collections

Coral tissue samples were collected using SCUBA. Two to three plugs of tissue and skeleton were removed from each *M. annularis* colony (Figure 2.1) using a 2-cm diameter corer and hammer (USVI Department of Planning and Natural Resources permit #STT-050-10). From the 7 WP Diseased colonies, tissues were cored from both the bleached top "Bleached+WP Diseased (BD)" and the margin of lesions "WP Diseased

(D)," which did not show signs of bleaching. Tissue from an additional 5 "Bleached (B)"

non-WP Diseased corals and 2 "Healthy (H)" corals (normal pigmentation, non-diseased)

were taken as controls (Figure 2.1). Tissue samples were placed in individual sterile bags

underwater, stored on ice, and processed on shore within 4 hours. All sampled colonies

were examined for diseases signs and progression (if applicable) two days after sample

collections. In all sampled WP Diseased colonies lesions had expanded, indicating that

the disease was active when samples were taken. In all sampled non-WP Diseased

colonies, no lesions had developed.

Cored specimens were rinsed with 0.02 µm filtered seawater. Tissue was removed

by airbrushing with ~40 ml of 0.02 µm filtered phosphate buffer saline solution (pH 7.3).

Tissue homogenates were 0.22 µm filtered, preserved in molecular biology grade

chloroform (2% final concentration), and stored at 4°C until viral metagenome generation

processing.

Seawater sampling, viral concentration and purification

Three liters of seawater were collected ~16 cm above 3 diseased coral colonies

using sterile containers. Replicate samples were pooled into one 9 liter-sample from

which the "SW Bleached+WP Diseased (SWBD)" virome was generated. Seawater also

was collected and pooled from above 3 Bleached colonies for the "SW Bleached (SWB)"

virome.

Virus-like particles (VLPs) were concentrated using a 100 Kd tangential flow

filter and purified via passage through a 0.22 µm sterivex (Vega Thurber et al, 2009). The

resulting viral concentrate was preserved in molecular biology grade chloroform (2%

final concentration), and stored at 4°C until DNA extraction was performed as described below. The cesium chloride (CsCl) gradient ultracentrifugation steps were not conducted prior to extracting DNA from the seawater samples.

Viral metagenome generation

VLPs were isolated from coral tissues using CsCl density gradient ultracentrifugation, with buoyant densities ranging from 1.2 to 1.7 g/ml before addition of samples (Vega Thurber et al, 2009). After comparing all CsCl density layers from each tissue type for the presence of viral particles, viruses were isolated from the 1.2 g ml^{-1} density layer, where the majority of VLPs were present. To confirm the presence of VLPs and that bacterial/eukaryotic contamination was minimal, an aliquot of every viral fraction from all samples and density layers were stained with SYBR Gold (Invitrogen) and imaged using an epifluorescent microscope. Following this, all samples were again 0.22 µm Sterivex filtered to remove residual bacteria.

DNA was isolated using an organic extraction protocol (Vega Thurber et al, 2009) and amplified using nonspecific multiple displacement amplification (MDA) according to manufacturer's protocol (GenomPhi, GE Healthcare). PCR reactions using 16S and 18S primer sets were performed to determine whether bacterial or eukaryotic DNA contaminated the viromes. No contamination was detected.

The coral viromes (24 samples total, 1 plate) were barcoded and pyrosequenced on a Titanium 454 platform from Roche at EnGencore (University of South Carolina). The final numbers of replicate libraries for each coral health state or seawater type were: H (n=2), B (n=5), BD (n=7), D (n=7), SWB (n=1), and SWBD (n=1).

Virome processing and bioinformatic analyses

Sequence reads underwent several preliminary bioinformatic steps. SFF files were

converted to FASTA/FASTQ files and de-replicated using the program GALAXY

(Geock et al, 2010). Low quality reads (i.e., those < 100 base pairs in length and/or with

quality scores < Q20) were removed. To eliminate any potential non-viral sequences

from the datasets, the program DeconSeq was used to identify and remove reads with

nucleic acid homology (based on ≥ 60% identity and 94% similarity) to eukaryotes

(mouse, fish, human and mosquito), bacteria, and/or archaea (Schmieder & Edwards,

2011). These conservative quality and similarity parameters may have underestimated

viral sequence abundance since viral genomes commonly contain gene sequences

homologous to bacteria, archaea, and eukaryotes, but importantly, they reduced the

likelihood that sequence similarities in this study were false positives. Sequences

designated as contamination by Deconseq also were run through CAMERA (see below),

in order to confirm that they were in fact not similarities to possible coral-infecting

viruses (i.e. were truly human or bacterial contamination).

Using the CAMERA (Community Cyberinfrastructure for Advanced Microbial

Ecology Research and Analysis) platform, the tBLASTx algorithm (e values ≤ 1×10^{-5})

was used to find similarities to sequences in the National Center for Biotechnology

Information (NCBI) non-redundant (NR) viral database (Altschul et al, 1990; Sun et al,

2010). Hierarchical taxonomic information (e.g. viral order, family membership) was

manually assigned for the strongest similarity identified to a known viral genome.

Similarities to viruses that lacked any phylogenetic information (e.g., "unclassified virus"

or "fecal metagenome") or those describing paraphyletic groupings (e.g., "chimp virus")

were removed from the datasets. Sequence similarities at the viral family or satellite level were normalized to the total number of viral similarities identified in each library by dividing significant hits to known viral types by total known viral hits.

Viral family diversity analyses

Sequence similarity richness and evenness were determined using the Shannon Index diversity measure, $H'=-\sum_i (p_i)(\log_e p_i)$, where p_i is the proportion of the total sample belonging to the ith viral family/satellites (Clarke &Warwick, 2001). The index was calculated for all 24 viromes and averaged for each virome type where applicable.

Statistical analyses

To compare differences among the ratios of phage and eukaryotic viral similarities as well as among Shannon diversity values, one-way Analysis of Variance (ANOVA) followed by Tukey's HSD post hoc (95% confidence) tests (when statistical differences of $p \le 0.05$ were found) were performed using Analyse-it V2.2 Ltd. In addition, significant differences in viral taxa among the virome types were determined using a Kruskal-Wallis test followed by pairwise comparisons with Bonferroni corrections, when statistical differences ($p \le 0.05$) were found.

Viral consortia variability was determined using Bray-Curtis similarity matrices and non-metric multidimensional scaling plots (MDS) of all normalized eukaryotic viral family similarities with 25 iterations. To test for statistical differences among the resulting MDS clusters, Analysis of Similarity (ANOSIM) tests were performed while Similarity of Percentage (SIMPER) analyses were executed to determine which viral types drove dissimilarity among samples (Clarke & Warwick, 2001). To further examine the difference in viral sequence similarities between the paired WP Diseased and WP

Diseased-Bleached tissues isolated from individual colonies, a CLUSTER analysis was

performed only on the WP Diseased coral colonies (D vs. DB). Shannon Diversity, MDS,

ANOSIM, SIMPER, and CLUSTER analyses were all performed in PRIMER v.6 (Clarke

et al, 2006).

SCSDV replication gene phylogenetic analysis

Phylogenetic analysis of the SCSDVs was performed using the replication

initiator protein genes (*rep*) found in all WP Diseased and both Seawater viromes (SWB

and SWBD) using the Metavir tool with the "compute phylogenic trees from multiple

viromes" option (Roux et al, 2011). The replication initiator protein (Rep) was selected as

a marker due to its evolutionary conservation in all SCSDVs and their associated satellite

DNAs (Delwart & Li, 2012; Martin et al, 2011; Gibbs and Weiller et al, 1999; Ilyina &

Koonin, 1992). METAVIR conducts the following steps to construct phylogenetic

comparisons: 1) assembly of reads using CAP3, 2) sequence translation of un-assembled

reads, and 3) determination of reads with similarities to Rep proteins (BLASTx to the NR

database, e value $< 10^{-3}$) to SCSDV genomes in the PFAM database. Using the Metavir

FASTA output, GENEIOUS VR6 (Biomatters) was used to construct a Neighbor Joining

(NJ) tree using the Jukes-Cantor model with 10,000 bootstraps. Only branches with $>$

60% support were retained.

Viral metagenomic sequence alignments to SCSDV genomes and verification of SCSDV
features

To confirm that our libraries contained sequences similar to all regions of SCSDV

genomes, contigs from each individual library were constructed in Newbler using default

settings (Margulies et al, 2005). Contigs from WP Diseased libraries were analyzed in Metavir's "Contig Map" feature. Representative contigs of 1000-3000 bp length that had similarities to SCSDVs were compared to annotated genomes from NCBI in GENEIOUS VR6 (Biomatters) by generating multiple alignments in MUSCLE (1000 iterations) (Edgar, 2004). Average Nucleotide Identities (ANI) (percentages) were derived from multiple nucleotide alignments of WP Diseased contigs and the genomes of known circoviruses, nanoviruses, and satellite DNAs. These percentages were compared across each major category (e.g. known circoviruses to known nanoviruses or putative circoviurses to known circoviruses) using univariate nonparametric statistics. Various SCSDV features also were annotated in GENEIOUS R6 (confirmed by tBLASTx to the NR database), such as Rep and capsid genes, as well as stem loops, to further confirm that these sequences were similar to known SCSDVs (data not shown).

Transmission electron microscopy (TEM)

Coral tissue and skeleton samples (~2 mm) for TEM were collected in tandem with all samples obtained for viral metagenome generation. Samples were preserved in 0.02 µm filtered 2% gluteraldehyde and 0.05 M sodium cacodylate-buffered sea-water and stored at 4°C. Samples were post-fixed in osmium tetroxide, dehydrated in ethanol, embedded in Spurr® resin, sectioned with a diamond knife in a Sorval MT-2 ultra-microtome, and mounted onto copper grids. Sections were stained with lead citrate and uranyl acetate as needed and then imaged on a JOEL 1400 transmission electron microscope at the University of Miami Center for Advanced Microscopy (Miller et al, 2011). Two individuals from each health state were examined for the presence of virus-

like particles.

2.4 Results

To determine if specific viruses are associated with the documented St. Thomas, USVI WP-like Disease outbreak, we generated 24 pyrosequenced shotgun viromes from Healthy (H), Bleached (B), Bleached+WP Diseased (BD), and WP Diseased (D) coral tissues, as well as from seawater adjacent to Bleached (SWB) and Bleached+Diseased colonies (SWBD). These libraries totaled over 1 million reads, of which >360,000 passed quality control and *in silico* contaminant screening. Over 21% (~78,000) of the curated sequences had similarity to known annotated viral genomes (Table 2.1).

A majority of these sequences (averaged from all coral and seawater samples) were similar to phages (72.0% ± 16.8) in the Order Caudovirales (*Myo-*, *Sipho-*, and *Podoviridae*). Within only the coral tissues libraries, similarities to large eukaryotic viruses in the families *Herpesviridae* (30.0% ± 18.2) and *Phycodnaviridae* (13.8% ± 11.8) were the most abundant eukaryotic viral similarities. These *Phycodnaviridae* and *Herpesviridae* similarities were found to have homology to genes (i.e. capsid and topoisomerase genes) located across multiple regions of the known genomes (data not shown). Of eukaryotic viral comparisons, percentage of similarities to *Circoviridae* (15.2 ± 17), *Nanoviridae* (7.9 ± 13), and satellite DNAs (alpha satellites) (8.6 ± 16) ranged from 0% (in Healthy tissue) to 64% (WP Diseased tissue).

Ratios of phage to eukaryotic viral similarities vary among coral tissue health states

Theoretically, eukaryotic viruses should increase in abundance relative to bacteriophages in coral tissues or seawater when an active eukaryotic viral infection is

occurring. Although bacteriophage similarities dominated all libraries, the percentage of sequences similar to eukaryotic viruses was significantly higher (d.f. = 3) in the Bleached (34.47±17.0%) and Bleached+WP Diseased (32.61±18.8%) samples relative to the Healthy ones (11.11±8.3%) (Table 2.2). In addition, the ratio of phage to eukaryotic viral sequence similarities trended towards a decrease in WP Diseased (4.77±1.8) compared to Healthy tissues (19.21±15.2). The ratio of bacteriophage to eukaryotic virus sequence similarities in the SWB sample also was 1.47-fold higher than in the SWBD library (Table 2.2).

SCSDV and satellite DNA similarities dominated diseased coral tissues

All viral types comprising ≥ 4% of known eukaryotic virus similarities in at least one coral tissue or seawater sample were compared among the coral tissues health states and seawater viromes (Figure 2.2A). These comparisons indicated that significant differences (d.f = 3) in viral consortia exist among coral tissue health states. For example, similarities to SCSDVs, including *Circoviridae, Nanoviridae,* and satellite DNAs were each statistically more abundant in the WP Diseased libraries, relative to the Healthy libraries (p<0.05 for all tests). Collectively, SCSDV similarities comprised 64.5% of known eukaryotic viral similarities in WP Diseased tissues (Figure 2.3), whereas similarities to SCSDVs were not detected in Healthy coral viromes (Table 2.3). Furthermore, similarities to *Nanoviridae* were more abundant in WP Diseased than in Bleached+WP Diseased viromes (17.57 ± 5.1% vs. 0.35 ± 0.4%; p<0.03) (Table 2.3). Satellite DNA similarities also were in higher relative abundance in WP Diseased (14.05 ± 5.2%) than Bleached (0.00%) tissue libraries (p<0.01). Both seawater viromes also

contained high abundances of SCSDV similarities (SWD=41.29% and SWB=55.59%) (Figure 2.2A).

Herpesviridae similarities were identified in all coral tissue types but at a higher relative abundance in Healthy than in WP Diseased tissue (62.18 ± 4.5% vs. 16.47 ± 3.4%) (p < 0.03) (Table 2.3). Although common in coral tissues, these herpesvirus similarities were rare in adjacent seawater and comprised < 1.5% of the similarities in either seawater virome (Figure 2.2A). Sequence similarities to at least some members of the nucleocytoplasmic large DNA virus (NCLDV) group also were present in all six virome types including similarities to members of the *Phycodnaviridae, Mimiviridae* and *Ascoviridae*. A higher relative proportion (> 40%) of these viral sequences were identified in both bleached (B and B+D) tissue types compared to Healthy or WP Diseased tissues (33% and 18%, respectively) (Figure 2.2A and 2.3). Viral sequence similarities that constituted a minority (i.e., <4% of eukaryotic viruses similarities) of the best annotations for each read also were examined for apparent patterns (Figure 2.2B). With the exception of the Healthy viromes, *Baculoviridae* and *Iridoviridae* similarities were present in viromes generated from all coral health states and seawater samples.

Diseased coral tissues contain a unique consortium of viral sequence similarities

To determine whether viral consortia differed among viromes generated from different coral health states as well as from adjacent seawater, multivariate analyses were performed. The WP Diseased viromes grouped (Figure 2.4, red stars) in this analysis, and ANOSIM confirmed that these viromes were statistically different from the other three tissue type viromes (Global R = 0.238 and p-value = 0.012) (Table 2.4). The two Healthy

samples (green hexagons) were located furthest from the WP Diseased tissues, depicting

the minimal similarity between their viral consortia (Figure 2.4). Seawater viromes (dark

and light blue circles) also grouped closer to each other than to viromes generated from

any coral tissue types (Figure 2.4). CLUSTER analysis depicted relatedness between

paired viromes generated from Bleached+WP Diseased and WP Diseased tissue of an

individual colony; viral consortia from the same individual colonies clustered on different

branches, with up to 55% dissimilarity (Figure 2.5).

SIMPER analysis determined which viral families contributed to virome

dissimilarity (Table 2.5). While similarities to *Herpesviridae* were present in viromes

generated from all tissue health states, these sequences contributed to more than 31% of

the dissimilarity between Healthy and WP Diseased tissue viromes, with herpesvirus

similarities being the most abundant in Healthy tissues (Table 2.5). Sequences similar to

members of the SCSDVs contributed from 9 to 20% of the dissimilarity between WP

Diseased and other coral virome types, and are strongly responsible for the uniqueness of

the WP Diseased viral consortia (Table 2.6). *Poxviridae* similarities contributed to

dissimilarities among the Bleached+WP Diseased and Bleached viromes compared to the

Healthy viromes (9.78% and 9.46%, respectively) (Table 2.5). Out of all health states,

SIMPER analysis showed that the Healthy viromes were most similar to each other

(70.94% similarity). Both Bleached+WP Diseased viromes and Bleached viromes each

had approximately 43% similarity, whereas WP Diseased tissues viromes had

intermediate similarity at 55.90% (Table 2.5).

Diseased viromes contain higher eukaryotic viral diversity than healthy corals

To determine whether there were differences in viral diversity among coral tissue health states, Shannon's diversity index was calculated (Table 2.6). Eukaryotic viral diversity was statistically variable among coral tissue types ($p<0.05$), with WP Diseased viromes having higher diversity than Healthy viromes (1.96 ± 0.08 vs. 0.98 ± 0.19). Diversity between different types of bleached tissues (B and BD) was similar (1.30 ± 0.10 and 1.35 ± 0.11) (Table 2.6).

Diseased coral SCSDVs are distinct from Seawater SCSDVs

Phylogenetic trees were created using the viral replication (Rep) protein of SCSDVs identified within the 7 WP Diseased and 2 Seawater viromes. The tree contained over 50 sequences, with all of the WP Diseased and Seawater viromes contributing at least one Rep sequence similarity (Figure S3). Rep sequences from both Seawater viromes were generally located on separate branches ($> 60\%$ support) of the tree than Rep sequences from WP Diseased coral viromes (Figure 2.6). For example, two main coral SCSDV clades (stars) were distinct (72.4% and 95.0% bootstrap support) from a well-supported Seawater clade (89.9% bootstrap support) (triangle) (Figure 2.6).

To confirm the origin of SCSDVs in WP Diseased libraries, representative SCSDV contigs were aligned to completely assembled and annotated genomes of circoviruses, nanoviruses, and satellite DNAs. It was determined that putative WP Diseased contigs had broad similarities to fully sequenced and annotated circo- and nanoviruses, and not just within the Rep gene (Figure 2.7). Further, Average Nucleotide Identity (ANI) of putative circoviruses were more similar to known circoviruses than

other viral types (Figure 2.7) (d.f.= 11, p < 0.01) when all pairwise comparisons were evaluated. Surprisingly, the putative nanoviruses from WP diseased libraries also were more similar to known circoviruses and our own putative circoviruses than to known and annotated nanoviruses (d.f. = 11, p < 0.01).

Identification of intracellular virus-like particles corroborates genomic-based findings

Electron micrographs were used to identify potential active viral infections within corals, and to corroborate the sequence-based findings that herpes-like viruses, SCSDVs and NCLDVs were present in coral tissue. However, quantitative TEM analysis could not be performed due to the extensive variation in the quality of the tissues among different health states. For example, tissues were degraded in the WP Diseased samples and cell layers were difficult to discern, whereas Bleached tissues appeared more intact than either WP Diseased or Bleached+WP Diseased tissues. Healthy tissues exhibited intact *Symbiodinium*-host cell attachment and defined tissue layers, whereas signs of degradation were evident in Bleached tissue types (i.e. *Symbiodinium* detachment) (data not shown). *Herpesvirus*-like particles with a characteristic envelope that were ~180 nm in diameter were observed in Bleached+WP Diseased and WP Diseased tissues (Figure 2.8A). In addition, distinctive figure 8-shaped poxvirus-like particles were visualized in WP Diseased tissues (Figure 2.8B). Lastly, SCSDV-like particles were observed in WP Diseased tissues (Figure 2.8C; twinned gemini-like particle), however, TEM resolution was low, ~20 nm (the size of a typical SCSDV particle), so the features of these VLPs are not well-defined. No bacterial cells were observed within the degraded WP Diseased tissue, while in Healthy tissues small cell-like structures (< 0.22 um) were commonly

identified (data not shown).

2.5 Discussion

SCSDVs are associated with WP

Combining TEM and next generation sequencing, we have shown here that viruses are variably associated with different *M. annularis* coral health states. To examine the local oceanic viral consortia and to give insight into transmission mechanisms, we also generated viromes from seawater above Bleached and WP diseased corals. Our robust sampling, which in some cases generated up to 7 replicate viromes per health state, allowed us to determine that a unique viral group, the coral small circular ssDNA viruses (SCSDVs), was associated with a WP disease outbreak in the Caribbean (Figure 2.2,2.3; Table 2.3).

SCSDVs are common pathogens of plants and animals and include the families: *Circoviridae*, *Nanoviridae*, *Geminiviridae*, but their prevalence and distribution in the environment was unknown until recently. Based on metagenomic analyses of animal hosts (e.g., human, bat, rodent, pig and chimpanzee) and water samples, SCSDVs are now thought to be more common than previously thought (for review, Rosario et al, 2012).

Interestingly, SCSDVs have been found to be abundant in reclaimed waters and sewage, suggesting that SCSDVs in the diseased corals examined here could be linked to environment degradation (Rosario et al, 2009; Blinkova et al, 2009). Previously it has been shown that environmental viruses such as human enteroviruses and adenoviruses are present on coral mucus, suggesting that these associations were the result of anthropogenic pollution (e.g. runoff) (Lipp et al, 2002; Lipp et al, 2007; Futch et al,

2010). *Serratia marcescens*, a human bacterial pathogen, also found in sewage, was demonstrated to be the cause of white pox disease in acroporids; it is likely that other pathogens including viruses originate from sewage and negatively affect corals (Patterson et al, 2002; Sutherland et al, 2011). However, our analysis of the Rep proteins and genomes of coral and seawater SCSDVs sequenced in this study suggested that the coral SCSDVs are genetically distinct from those found in the surrounding seawater samples and are likely a unique component of the coral virome. An alternate hypothesis is that SCSDVs are present in healthy corals but are undetectable because they are either below the detection threshold of the methods employed or present in a quiescent stage.

Nevertheless, it is evident from our analysis of both the conserved SCSDV Rep (Figure 2.4 red lettering) sequences and the genome-genome alignments (Figure 2.7) of our putative SCSDVs and known circo-, nano- and satellite viruses that these white plague-associated SCSDV types are novel.

The host for the coral-associated SCSDVs presented here is yet to be determined, but may include the algal endosymbiont (*Symbiodinium* spp., since nanovirus/gemniviruses infect plants), the coral host itself (since circoviruses infect animals), or another member of the coral holobiont (Rosario et al, 2012; Delwart &Li, 2012; Yu et al, 2010). However, a previous study examining viruses associated with *Montastraea cavernosa* coral colonies searched *Symbiodinium* EST libraries and found few similarities to SCSDVs (Correa et al, 2013) suggesting that the SCSDVs associated with diseased corals in this study are infecting the coral animal. In addition, white plague disease signs include rapid tissue loss that suggests a coral (and not algal) pathogen is causing tissue necrosis. Furthermore if algal symbionts were affected, bleaching also

would have been expected in the area of lesions; this was not observed (Figure 2.1).

NCLDVs and bleaching

Sequence similarities to nucleocytoplasmic large DNA viruses (NCLDVs), including similarities to members of the *Phycodnaviridae, Poxviridae, Mimivirdae* and *Ascoviridae,* were relatively more abundant in bleached coral tissue types than in non-bleached tissue types (Figure 2.3). Previously, poxvirus sequences were found to be more abundant in temperature-stressed corals (Vega Thurber et al, 2008), and a recent study on the scleractinian coral, *Acropora millerpora,* which is both geographically and evolutionary distinct from the Caribbean *Montastraea annularis*, also contained pox-like virus sequences (Littman et al, 2011). This study also corroborates findings that have implicated NCLDVs in the infection of the algal symbiont *Symbiodinium* and provides more evidence that bleached host tissue contains viral types different from those found in healthy coral tissues, suggesting viruses may be involved in some thermally induced bleaching responses (Correa et al, 2013; Marhaver et al, 2008).

Herpesviruses dominate healthy tissues

Previous studies have shown that herpes-like viruses are a commonly observed in cnidarian viromes (Vega Thurber et al, 2008). This new work provides physical evidence that herpes-like particles are produced in coral tissues (Figure 2.8A). Given their cosmopolitan presence in healthy individuals of every coral genus tested (e.g., *Porites*, *Acropora*, *Montastraea*, *Diploria*), we hypothesize that herpes-like viruses establish long-term non-fatal infections in corals, in a manner similar to their infections of

vertebrate hosts (Knipe & Cliffe, 2008).

Viral diversity is altered in diseased corals

WP Diseased corals hosted the highest diversity of eukaryotic viruses, bleached corals had an intermediate viral diversity, and healthy corals exhibited the lowest viral diversity. Since both the WP Diseased and Healthy tissues contained high abundances of *Symbiodinium* (based on qualitative analysis of TEM images), we suggest that the higher viral diversity in WP Diseased viromes (relative to Healthy viromes) was not related to the relative abundance of *Symbiodinium* in specimens of the two health states. Rather, the higher diversity of viral types found in WP Diseased corals may be a consequence of secondary infections resulting from a coral weakened from other viral infections. On the other hand, a higher viral diversity in WP Diseased corals may be the direct cause of disease signs. In either case, higher viral diversity may be an indicator of coral stress and may be used to diagnostically characterize corals in a disease state.

Caveats

Multiple displacement amplification (MDA) has been shown to bias metagenomic libraries towards ssDNA sequences and genomes due to the rolling circular amplification method that the Phi29 polymerase employs (Kim et al, 2008; Kim & Bae, 2011). Although it is unclear whether MDA bias is stochastic (Abulencia et al, 2006) or linear (Yilmaz et al, 2010), we calculated that the probability that all WP Diseased (n=7) but no Healthy (n=2) samples contained SCSDV-like sequences was less than 0.0079 (assuming MDA bias towards ssDNA is 50% or less). Even with a 95% bias of MDA towards SCSDVs, we calculated that there is still less than a 0.7% chance of obtaining these results. Further, much of the debate about the utility of MDA for viral metagenomics

comes from studies where samples were processed in different ways. For example, some

studies compared the results of MDA amplified versus unamplified libraries, or to

datasets generated using amplification methods that do not amplify ssDNA viruses (such

as LASLs), or even after the elimination of a denaturing step that would enrich for

ssDNA viruses (Kim et al; 2008; Kim & Bae, 2011). Since all of our samples were

processed in an identical, scientifically rigorous manner, any bias towards ssDNA

sequences should be expressed uniformly in each of the sample libraries. Since only the

WP Diseased and seawater viromes, but not the bleached and healthy viromes, contained

high amounts of these viral types, it is evident that the changes detected in the relative

abundance of similarities to these viral types are not the result of MDA. Lastly, a

previous comparative study on stressed Pacific coral species (not infected with white

plague) also used MDA but detected SCSDV sequences only in two viromes out of 6

(Vega Thurber et al, 2008), while another study on another Pacific coral species using

MDA amplification identified less than 5% nano/circo viruses with no similarities to

satellite DNAs or geminiviruses (Wegley et al, 2007).

These conclusions are based on correlated data, yet, ultimately only direct

infection studies, such as exposing healthy corals to viruses isolated from diseased corals

in a controlled laboratory setting, can determine whether these suspected SCSDV

pathogens cause white plague-like disease or are alternatively secondary infections

resulting from altered coral physiology. Until a proper infection model is developed,

correlation with disease prevalence and incidence will be the best evidence as to causes

of coral diseases. Additionally this study only examined DNA viruses; it is possible RNA

viruses are involved in WP and future experiments should aim to evaluate viruses with

RNA genomes.

Lastly, a majority of our viral sequences (78.33%) were not similar to a known virus or group of viruses. Therefore, although we find significant differences in these libraries, they are based on a fraction of the total data. Yet to pointedly assess the prevalence of already known, described disease agents across these healthy and disease states, we narrowed our focus to taxonomically described viruses.

2.6 Conclusions

This study aimed to determine the viruses associated with white plague-infected corals. Our microscopy data found no evidence of foreign microbial cells present in WP Diseased corals, strongly suggesting that bacterial or small eukaryotic pathogen infection are not the causes of the examined disease. We also found heterogeneity in the viral consortia among tissue types isolated from the same coral colonies. Bleached+WP Diseased tissues were more similar to Bleached tissues than the WP-Diseased area of the same colony. We thus hypothesize that white plague infection is only localized to the disease front, and that bleached and WP Diseased tissues are distinct in their viral composition. Bacteria associated with coral mucus have been shown to be spatially heterogeneous (Daniels et al, 2011), and here we demonstrate viral heterogeneity in a coral colony. Ultimately we have shown that healthy corals have more abundant viral similarities to *Herpesviridae*, bleached corals possess more viral similarities to NCLDVs, such as *Phycodnaviridae* and *Poxviridae*, and diseased tissues contain an abundance of unique SCSDVs including members similar to C*ircoviridae* and *Nanoviridae*, as well as their associated satellites; this novel SCSD viral group therefore may be responsible for

white plague infections in *M. annularis*.

2.7 Acknowledgments

Figures

Figure 2.1. Locations of sampled tissue from *Montastraea annularis* colonies of different health states. BD tissue was taken from ~5 cm from the D tissue, where disease was progressing from the base of the coral colony. Seawater samples were taken ~16 cm above BD and B coral colonies. H= Healthy tissue, B= Bleached tissue, BD= Bleached+WP Diseased tissue, D= Diseased tissue, SWB= Seawater Bleached, SWBD = Seawater Bleached+WP Diseased.
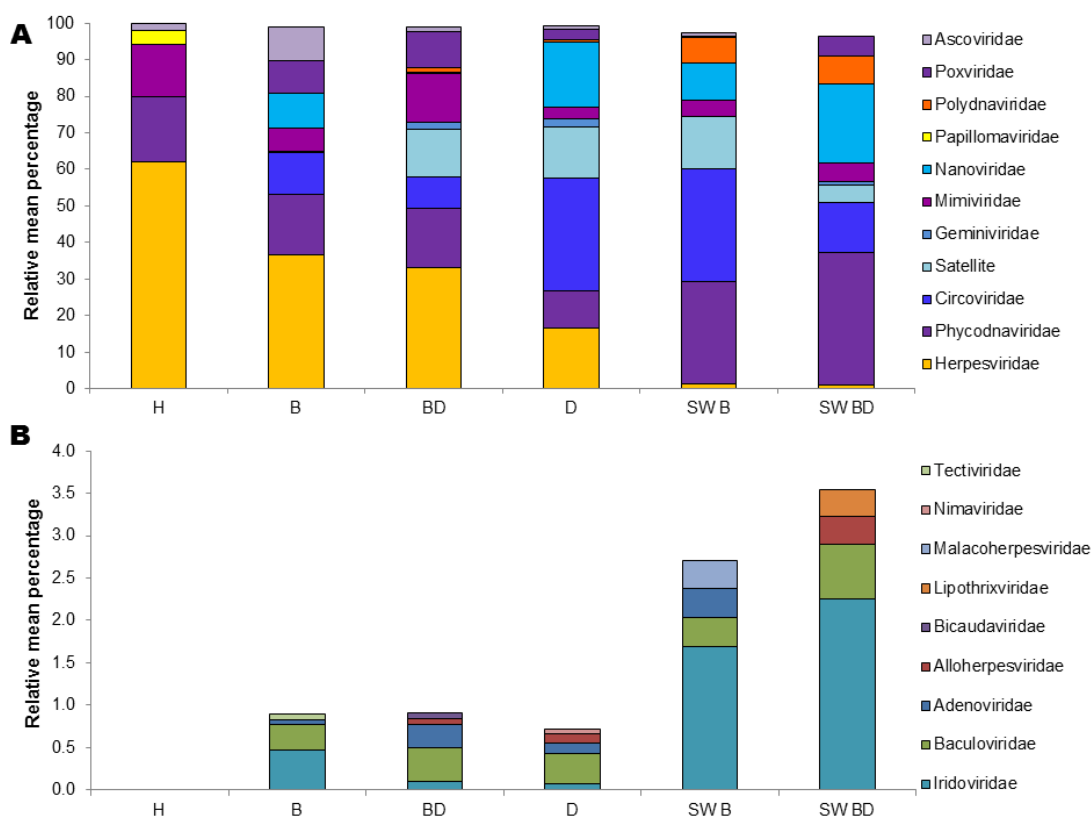
Figure 2.2. Mean percentage of similarities to viral families (and satellite DNAs) in metagenomes generated from different coral health states and seawater. Viral similarities that comprised ≥4% of the total known eukaryotic viral similarities for a given sample type (Figure 2A). The rare virome (Figure 2B), or the viral similarities comprising <4% of the total known eukaryotic viral similarities detected for a given sample type.
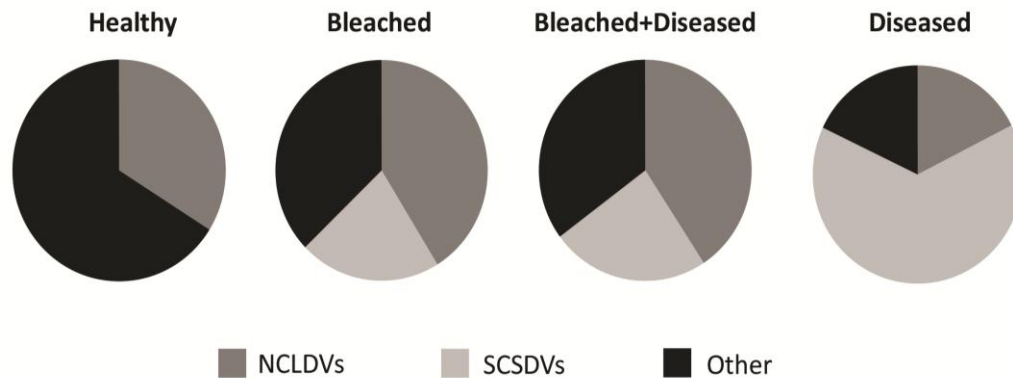
Figure 2.3. Viral "groups" among different coral health states. The mean relative percentage of similarities to each viral type was lumped into "groups" based on their common evolutionary history. 'NCLDVs' are nucleocytoplasmic large dsDNA viruses, which include *Ascoviridae*, *Phycodnaviridae*, *Poxviridae*, and *Mimiviridae*. 'SCSDVs' are small circular ssDNA viruses and their associated satellites and include: *Nanoviridae*, *Circoviridae* and *Gemniviridae*, and satellite DNAs. The 'other' category includes similarities to all viral types not fitting into the two previous groups (i.e., in this study: *Herpesviridae*, *Papillomaviridae* and *Polydnaviridae*).
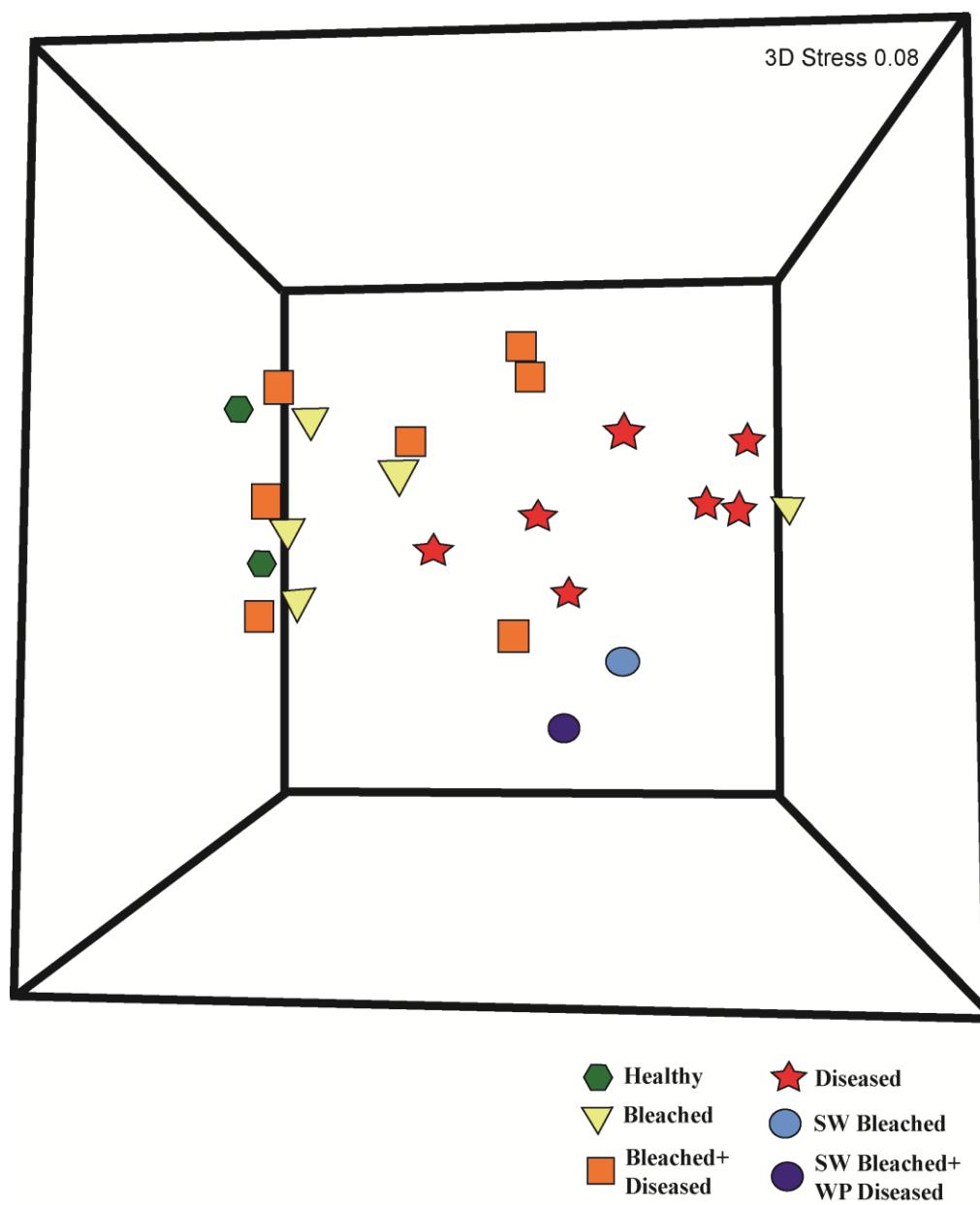
Figure 2.4. Non-metric multidimensional scaling (MDS) 3D plot comparing viral consortia from viromes. MDS plot was constructed from a Bray-Curtis similarity resemblance matrix based on relative percentage of similarities to viral family.
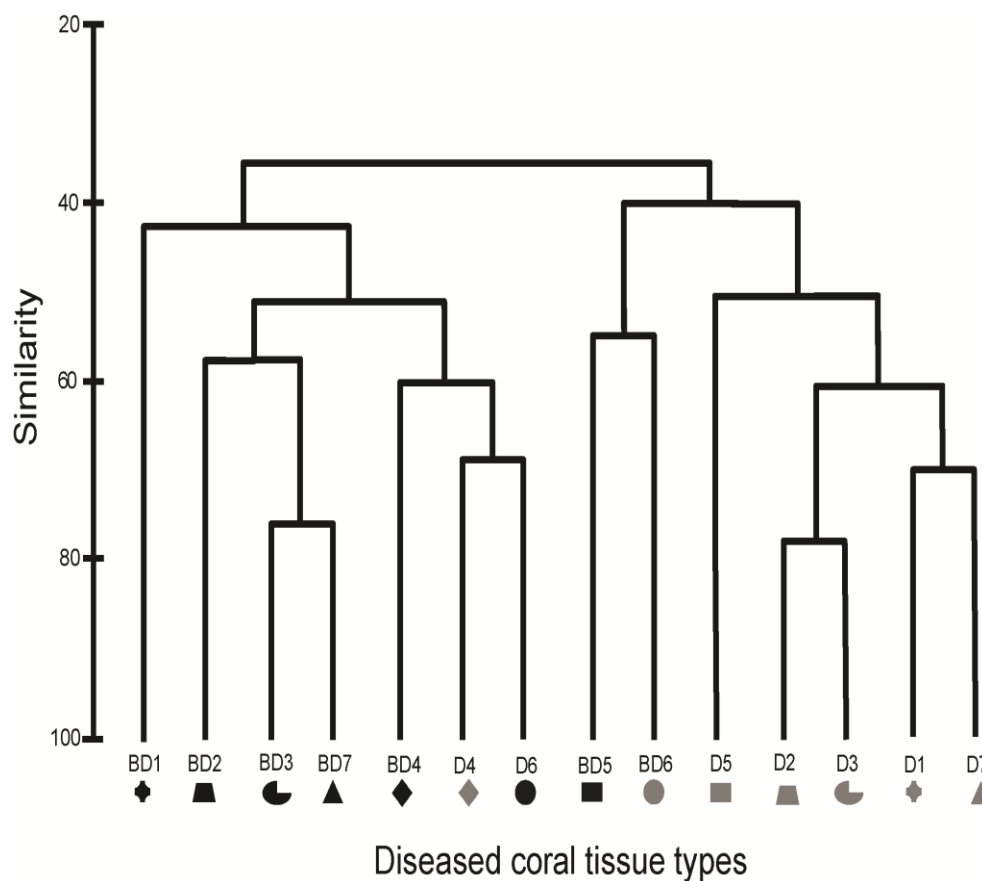
Figure 2.5. Cluster analysis of viral consortia from both diseased (intra colony) coral tissue types: Bleached+WP Diseased and WP Diseased. Cluster dendogram was constructed using group-average linking (similarity was calculated from means of clusters and not the max. or min. values) and Bray Curtis similarities of relative percentages for only Bleached+WP Diseased (BD) and WP Diseased (D) coral colony health states. Matching icons indicate health states from the same coral colony. Black icons are BD tissues, while gray icons are D tissues.
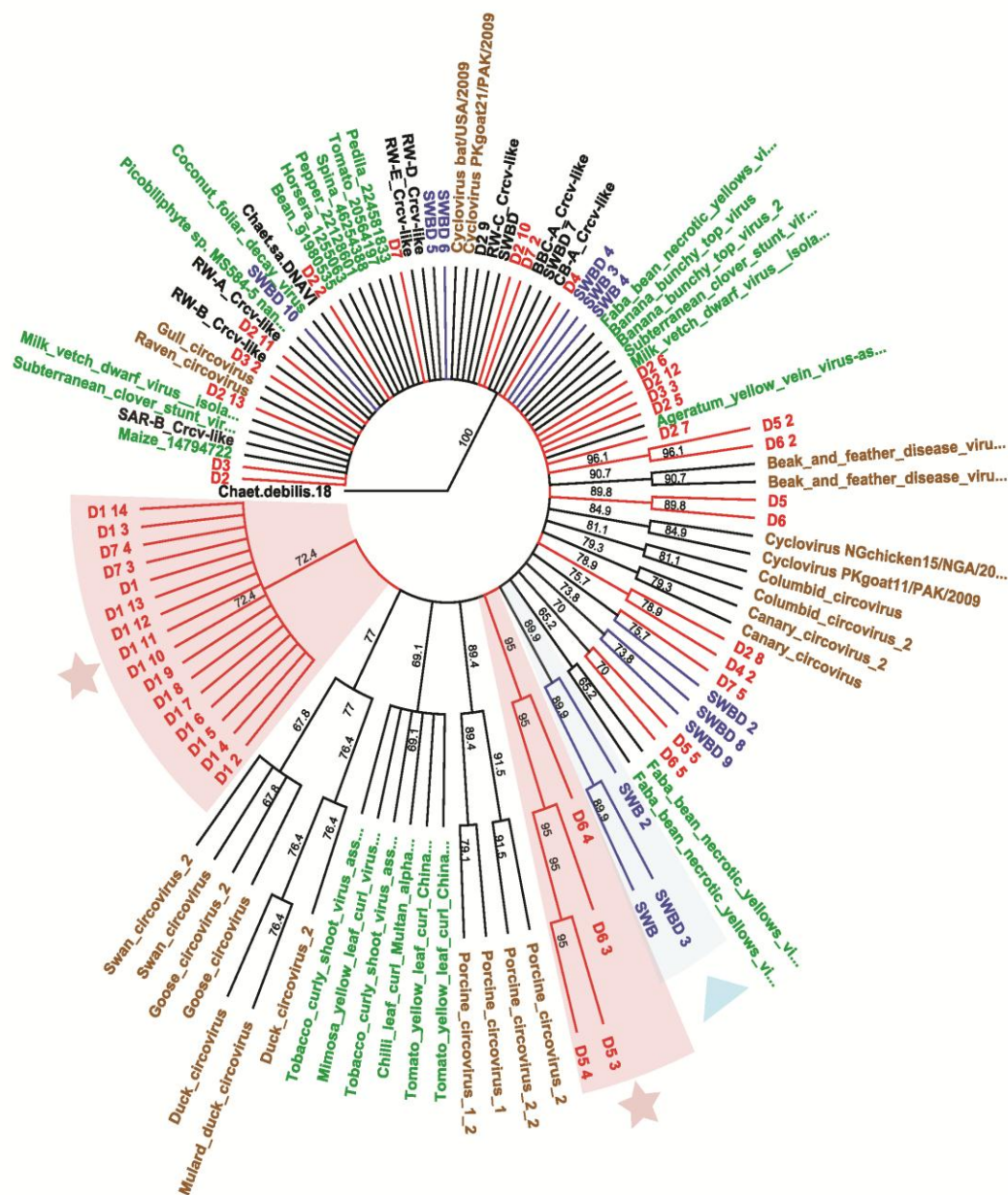
Figure 2.6. Neighbor-Joining phylogenetic tree of SDSDV Rep proteins from WP Diseased health types (D, colored red) and both seawaters (SWD, SWBD, colored blue). Branch length and scores 0-1 represent branch-support based on bootstrap percentages (10,000 bootstraps). Numbers indicate from which sample (i.e. D1.2) the sequence originated. SCSDVs known to infect plants are colored green, while those known to infect animals are colored mustard. Sequence names starting with RW are from reclaimed water (Rosario et al, 2009).A novel SW clade is indicated with a triangle, while stars designate coral specific SCSDV clades.

	Duck	Porcine	Raven	Beak	D2 putative circo2	D2 putative circo1	D1 putative circo	Coconut foliar disease	Abaca	Banana	D5 Putative nano	D3 Putative nano	D1 putativenano1	Ageratum	Tobacco	cottonalpha
Duck																
Porcine	31.7															
Raven	34.8	32.3														
Beak	34.6	32.6	44.4													
D2putativecirco2	22.8	23.7	22.4	23.7												
D2putativecirco1	22.3	23.6	23.1	23	21.3											
D1putativecirco	21.1	25	20.8	20.4	20.8	19.9										
Coconut foliar disease	20.1	21.1	19.6	19.5	20.6	16.9	19.6									
Abaca	19	20.2	18.6	18.5	18	16.3	21.6	25.6								
Banana	18.6	20	18.2	17.7	17.4	15.6	21.8	25.2	66.9							
D5putativenano	23.6	21.7	22.2	22.1	21.6	18.6	19	20.8	20.6	20.7						
D3putativenano	24.5	23.1	24.1	24.9	20	21.6	18.7	18.2	16.9	16.9	19.7					
D1putativenano1	24.9	24.5	25.5	24.3	22.3	23.4	21.5	19.9	18.3	19.6	22.4	21.7				
Ageratum	21.3	21.8	21.9	21.2	20.6	20	21.4	29.4	24.7	26.1	20.8	19.2	22.2			
Tobacco	20.3	21.6	21.4	21.3	20	17.3	18.4	22.1	19	19.5	19.6	17.2	21.7	24		
Cottonalpha	22.9	25.2	21.7	23.9	21	19.5	19.7	20.1	19.9	20.5	20.2	19.3	21.9	23	21.8	
D2putativealpha	26.1	24.6	23	24.1	20.5	23.2	23.6	18	19	18.3	20.9	21.4	22.9	22	19.9	19.3

Figure 2.7. Alignments (above) and ANI distances in percentages (below) of circoviruses, nanoviruses, and satellite DNA genomes to representative SCSDV contigs (noted with red asterisks - i.e: "putative circovirus") from WP Diseased libraries. As a control, known ANI distances of known circoviruses to each other and known nanoviruses to each other were compared, and statistical differences in ANI were found (d.f. =11, p<0.01). Green bars denote 100% nucleotide agreement, mustard bars denote 30-99% agreement, and red bars denote <30% agreement among sequences. Black squares represent >25% identity to the consensus, while gray squares represent <25% identity to the consensus alignment. Reference whole genomes were from NCBI with respective accession numbers: **circoviruses**: Beak + feather= ref|NC_001944.1; Porcine= ref|NC_001792.2; Raven=ref|NC_008375.1; Duck=ref|NC_007220.1; **nanoviruses:** Abaca bunchy= ref|NC_010319.1|; Banana bunchy=ref|NC_003479.1; coconut folior decay=ref|NC_001465.1; **satellites**: Ageratum alphasatellite=ref|NC_019547.1; Cotton alphasatellite = ref|NC_013593.1; Tobacco necrosis satellite= ref|NC_001557.1|
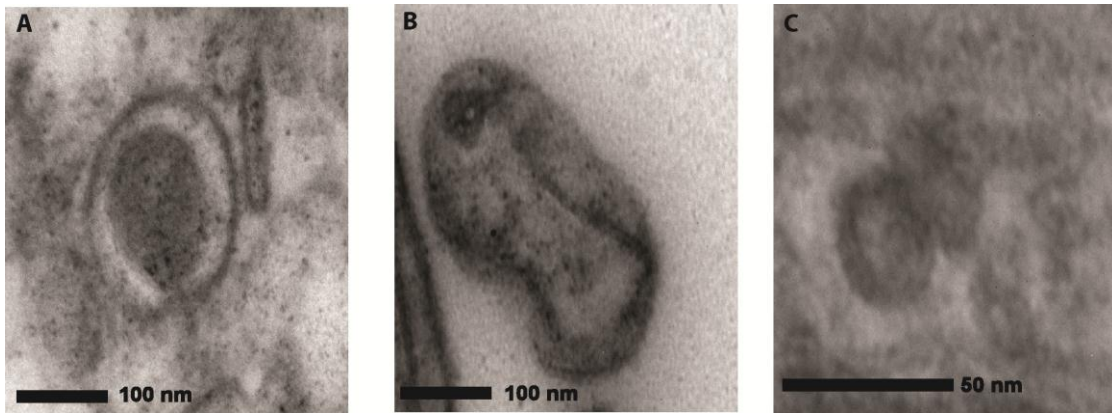
Figure 2.8. Transmission electron micrograph of viral particles detected in diseased *Montastraea annularis* tissues. A herpes-like viral particle approximately 180 nm in width (5A). A pox-like viral particle, approximately 200 nm in length (5B). A gemini-like particle approximately 40 nm length (5C).

Tables

Table 2.1. Number of sequence reads before and after quality processing and contamination screening.

Sample	# Raw Reads	# Reads post-QC	# Reads post-QC +Deconseq	# of Similarities to Viral Database	# of similarities to Euk viruses
Healthy Total	**68522**	**21715**	**11601**	**4077 (35.14%)**	**185**
Healthy1	46634	11311	1608	429	83
Healthy2	21888	10404	9993	3648	102
Bleached Total	**177786**	**71535**	**57173**	**7030 (12.62%)**	**2478**
Blch1	63252	24612	17786	1907	915
Blch2	7035	2423	2336	206	115
Blch3	24432	11337	9409	808	363
Blch4	77208	30529	25037	2743	798
Blch5	5859	2634	2605	1366	287
Bleached and WP Diseased Total	**201986**	**82382**	**78536**	**18438 (23.45%)**	**3601**
Blch+Dis1	19087	5892	5677	728	342
Blch+Dis2	7424	3371	3033	459	106
Blch+Dis3	11079	4568	4068	447	304
Blch+Dis4	62793	26118	24953	10317	1197
Blch+Dis5	30660	12147	11924	1904	392
Blch+Dis6	28843	13848	12942	2122	828
Blch+Dis7	42100	16438	15939	2461	432
WP Diseased Total	**494119**	**184309**	**172690**	**41382 (23.96%)**	**12065**
Dis1	153916	65278	60629	16488	6760
Dis2	47745	16652	14905	1781	1057
Dis3	70392	26265	25484	8776	1919
Dis4	58522	22674	20186	3562	821
Dis5	83522	28283	27065	4190	934
Dis6	34474	12598	12108	2098	285
Dis7	45548	12559	12313	4487	289
SW Bleached Total	**45290**	**18009**	**17405**	**4028 (23.14%)**	**699**
SW Bleached + WP Diseased Total	**54645**	**22689**	**22685**	**2965 (13.07%)**	**515**
Grand Total	**1044444**	**400639**	**360788**	**77920 (21.60%)**	**19543**

Table 2.2: Mean percentage of reads with similarity to eukaryotic viruses and mean ratio of bacteriophage (phage) to eukaryotic (euk) virus similarities in metagenomes generated from corals of different health states or adjacent seawater. Values in bold are statistically different from healthy sample values.

	Healthy (N=2)	Bleached (N=6)	Bleached+ WP Diseased (N=7)	WP Diseased (N=7)	SW Bleached (N=1)	SW Bleached+ WP Diseased (N=1)
Mean % Euk viral similarities (mean ± SE)	11.11±8.30	34.47±17.00	32.61±18.79	26.82 ±16.53	17.37	12.49
Mean ratio of Phage : Euk viral similarities (mean ± SE)	19.31±15.16	**3.80±2.03**	**3.23±0.93**	4.77±1.76	7.00	4.76

Table 2.3: Univariate comparisons of the relative abundance of the sequence similarities to eukaryotic viral families and satellite DNAs comprising ≥4% of coral tissue metagenomes. H=Healthy, B=Bleached, B=Bleached+WP Diseased, D=WP Diseased. Bold indicates significant difference (p<0.05).

Viral Type	Significant pairwise differences	Kruskall-Wallis Statistic	P-Value
Circoviridae	H-D	8.42	**P≤0.04**
Herpesviridae	H-D	9.20	**P≤0.03**
Nanoviridae	H-D, BD-D	9.57	**P≤0.02**
Satellite DNAs	H-D, B-D	10.92	**P≤0.01**
Papillomaviridae	H-B, H-BD, H-D	9.50	**P≤0.02**
Ascoviridae,	---------	2.33	P>0.05
Gemniviridae	---------	4.22	P>0.05
Mimiviridae	---------	1.45	P>0.05
Phycodnaviridae	---------	1.78	P>0.05
Polydnaviridae	---------	1.01	P>0.05
Poxviridae	---------	4.53	P>0.05

Table 2.4. Analysis of Similarity (ANOSIM) results comparing sequence similarities in viral consortia from different health states and adjacent seawater. Bold text indicates a significant difference between sample types.

Sample Type	H	B	BD	D	SWB	SW BD
H (n=2)						
B (n=5)	R=-0.16 P=0.52					
BD(n=7)	R=-0.18 P=0.69	R=-0.08 P=0.76				
D (n=7)	**R=0.83 P=0.03**	**R=0.36 P=0.03**	**R=0.37 P=0.01**			
SW B (n=1)	R=1.00 P=0.33	R=0.24 P=0.33	R=0.36 P=0.25	R=-0.03 P=0.50		
SWBD (n=1)	R=1.00 P=0.33	R=0.20 P=0.33	R= 0.43 P=0.25	R=0.33 P=0.25	NA	NA

Table 2.5. Similarity Percentage (SIMPER) analysis describing variation among sample types. Mean similarity (Avg. Sim.) among like sample types, and mean dissimilarity (Avg. Diss.) among different sample types are listed. All values are expressed as mean percentages. Viral types contributing to the dissimilarity are denoted by x or y superscript. Y denotes that the sample type from the table vertical column is contributing, while x denotes sample type from the horizontal row axis is contributing. Some samples have less than 1% difference in their contribution, and are labeled with xy.

Table 2.5

Sample	Healthy	Bleached	Bleached+ WP Diseased	WP Diseased	SW Bleached
Healthy	**Avg. Sim.** **70.94** *Herpesviridae* 81.33 *Phycodnaviridae* 10.84				
Bleached	**Avg. Diss.** **46.12** *Herpesviridae* 27.66^X *Phycodnaviridae* 13.69^{xy} *Circoviridae* 12.55^Y *Mimiviridae* 10.88^X *Nanoviridae* 10.43^Y *Ascoviridae* 9.63^Y *Poxviridae* 9.46^Y	**Avg. Sim.** **44.38** *Herpesviridae* 58.76 *Phycodnaviridae* 17.97 *Mimiviridae* 7.64 *Ascoviridae* 5.44 *Poxviridae* 5.37			
Bleached + WP Diseased	**Avg Diss.** **49.72** *Herpesviridae* 29.26^X *Mimiviridae* 14.68^{xy} *Phycodnaviridae* 13.60^{xy} *Poxviridae* 9.78^Y *Circoviridae* 8.86^y *Satellite* 13.12^Y *Papillomaviridae* 3.87^X	**Avg. Diss.** **54.23** *Herpesviridae* 15.55^x *Phycodnaviridae* 13.33^{xy} *Mimiviridae* 12.55^Y *Circoviridae* 12.76^X *Poxviridae* 11.89^Y *Nanoviridae* 8.94^X *Ascoviridae* 8.34^X	**Avg. Sim.** **42.44** *Herpesviridae* 57.55 *Phycodnaviridae* 17.95 *Mimiviridae* 10.06 *Circoviridae* 6.87		
WP Diseased	**Avg. Diss.** **71.99** *Herpesviridae* 31.75^X *Circoviridae* 21.39^Y *Nanoviridae* 12.21^Y *Satellite* 9.76^Y *Phycodnaviridae* 8.50^X *Mimiviridae* 7.91^X	**Avg. Diss.** **59.84** *Circoviridae* 19.51^Y *Herpesviridae* 19.22^X *Nanoviridae* 15.80^Y *Satellite* 11.74^Y *Phycodnaviridae* 10.49^X *Ascoviridae* 7.59^X *Poxviridae* 6.48^X	**Avg. Diss.** **61.93** *Circoviridae* 19.51^Y *Satellite* 15.62^Y *Herpesviridae* 15.58^Y *Nanoviridae* 13.99^Y *Mimiviridae* 10.70^X *Phycodnaviridae* 10.29^X *Poxviridae* 7.81^X	**Avg. Sim.** **55.90** *Circoviridae* 35.94 *Herpesviridae* 19.51 *Nanoviridae* 16.62 *Satellite* 11.09 *Phycodnaviridae* 9.49	
SW Bleached	**Avg. Diss.** **75.99** *Herpesviridae* 40.02^Y *Circoviridae* 20.30^Y *Satellite* 9.59^Y *Nanoviridae* 6.69^Y *Phycodnaviridae* 6.62^Y *Mimiviridae* 6.55^X *Polydnaviridae* 4.46^y	**Avg. Diss.** **66.47** *Herpesviridae* 26.56^X *Circoviridae* 17.92^Y *Satellite* 10.96^Y *Phycodnaviridae* 10.81^Y *Nanoviridae* 10.72^X *Ascoviridae* 6.72^x *Poxviridae* 6.41^X	**Avg. Diss.** **66.36** *Herpesviridae* 23.91^x *Circoviridae* 16.61^y *Satellite* 14.09^Y *Phycodnaviridae* 12.02^y *Mimiviridae* 9.93^x *Nanoviridae* 7.40^x *Poxviridae* 7.15^x	*Avg. Diss.* **42.62** *Phycodnaviridae* 20.28^Y *Herpesviridae* 17.73^X *Circoviridae* 15.06^{Xy} *Nanoviridae* 13.84^X *Satellite* *Polydnaviridae* 12.82^{Xy} *Mimiviridae* 6.99^y *Poxviridae* 3.06^y 2.95^x	NA (less than 2 samples)
SW Bleached + WP Diseased	**Avg. Diss.** **76.46** *Herpesviridae* 40.03^X *Nanoviridae* 14.13^Y *Phycodnaviridae* 12.03^Y 59.07^y *Circoviridae* 6.20^x *Mimiviridae* 5.06^Y *Polydnaviridae* 3.59^y *Poxviridae*	**Avg. Diss.** **63.45** *Herpesviridae* 28.13^X *Nanoviridae* 16.64^Y *Phycodnaviridae* 15.59^Y 10.87^y *Circoviridae* 7.41^X *Ascoviridae* 5.98^y *Polydnaviridae* 5.70^x *Poxviridae*	**Avg. Diss.** **68.39** *Herpesviridae* 23.48^X *Phycodnaviridae* 16.01^Y 15.54^Y *Nanoviridae* 10.62^X *Satellite* 9.68^X *Mimiviridae* 7.51^x *Poxviridae* 6.87^y *Circoviridae* 4.70^y *Polydnaviridae*	*Avg. Diss.* **51.22** *Phycodnaviridae* 25.17^Y 19.00^X *Circoviridae* 15.13^X *Herpesviridae* 11.68^Y *Nanoviridae* 10.33^x *Satellite* 26.67^X *Polydnaviridae* 2.96^y *Poxviridae*	**Avg. Diss.** **28.80** *Circoviridae* 29.48^X *Nanoviridae* 19.87^Y *Satellite* 16.91^X *Phycodnaviridae* 14.47^Y 8.93^Y *Poxviridae* 1.77^X *Ascoviridae*

Table 2.6. Shannon diversity index of mean relative percentage of eukaryotic viral types of all viromes generated. Bold denotes significantly different than Healthy.

Sample	Shannon Diversity (H')	Standard Error
Healthy	0.98	0.19
Bleached	1.35	0.11
Bleached+WP Diseased	1.30	0.10
WP Diseased	**1.62**	0.08
SW Bleached	1.80	NA
SW Bleached+WP Diseased	1.87	NA

PHAGE-BACTERIA NETWORK ANALYSIS AND ITS IMPLICATIONS FOR CORAL DISEASE

Nitzan Soffer, Jesse Zaneveld, Rebecca Vega Thurber

Chapter 3 PHAGE-BACTERIA NETWORK ANALYSIS AND ITS IMPLICATIONS FOR CORAL DISEASE

3.1 Summary

Multiple studies have explored microbial shifts in diseased and stressed corals, however, little is known about changes in bacteriophage (phage) consortia and their interactions with microbes in this context. This study characterized both microbial and phage consortia associated with *Montastraea annularis* corals during a concurrent white plague disease outbreak and bleaching event. Phage consortia, based on shotgun metagenomes, were different in bleached compared to diseased tissues. Similarities to viruses in the family *Inoviridae* were elevated in diseased and healthy compared to bleached tissues. Sequencing of the bacterial/archaeal 16S rRNA gene revealed that microbial communities were different in diseased and bleached corals. Bacteria in the orders *Rhodobacterales* and *Campylobacterales* were increased while *Kiloniellales* was decreased in diseased compared to other tissues. 11 bacterial genera differed across health states overall. To infer which phages interact with these 11 bacterial network of phage-bacteria co-occurrence and mutual exclusions was constructed. Phages and bacteria both exhibited a range of specificity and six phages were found to interact with two disease-associated taxa. These results suggest that phages have a role in controlling stress associated bacteria, and that networks can be utilized to select potential phages for mitigating detrimental bacterial growth, (i.e. phage therapy). Overall this study examines microbial and phage shifts in diseased corals using a novel three-pronged approach.

3.2 Introduction

Coral reefs are considered some of the most diverse environments in the world (Moberg and Folke, 1999; Veron et al., 2009). Scleractinian (stony) corals generate the physical structure of coral reefs, and thus are ecologically important members of many tropical marine ecosystems. In addition to supporting macroscopic reef communities, corals also host diverse microbial consortia that include *Symbiodinium* dinoflagellates, bacteria, archaea, fungi and other microbial eukaryotes (Knowlton and Rohwer, 2003; Croquer et al., 2006). Culture-based studies have demonstrated that these coral-associated microbes (the coral microbiota) take on a variety of roles ranging from mutualistic, to pathogenic (Rohwer et al., 2001; Ritchie et al., 2006; Mouchka et al., 2010; Rosenberg and Kushmaro, 2011; Cook et al., 2013). For example, while bacteria such as *Serratia marcescenes, Vibrio shiloi*, and *Vibrio coralliilyiticus* have been shown to cause disease signs (Ben-Haim et al., 2003; Rosenberg and Falkovitz 2004; Sutherland et al., 2011), *Photobacterium spp*. cultured from coral mucus secrete antibiotics that can reduce pathogen growth (Ritchie et al., 2006).

The coral microbiota has been posited to play important roles in mediating the effects of global environmental changes on coral health (Williams et al., 1987; Rosenberg et al., 2007; Ainsworth et al., 2009). Coral reefs are declining globally due to changes in environmental conditions, such as eutrophication of water due to coastal development, overfishing of herbivores, and increased sea surface temperatures (Nyström et al., 2000; Pandolfi, 2005; Harvell et al., 1999; Pandolfi et al., 2011; Vega Thurber et al., In press). These environmental stressors leave the corals vulnerable to disruption of their microbial symbioses, including susceptibility to opportunistic pathogenesis. For example,

temperature stress can lead to bleaching, a phenomenon where the symbiotic

dinoflagellates (*Symbiodinium* spp.) are either expelled or degraded, leaving the coral

host bereft of its main energy source (Brown, 1997; McClanahan et al., 2009; Tolleter et

al., 2013). Interactions in the coral microbiota may inhibit or exacerbate this bleaching.

For example, *Vibrio spp.* have been shown to cause bleaching in corals that are heat

stressed (Kushmaro et al., 2001; Ben-Haim and Rosenberg, 2002, reviewed in Rosenberg

et al., 2007). Therefore stress can induce changes in the microbiota that lead to additional

stress or disease (Brandt and McManus, 2009).

Although there are over 3 dozen coral diseases described, most have no known

etiological agent (Green and Bruckner, 2000; Sutherland et al., 2004; Rosenberg et al.,

2007; Bourne et al., 2009; Pollack et al., 2011). Some of these diseases may represent

generic responses to stress (Kuntz et al., 2005) that ultimately lead to opportunistic

infection by diverse combinations of copiotrophic bacteria. These opportunistic bacteria

are typically ubiquitous in the environment but replicate in corals under conditions where

the host is stressed or immune compromised, which may be the result of another infection

(Burge et al., 2013). Some examples of these hypothesized opportunistic bacteria include

members of orders *Rhodobacterales, Campylobacterales*, *Clostridiales* and *Vibrionales*

(Frias-Lopez et al., 2002; Cooney et al., 2002; Rosenberg et al., 2007; Sekar et al., 2008;

Sunagawa et al., 2009; Vega Thurber et al., 2009; Mouchka et al., 2010).

Viruses also infect many members of the coral-holobiont including the coral animal

itself (Vega Thurber et al., 2008), the photosynthetic *Symbiodinium* algae (Correa et al.,

2012) and mucus- tissue- or skeleton associated bacteria (Wegley et al., 2007; Vega

Thurber et al., 2008; Marhaver et al., 2008; Littman et al., 2011). Although the diversity

and roles of eukaryotic viruses associated with coral diseases and bleaching have been recently described (e.g., Soffer et al., 2013; Littman et al., 2011), less is known about the roles of bacteriophages. Bacteriophages can influence their bacterial hosts positively and negatively (Rohwer and Vega Thurber, 2009). For example, lytic phages are estimated to cause 10^{28} infections per day (Suttle, 2007). Yet some lysogenic phages prevent infection from other phages and/or add new beneficial genes via horizontal gene transfer, potentially increasing bacteria host fitness as a result (Brussow et al., 2004; Mann et al., 2005; Lindell et al., 2007; Breitbart, 2012).

Previous metagenomics studies have determined that myo-, sipho-, micro- and podo-phages are found in coral mucus/tissue (Wegley et al., 2007; Vega Thurber et al., 2008; Marhaver et al., 2008; Littman et al., 2011). It is likely that interactions among bacteriophage and the coral bacteria and archaea result in alterations of the microbiome (van Oppen et al., 2009) such as controlling coral infection from either bona-fide pathogens or opportunists. For example, the application of host-specific phages to diseased individuals has been shown to prevent *Vibrio* disease in Red Sea *Favia spp.* corals. This form of 'phage therapy' has been suggested to be used for potential control of disease-causing bacteria in natural settings (Efrony et al., 2007; Efrony et al., 2009).

However, unless the target host is amenable to culturing, identifying the phages that associate with target bacteria and can therefore be used for phage therapy will be constrained. Since 35-90% of bacteria from the environment are not cultivable we are limited in our understanding of the interactions between microbiota and their phage predators (Rappe and Giovanoni, 2003; Cook et al., 2013). Furthermore, it has been difficult to predict bacteria-phage interactions as phages have variable host ranges while

bacteria differ in their susceptibility to individual phages or multiple phages (Weitz et al., 2012; Flores et al., 2011). Yet, these complex and underexplored top-down forcings likely influence the overall microbial ecology of corals and coral reefs (Rohwer and Vega Thurber, 2009). Networks of interactions between bacteria-bacteria, bacteria-eukaryotes, phage-encoded bacterial genes, and metabolic networks are increasingly used to describe complex ecosystem interactions, and similar methods can be applied to determine interactions among uncultured phage and bacteria from host samples (Zhou et al., 2010; Steele et al., 2011; Faust et al., 2012; Faust and Raes 2012, Rodriguez-Lanetty et al., 2013: Modi et al., 2013, Chow et al., 2013).

Here we investigate the communities of bacteria, archaea, and bacteriophages associated with *Montastraea annularis* (also referred to as *Orbicella annularis*) corals during a simultaneous outbreak of white plague (WP) disease and coral bleaching in the U.S. Virgin Islands. By assessing microbial and bacteriophage relative abundances across conditions, we sought to gain new insights into the ecological interactions between phage and bacteria. Using a combination of 16S rRNA and shotgun metagenomic analysis, we found that bacterial and phage communities varied among different health states, with bacterial types previously determined to be affiliated with coral disease and other stress conditions (e.g., *Campylobacterales* and *Rhodobacterales*) elevated in diseased corals. We also construct a network using multiple correlation methods with CoNet (Faust et al., 2012) in Cytoscape (Shannon et al., 2003). We found 6 phages interact with the 2 disease-associated bacteria, but no mutualists, therefore making potential candidates for phage therapy. This network analysis allowed us to infer phage-bacterial interactions

from our non-cultured environmental coral samples and highlight their potential roles in coral microbial ecology and phage therapy of coral diseases.

3.2 Experimental Procedures

Sample collections

White plague-like diseases are of particular importance, affecting dozens of reef building species and causing rapid tissue loss (Weil et al., 2006; Miller et al., 2009; Richardson et al., 1998). The etiological agent/s of WP remains controversial, with multiple studies on the bacterial communities of white plague affected corals, finding different shifts in bacterial communities (Pantos et al., 2003; Sunagawa et al., 2009; Cardenas et al., 2012; Roder et al., 2013; Garcia et al., 2013; Cook et al., 2013) and now viral consortia of WP affected corals (Soffer et al 2013).

Coral samples were collected using SCUBA, where two to three cores of tissue attached to skeleton were removed from each *M. annularis* colony (Fig. 3.1) using a 2-cm diameter corer and hammer (USVI Department of Planning and Natural Resources permit #STT-050-10). Colonies showing signs of white plague (which progressed from the base of the colony) were also bleached on the top of the colony. From the 7 WP Diseased colonies, tissues were cored from both the bleached top "Bleached+diseased (BD)" and the margin of lesions "Diseased (D)," which did not show signs of bleaching. Tissue from an additional 6 "Bleached (B)" non-WP Diseased corals and 2 "Healthy (H)" corals (normal pigmentation, non-diseased) were taken as controls (Fig. 3.1). Coral plugs were rinsed with 0.02 μm filtered seawater. For virome libraries, tissue was removed by airbrushing with ~40 ml of 0.02 μm filtered phosphate buffer saline solution (pH 7.3).

Tissue homogenates were 0.22 µm filtered, preserved in molecular biology grade

chloroform (2% final concentration), and stored at 4°C until viral metagenome generation

processing. For bacterial libraries, an intact coral plug was rinsed with 0.02 µm filtered

seawater and preserved in 95% ethanol until extractions.

Bacterial libraries

Most of the tissue sloughed off during ethanol preservation, therefore, 500 µl of

Ethanol/tissue slurry was pipetted for DNA extractions. A modified organic extraction

protocol that excluded the tRNA and phenol steps was used to purify DNA (Rowan and

Powers, 1991). Isolated nucleic acids were amplified using barcoded primers 515F and

806R, which were chosen due to their ability to amplify both Bacteria and Archaea

(Caporaso et al., 2011, Walters et al., 2011). Triplicate amplicon libraries were prepared

using GoTaq Flexi reagents from Promega (Madison WI,USA) using standard protocols

and the following PCR cycle:1 cycle of 3 mins 94°C, 35 cycles of 94°C for 45 seconds,

50 °C for 60 seconds, 72 °C for 90 seconds, and then 1 cycle of 72 °C for 10 minutes.

PCR products were run on a 1.5 agarose gel, triplicates pooled, cleaned using AMPure

magnetic beads from Agencourt (Brea CA,USA) and quantified with a Qubit HS dsDNA

kit (Invitrogen, Eugene OR, USA) into equimolar ratios. Quality of amplicons were

determine on an Agilent Bioanalyzer 2100 before being pyrosequenced on a 454 GS

Junior Roche at the Oregon State University Center for Genome Research and

Biocomputing Core Laboratories (CGRB).

16S rRNA gene analysis

16S rRNA gene sequence libraries were analyzed in QIIME and PRIMER 6 (Caporaso et al., 2010; Clarke and Gorely, 2006). First, reads were de-multiplexed based on their error-correcting barcodes and filtered for quality using default parameters (quality score >= 25, min length = 200, max length = 1000, and no ambiguous bases and mismatches allowed). Next Operational Taxonomic Units (OTUs) were assigned at a 97% similarity threshold UCLUST (Edgar, 2010), and OTU tables constructed from the assignments. Lastly, taxonomic annotations were made to the Ribosomal Database Project (RDP) database using the RDP classifier (Wang et al., 2007). OTUs identified as chloroplasts were removed from the analysis (mean 23% ± 0.2). Amplicon libraries were paired with all virome samples with the exception that there was an additional B sample processed for bacterial analysis.

Viral metagenome generation

Bacteriophages (phages) were isolated from coral tissue and microbes using CsCl density gradients (Vega Thurber et al, 2009; more details in Soffer et al., 2013). DNA was then extracted with an phenol-chloroform extraction protocol (Vega Thurber et al, 2009, Soffer et al., 2013) and amplified using nonspecific multiple displacement amplification (MDA) according to manufacturer's protocol (GenomPhi, GE Healthcare-Pitttsburgh, PA, USA). PCR reactions using 16S and 18S primer sets were performed to determine whether bacterial or eukaryotic DNA contaminated the viromes. No contamination was detected.

The coral phage libraries (21 coral samples), were barcoded and pyrosequenced at EnGencore (University of South Carolina) on a Roche Titanium 454 platform. The final numbers of replicate libraries for each coral health state were: H (n=2), B (n=5), BD (n=7), D (n=7).

Phage library processing and bioinformatic analyses

Sequence reads underwent several preliminary bioinformatic steps. SFF files were converted to FASTA/FASTQ files and de-replicated using the program GALAXY (Geock et al, 2010). Low quality reads (i.e., those < 100 base pairs in length and/or with quality scores < Q20) were removed. Using the CAMERA (Community Cyberinfrastructure for Advanced Microbial Ecology Research and Analysis) (Sun et al, 2010) platform, the tBLASTx algorithm was used to find similarities to sequences in the National Center for Biotechnology Information (NCBI) non-redundant (NR) viral database (Altschul et al, 1990). This annotation level will be referred to as "strain level". Family level taxonomic was manually assigned for the strongest similarity (best tBLASTx e-value $\leq 10^{-5}$) identified to a known viral genome. For this study, only sequences similar to bacteriophage were utilized for network analysis (for eukaryotic viral analysis see Soffer et al., 2013).

Community and consortia statistical analyses

A summary table of relative bacterial abundance (genus level) or bacteriophage relative abundance (strain level) were used to analyze microbial community and viral consortia structure. β-diversity of normalized and log-transformed Bray-Curtis distances were summarized in non-metric multidimensional scaling (MDS) plots (25 iterations). An

Analysis of Similarity (ANOSIM) was used to test for significant differences among overall bacterial or bacteriophage communities (Clarke & Warwick, 2001). Similarity percentage (SIMPER) (Clarke & Warwick, 2001) analysis using Bray-Curtis distances was used to determine which bacteria or phage taxa contributed to dissimilarity. All of these were computed in Primer 6 (Clarke and Gorley, 2006). The phage or bacterial taxa that drove differences between these clusters were identified with SIMPER analyses. Significant differences were subsequently tested using Kruskall-Wallis and a Bonferonni post hoc test (if p≤0.05) in Analyse-It (V2.3).

Construction, visualization and analysis of phage-bacteria interaction networks

Significant correlations between phage strains and bacterial genera were identified using the CoNet Cytoscape plugin (Faust et al., 2012; Shannon et al., 2003). Co-occurrence or mutual exclusion interactions were identified using an ensemble of correlation measures of a recently described bootstrap and renormalization approach to reduce false positive and compositionality biases (Faust et al., 2012). In order to focus on bacteria potentially associated with disease and/or bleaching, bacterial genera of interest for the network analysis were chosen based on whether they were significantly different in any one of the health states; this was determined using ANOVA and a False Discovery Rate (FDR) of 0.2 in QIIME (Benjamini and Hochberg, 1995). For all phage-bacteria pairs, correlation or dissimilarity scores were calculated using Pearson and Spearman correlation, or Bray-Curtis and Kullback-Liebler dissimilarities respectively. Annotated bacteriophage strain level relative abundance and bacterial 16S genus abundance (normalized to column sum) were input as separate matrices for all health states

combined, with a minimum row filter (for zeros) of 3. The ReBoot procedure using 100 permutations was used to control for potential false-positive correlations due to the compositional nature of relative abundance data (Faust et al., 2012). The resulting distribution was run with 1000 bootstraps. Finally, an FDR correction (Benjamin Hochberg, P-value threshold or q≤ 0.05) was applied to the p-value of all correlations based on the number of phage strain/bacterial genus pairs tested to control the false discovery rate for multiple comparisons. In each analysis, the p-value for correlations was combined across multiple correlation measures (Pearson, Spearman , Bray-Curtis, Kullback-Liebler) using Simes' method (Sarker and Chang, 1997), and only correlations supported by at least two correlation methods were included. Variances were pooled.

Inferred interactions between phage and bacteria were visualized as a network in Cytoscape (Shannon et al., 2003). Networks were arranged using the Edge-weighted spring algorithm, which treats each node as connected by springs of varying strength (bacteria and phages with more interactions are closer together). The Cytoscape plugin NetworkAnalyzer (Assenov et al., 2008) was used to compute the following: node degree distribution (power law fit), average shortest path length (character path), and heterogeneity. Degree node distributions were fit to the power law using NetworkAnalyzer to determine whether networks exhibited scale-free properties; networks exhibiting scale-free properties increase in size exponentially with increasing nodes, and nodes are more likely to attach to already existing nodes (Barabasi and Albert, 1999). The correlation value (R^2) was calculated based on logarithmic values. Modularity was not tested, as we did not infer interactions among the phages, or interactions among the bacteria, and modularity is computed by these same-microbe type

interactions (Ravasz et al., 2002). Comparisons among individual health state networks did not yield supported and consistent networks, due to low sample size, and therefore are not presented.

3. 3 Results and Discussion

Corals were dominated by Proteobacteria *and* Bacteriodetes

16S rRNA microbial libraries were constructed from coral tissues sampled during a concurrent white plague (WP) disease outbreak and bleaching event in the US Virgin Islands in 2010. Coral samples were taken from four health states: Healthy (H), Bleached (B), Bleached+Diseased (BD) and white plague Diseased (D) (Fig. 3.1). The BD tissues were sampled from bleached portions of the diseased colony not showing signs of WP, while D tissues were sampled at the leading edge of the disease lesion. In total 68,577 amplicon sequences passed quality filtering across the 22 samples. These sequences were assigned to 417 genera within 175 bacterial or archaeal orders and 38 phyla (Table 3.1) (1,302 sequences or 1.9% total, could not be assigned to any domain). The minimum sequences per sample was 957, the maximum 5,458 and the mean 3,117. Seven of these 175 orders (4.0%) were Archaea. Archaea have previously been found in corals using archaeal specific primers (Kellogg, 2004;Wegley et al., 2004; Beman et al., 2007), but most of the archaea identified here were both low-abundance and low-prevalence; none of the seven archaeal relative mean abundances rose above 0.35% per sample, and Archaea were entirely absent in 42% of the libraries. Archaea thus appear to be a numerically minor constituent of the tissue-associated community, similar to previous studies examining combined bacterial and archaeal communities in corals (Vega Thurber

et al., 2009; Sato et al., 2013). The remaining 167 orders for which taxonomy was assigned were bacterial.

Comparison of the abundance of phyla did not reveal differences across health states (Kruskall-Wallis, p>0.05). The phylum *Proteobacteria* was most common in all the libraries (57 ± 5 % mean relative abundance± SEM), followed by *Bacteriodetes* (23 ± 2% mean relative abundance± SEM). *Proteobacteria* abundances did not significantly differ across health states (Kruskall- Wallis p>0.05), corroborating previous studies on both WP and healthy 16S libraries (Pantos et al., 2003; Kellogg et al., 2012; Cardenas et al., 2012). *Bacteriodetes* were also not significantly different across health states (Kruskall-Wallis p>0.05), but this finding is in contrast with past studies that showed elevations of this taxa in WP and other diseased or stressed corals (Pantos et al., 2003; Barneah et al., 2007;Vega Thurber et al., 2009; Castro et al., 2013).

Bleached and WP diseased tissues harbor distinct microbes

To assess whether there were microbial shifts in WP, as well as bleached and healthy corals, whole bacterial and archaeal communities at the genus level were compared using Bray-Curtis distances, and tested for significance with multivariate statistics. Microbial communities from white plague disease (D) were significantly different than both bleached regions of corals (BD and B) (ANOSIM p ≤0.05; Global R =0.29), yet no communities were significantly different from healthy corals (ANOSIM p>0.05; Global R =0.29) (Fig. 3.2). However, due to the high prevalence of disease and bleaching in the sampled area there were only two healthy samples available for this study. Nevertheless, there are clear differences in the bleached and diseased tissues

overall microbial communities. One interpretation of this shift is that loss of symbionts (bleaching) contributes to alteration of the microbial community (*sensu* Littman et al., 2010) which is one of the major distinctions between tissue composition of D and BD, other than proximity to the disease lesion.

Campylobacterales *and* Rhodobacterales *are elevated in diseased tissues*

To assess which bacteria are associated with WP tissues, we first searched for the original proposed WP pathogen, *Aurantimonas coralicida* (an α-proteobacterium in the order *Rhizobiales*) (Richardson et al., 1998). *Aurantimonas* sequences were only found in one bleached sample (~0.5% relative abundance) but not in any white plague-affected corals (D or BD) in this study. Instead, the orders *Campylobacterales* and *Rhodobacterales* were elevated in D tissues compared to all others (Table 3.2). These orders are associated with corals afflicted with a variety of other diseases and general stressors (Frias-Lopez, et al., 2002; Cooney et al., 2002; Sekar et al., 2008; Sunagawa et al., 20009; Mouchka et al., 2010). When comparing microbial genera rather than orders, a similar pattern was found: significant increases were seen in the relative abundance of the genus *Arcobacter* (order *Campylobacterales*) and an unknown genus in the order *Rhodobacterales* in D tissues (P ≤ 0.05)(Fig. 3.3). *Vibrios* that are typically associated with various diseased and stressed corals (Kushmaro et al., 2001; Ben-Haim and Rosenberg, 2002; Cervino et al., 2004) did not vary significantly across health states, indicating that this genus it is unlikely to have a role in bleaching or white plague disease in this case. Additionally, *Vibrios* were found in low mean abundances (< 0.6%) in all health states.

Although members of the order *Rhodobacterales* are known associates of healthy corals, they are often found at higher relative abundance in various diseased corals, suggesting that it is an opportunistic bacterial group that proliferates during environmental perturbations (Mouchka et al., 2010). For example, *Rhodobacterales* has been previously found to be more abundant in white plague infected *Montastraea faveolata* than healthy specimens (Sunagawa et al., 2009). In addition *Rhodobacterales* have been found to be enriched in black band disease affected *Monstastraea annularis* (Cooney et al., 2002) and *Sidestraea spp*. (Sekar et al., 2008). Sharp et al., 2012 showed that *Rhodobacterales* are associated with corals in early life stages, as soon as 4 days post fertilization, which could indicate that *Rhodobacterales* are bacteria that thrive in the early succession of microorganisms during coral development. In other contexts, stress or disease have been shown to create disturbances that allow early successional ('weedy') microorganisms to flourish (Koenig et al., 2011; Lozupone et al., 2012; Shade et al., 2012). Likewise, stress or disease (e.g. white plague), can also create disturbed microbial communities similar to a transitional/fluctuating stage that may lead *Rhodobacterales* to opportunistically infect the coral.

Sharp et al., 2012 also detected *Campylobacterales* (the other bacterial order enriched in our disease libraries), in larvae. In Vega Thurber et al. 2009, *Epsilon-proteobacteria*, (the class that includes *Campylobacterales*) increased after stress treatment. Similarities specifically to the genus *Arcobacter* was found in higher relative abundance in our diseased libraries, and it has been shown to be a pathogen in human and animals (Ho et al., 2006; Collado and Figueras 2011). But some *Campylobacter* are non-pathogenic strains, and fix nitrogen which may be beneficial to stressed corals (McClung et al.,

1983). Interestingly, *Campylobacter* has been found on newly exposed skeleton resulting from black band disease lesions (Frias-Lopez et al., 2002). This may also explain why this group was found to be significantly enriched in D tissues (which are adjacent to exposed skeleton where tissue is lost), but not in BD tissue (where coral tissue is intact but *Symbiodinium* have been expelled).

Kiloniellales *are lost in diseased tissues*

Another shift in bacterial communities detected in WP was the loss of an unknown genus in the order *Kiloniellales,* which is a newly described bacterial order in the *alpha-proteobacteria* (to which the *Rhodobacterales* also belong) previously isolated from macroalgae and the surface mucus layer of coral larvae (Wiese et al., 2009; Sharp et al., 2012; Cleary et al., 2013). Interestingly, this was the only genera found to be significantly more abundant in healthy tissues compared to D (Kruskall-Wallis p<0.05) (Fig. 3.3). This may indicate that these microorganisms are members of the healthy tissue community that are lost during disease, although their contribution to host fitness (if any) is currently unknown. Future studies on the presence of *Kiloniellales* in corals and a description of its metabolic functions would further help determine the role of this bacterial group in coral health.

Bleached corals harbor low abundance taxa similar to known thermally tolerant bacteria

Multiple bacterial genera were significantly more relatively abundant in B corals than all of the other health states (Kruskal-Wallis, p≤0.05), including two thermally tolerant genera: *Caldicellulosiruptor* (order *Thermoanaerobacterales)* and *Thermus* (order *Thermales*) (Fig. 3.3). Another taxa similar to a thermally tolerant genus,

Thermoanaerobacterium (order *Clostridiales*), was found to be more relatively abundant

(p≤0.05) in B tissues relative to D tissues (Fig. 3.3)*.* In contrast, a genus from each order

Actinomycetales and *Bacillales* were found in higher relative abundance in bleached

corals than the other health states. However, some of these bacteria were not in higher

relative abundance in the BD tissues, so it is possible other factors are involved than

bleaching alone. Although these bacterial types were found to be significantly more

relative abundant (p≤0.05), they are still at low percentages (<2%) of the microbiome,

and their effects (if any) on coral bleaching remains to be determined.

Bacteriophage consortia differ between disease and bleached corals

To evaluate the differences in coral phage consortia among health states, we

generated viral shotgun metagenomic libraries using standard methods (Vega Thurber et

al., 2009), and annotated them using tBLASTx (E-val $\leq 10^{-5}$) to a curated viral database as

previously described (Soffer et al., 2013). Of 944,509 total metagenomic reads, there

were a total of 70,927 distinct high-quality sequences similar to viruses, of which 52,598

(74%) were similar to bacteriophages. Multivariate analysis of the overall consortia of

phage strains did detect differences among the health states. The results were similar to

the pattern of bacterial communities: D consortia clustered separately from both bleached

samples (B and BD) (P≤05: Global R=0.233), but none were significantly different from

healthy corals (P>0.05: Global R=0.233) (Fig. 3.4). The phage consortia consisted of 519

total strains, falling into 5 phage families: *Inoviridae, Myoviridae, Microviridae,*

Podoviridae and *Siphoviridae*. *Myo-, Podo-, and Sipho- viridae* are dsDNA phages in

order *Caudovirales*, while *Inoviridae* and *Microviridae* are ssDNA phages not currently

assigned an order. Furthermore, to understand the roles that phage may play in white plague and/or bleaching, we tested whether phage families exhibited general differences across health states. BD tissues had significantly lower *Inoviridae* abundances than H or D tissues (Kruskall-Wallis, p>0.05). Unclassified phages were decreased in H compared to B, but not others (Kruskall-Wallis, p>0.05). However, phage in families *Microviridae, Myoviridae, Podoviridae* and *Siphoviridae* did not vary across health states (Kruskall-Wallis, p >0.05)   (Fig. 3.5). These findings contrast with a previous study of phage consortia in healthy tissues from a different coral species, *Porites astreoides*. There, *Inoviridae* was the least abundant phage family (Wegley et al., 2007). Aside from *Inoviridae*, other phage families followed similar patterns to those previously reported were *Microviridae* were most abundant, followed by members of the *Caudovirales* (Wegley et al., 2007; Littman et al., 2011).

Phage- bacteria networks reveal hubs of interaction

In order to predict interactions (either co-occurrence or mutual- exclusion) among bacteria and phages, we constructed a network of correlations between the abundance of bacterial genera and phage strains from all health states (Fig. 3.6). Similar methods have been successfully applied to study bacteria-bacteria (Faust and Raes 2012; Rodriguez-Lanetty et al., 2013), bacteria-eukaryote (Steele et al., 2011) and metabolic networks in sequence data, (Zhou et al., 2010; Reviewed in Faust et al., 2012). Because we were specifically interested in phage control of disease-associated bacterial types, only the 11 bacterial genera that differed among health states (ANOVA and FDR (q=0.2) in QIIME) were compared against all 519 detected phage strains.

In the resulting network of significant phage-bacteria interactions, each node is either a bacterial genus (Fig. 3.6, square symbols) or phage strain (diamond symbols), and edges indicate significant co-occurrence (green) or mutual-exclusion (red) interactions. The network included 151 nodes and 332 edges (representing 205 co-occurrence and 125 mutual exclusion interactions). Co-occurrence relationships between phage and bacterial abundances reflect several likely interactions: (i) the increase of bacterial host abundance directly allows growth of phage populations, (ii) the increased phage populations remove a major competitor of the co-occurring bacterial population, and (iii) the increased phage populations directly infect and benefit the co-occurring bacterium (e.g. by facilitating gene transfer). By contrast, mutual-exclusion relationships might reflect: (i) lytic phages directly reducing bacterial populations or (ii) bacteria competing with the excluded phage's host, lowering phage populations.

In addition to paired interactions, some network properties describe the overall interaction structure. The node degree distribution of the resulting phage-bacteria network approximately fit a power law (R^2=0.83) and therefore had properties of a scale-free network, (i.e. non-random network) (Barabasi and Albert, 1999) (Fig. 3.7). True scale-free networks are characterized by short paths separating nodes. Biologically, these short average path lengths have been interpreted as causing scale-free networks to respond rapidly to perturbation (Faust and Raes, 2012). We calculated the average shortest path lengths (AL) for the network and compared them against other biological interaction networks. The resulting AL for this network was 3.10, indicating that roughly three edges separate average nodes. This value was similar to those in networks of marine microbial (bacteria and archaea-3.05; bacteria, protist and virus-3.00) interactions, which

are considered to have small AL (Steele et al., 2011; Faust and Roen, 2012, Chow et al., 2013).

The small scale and scale-free properties of this network suggests that bacterial types that are prone to phage interactions (such as *Thermus* that had a total 59 phage interactions- Table 3.3), are likely to interact with new phages added to the network, or that it is a generalist bacteria. Along those lines, the heterogeneity value in networks describes the possibility of hubs. The heterogeneity value of this network was 1.799, almost double the value determined for a network of T4 virus-bacteria interactions from surface seawater (0.953) (Chow et al., 2013). Hubs are thought to describe keystone species that, if removed, would lead to large changes in the community (Steele et al., 2011). A possible keystone might be the phage similar to Geobacillus-phage-GBSV1. This phage was predicted to interact with 8 bacterial genera, the maximal number of interactions (all co-occurrence) that was determined for any single phage (Table 3.4) in this network. It is plausible that targeted removal of this phage would thus lead to greater changes in the bacterial community than the removal of the phage similar to Vibrio-phage-KV40, for example, which only interacts with one bacterial genus (Table 3.4, Fig. 3.8)

Theoretical use of networks to predict candidates for phage therapy

Phage therapy has been shown to be effective against *Vibrio* infections of corals (Efrony et al., 2007; Efrony et al., 2009). Although it may be impractical to add phages to reefs to prevent or mitigate infections, these therapies may be useful in a coral nursery setting. Phage-bacterial networks can be used to predict which phages may be useful

against pathogenic bacteria, while also preventing loss of beneficial mutualist bacteria. Although phage have traditionally been thought to have highly restricted host ranges, some phages were recently shown to infect multiple bacteria (Holmfeldt et al., 2007; Flores et al., 2011; Weitz et al., 2012; Flores et al., 2013). Conversely, bacteria are commonly susceptible to multiple phage strains (Flores et al., 2013). Network analysis can be used to navigate these complex interactions, for example by detecting phages that are predicted to only affect bacteria of interest. For example, *Rhodobacterales* and *Campylobacterales*, the two bacterial orders associated with white plague in this study, had 6 phages that were not only shared in common, but had the same interaction type, thus, they would make potential candidates for phage therapy (Fig. 3.9, Fig. 3.6).

In the case of the disease coral-associated *Rhodobacterales* and the healthy coral-associated *Kiloniellales*, it is interesting that 7 phages were shared between them (Fig.3.10, Fig. 3.6). However, 6 of the 7 phages that were interacting with both bacteria had different interaction types. Therefore it is possible that the presence of phages is either preventing the proliferation of one of those bacterial types in a healthy coral state (i.e. controlling *Rhodobacterales* populations), or the absence of phages is allowing uninhibited growth of these bacteria in a disease state (i.e. no control of *Rhodobacterales* populations). Interestingly, Barr et al., 2013 demonstrated that coral mucus contains receptors for bacteriophages, positing that mucus may retain beneficial phages. Perhaps a disease state interrupts the production of these receptors or alters the mucus such that the phages are not attaching, leading to disproportionate growth of detrimental bacterial types. The addition of beneficial phages can therefore reduce disease associated bacteria in cases where the natural defense mechanisms fail.

Further considerations

This phage-bacterial network was constructed by combining sequence data from bacterial and phage metagenomes. However, there are outstanding issues with the construction and interpretation of these networks. For example, our attempts to compare robust networks constructed from each one of the 4 different health states failed due to small sample sizes resulting in no significant interactions using our conservative methods. Analysis of alterations in general features of phage-bacteria interaction network topology between health states would be an informative topic for future studies, but will likely require many more biological replicates. Although we relaxed the statistical conditions (such as increasing the p-value), only networks constructed without the ReBoot method would form (i.e. q>0.05 FDR), and thus were not well supported.

One consideration in this network analysis is that many environmental phages are quite divergent from characterized phages (Rohwer and Edwards, 2002; Rohwer, 2003; Tucker et al., 2010). Therefore, we did not entirely rely on annotated names for interpreting which specific phages are interacting with bacteria, and phage names such as "Clostridium-phage-phiSM101" are provided for information, but do not indicate that a particular environmental phage necessarily infects that host to the exclusion of others. However, one advantage of using these networks is that these difficulties with phage taxonomy assignment are largely sidestepped: inferences are drawn from correlations in the sequence data, rather than taxonomy. On the other hand, we did find some biologically relevant interactions. For example a phage with similarities to Clostridium-phage-phiSM101 was found interacting with the *Clostridium* bacteria.

This same phage was interacting with *Bacillus*, another *Firmicutes* which shares many characteristics with *Clostridium*, such as endospore formation (Onyenwoke et al., 2004). Therefore this phage interaction can either be a direct interaction (and is phylum or lifestyle specific), or that *Bacillus* and *Clostridium* are interacting, and thus the phage is indirectly interacting with the bacteria.

To address the issue of direct/indirect interactions, we attempted to create bacteria-bacteria networks to extrapolate whether phage interactions were indirect or direct. However, no interactions were found significant for just the 11 bacterial genera of interest, all bacterial genera, and the combination of those two across all samples using the same conservative methods as the phage-bacteria network, or even with relaxing the FDR correction up to 0.2. This suggests that the predicted phage-bacteria interactions are likely direct (given lack of interactions among bacteria), or that sample sizes were too small without the phage data.

Despite these issues, networks are still a valuable and useful tool to answer questions about phage-bacteria interactions that currently cannot be answered in any other way with limited corals for sampling, and lack of cultured coral bacteria/phages.

Conclusions

The aims of this study were twofold, first to describe the bacterial and bacteriophage consortia across different coral health states, and secondly to infer interactions among the phage-bacteria. This study determined that both bleached coral tissues vs. diseased tissues had distinct microbial communities. Diseased tissues harbored an increased relative abundance of the genus *Arcobacter* in the order *Campylobacterales*

and an unknown genus in the order *Rhodobacteriales* compared to the other health states. Diseased corals also showed decreases in the abundance of one unknown genus in the order *Kiloniellales*. The bacteriophage consortia at the strain level demonstrated similar clustering patterns as the bacterial (genus level) communities. In addition, phages with similarities to *Inoviridae* were elevated in healthy and diseased tissues compared to bleached. Lastly, using phage-bacteriophage interaction networks, we were able to predict which phages were interacting with the bacteria genera shown to vary across health states, and therefore potentially controlling their abundances. Ultimately, this study has taken a multifaceted approach to describe and explain bacterial community changes post stressors in corals, by looking at phages and bacterial communities concurrently. Finally, this study also highlights the potential for phage-bacterial networks to aide in selection of therapeutic phages that target opportunistic pathogens without negatively influencing beneficial bacteria through interactions.

3.5 Acknowledgments
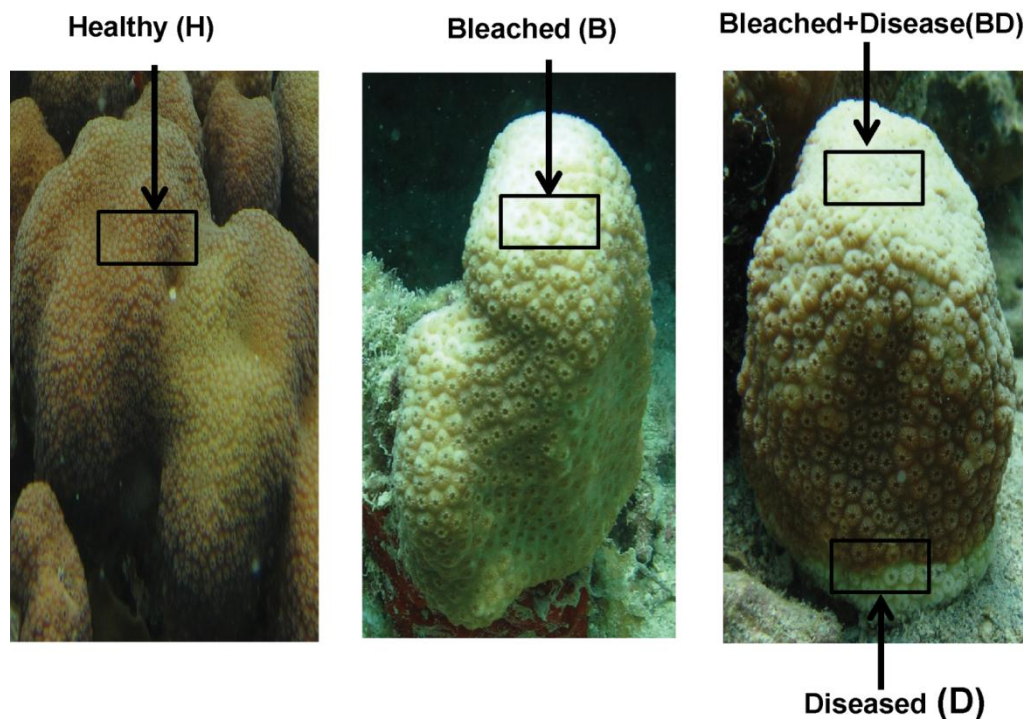
Figures

Figure 3.1 Coral health states sampled for bacteriophage and microbe metagenomes. Black boxes indicate sampling scheme. B samples were taken from the bleached portion of bleached coral colonies with no visible signs of white plague. BD samples are taken from corals affected by both bleaching and white plague disease, and were taken from bleached tissues not in contact with the leading edge of white plague tissue loss. H samples were taken from corals showing no signs of either bleaching or white plague. D tissues were sampled from the leading edge of white plague tissue loss, and included only live tissue with no signs of paling or bleaching.
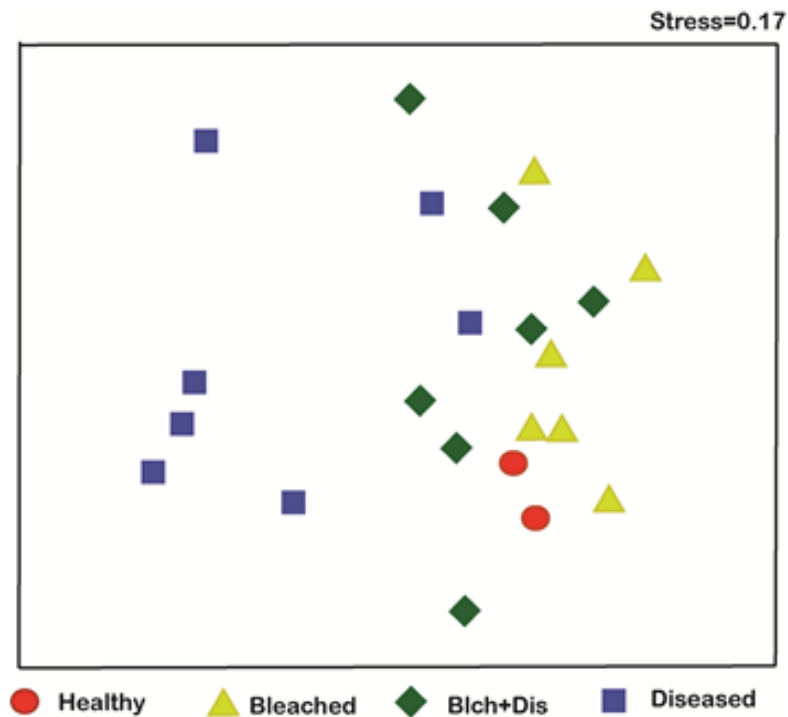
Figure 3.2 Non-metric Multidimensional scaling (MDS) plot of microbe communities from different health states at the genus taxonomic level. A log-transformed Bray Curtis resemblance matrix was used to construct the 2D MDS. Microbial communities from D tissues significantly differed from communities in B and BD tissues (ANOSIM P<0.05). No tissue type clustered significantly separately from H (ANOSIM P<0.05). Stress value is based on 2D MDS.
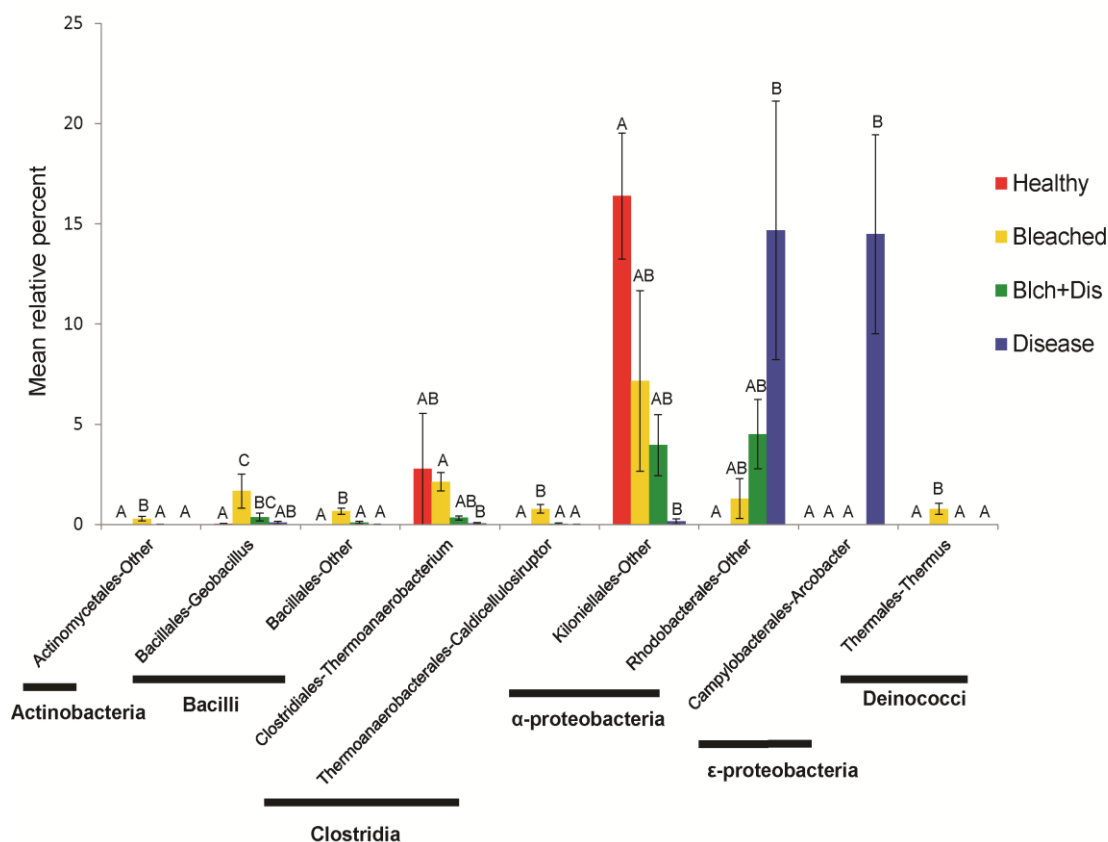
Figure 3.3 Relative abundance of bacteria across health states. Relative abundance for bacterial genera found to significantly vary across health states (Kruskall-Wallis, p ≤0.05) is plotted on the y-axis. The x-axis labels each order and genus (separated by a dash). Horizontal bars and bold labels group genera in the same phylum Bar colors represent the health states: H (red); B (yellow); BD (green); D (blue). Letters indicate significance groups: bars that share at least one letter were not significantly different from one another and bars without shared letters were significantly different (Kruskall-Wallis, p≤0.05). Error bars represent standard error. Relative abundance values for genera that differed across health states are reported as a portion of the whole microbial community (and therefore do not add up to 100%).
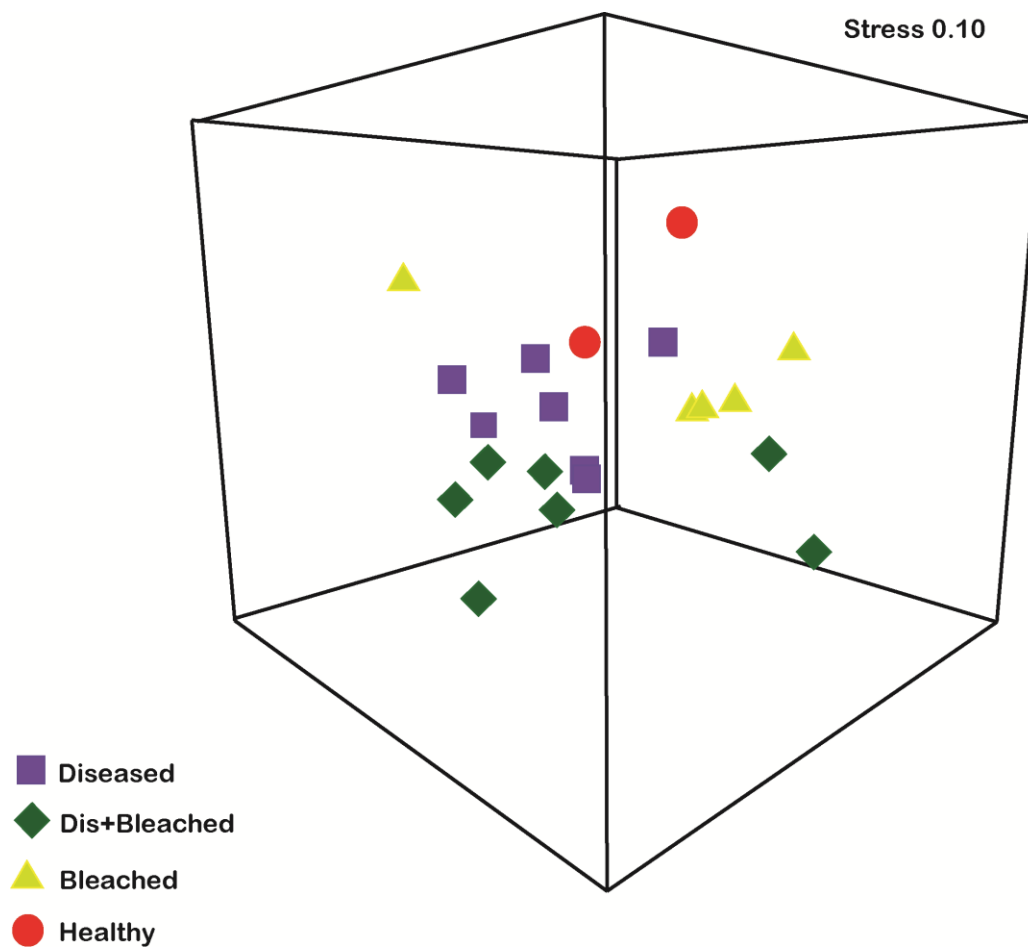
Figure 3.4 Non-metric Multidimensional scaling (MDS) plot of bacteriophage consortia from different health states at the strain level. Log transformed Bray Curtis similarity resemblance matrix was used to construct the MDS. A 3D MDS was selected to visualize clusters more accurately. Bacteriophage consortia showed similar overall clustering patterns to bacterial genera (Fig 3.2., above): D tissues cluster significantly different from B and BD (ANOSIM p≤0.05), but no tissue type clustered significantly separately from H (ANOSIM p≤0.05). Reported stress value is based on 3D MDS.
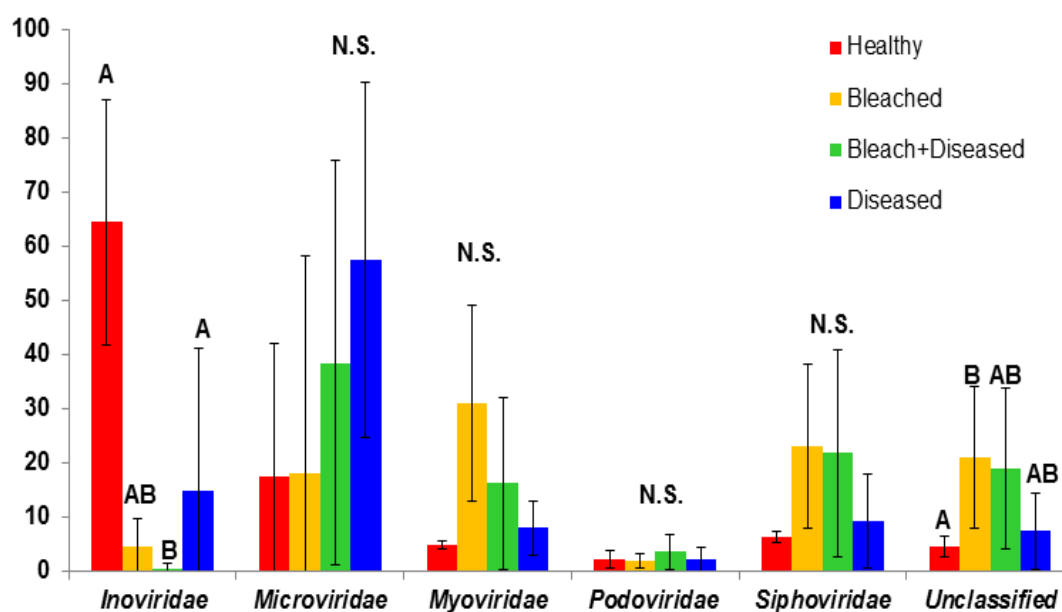
Figure 3.5 Mean relative percent of bacteriophage families (and unclassified). Letters denote significantly different relative percent abundances out of 100% (Kruskall-Wallis, $p \leq 0.05$). N.S are not significantly different. Error bars are standard error. Colors of the bars indicate: Healthy (red); Bleached (yellow); Bleach+Diseased (green); Diseased (blue).
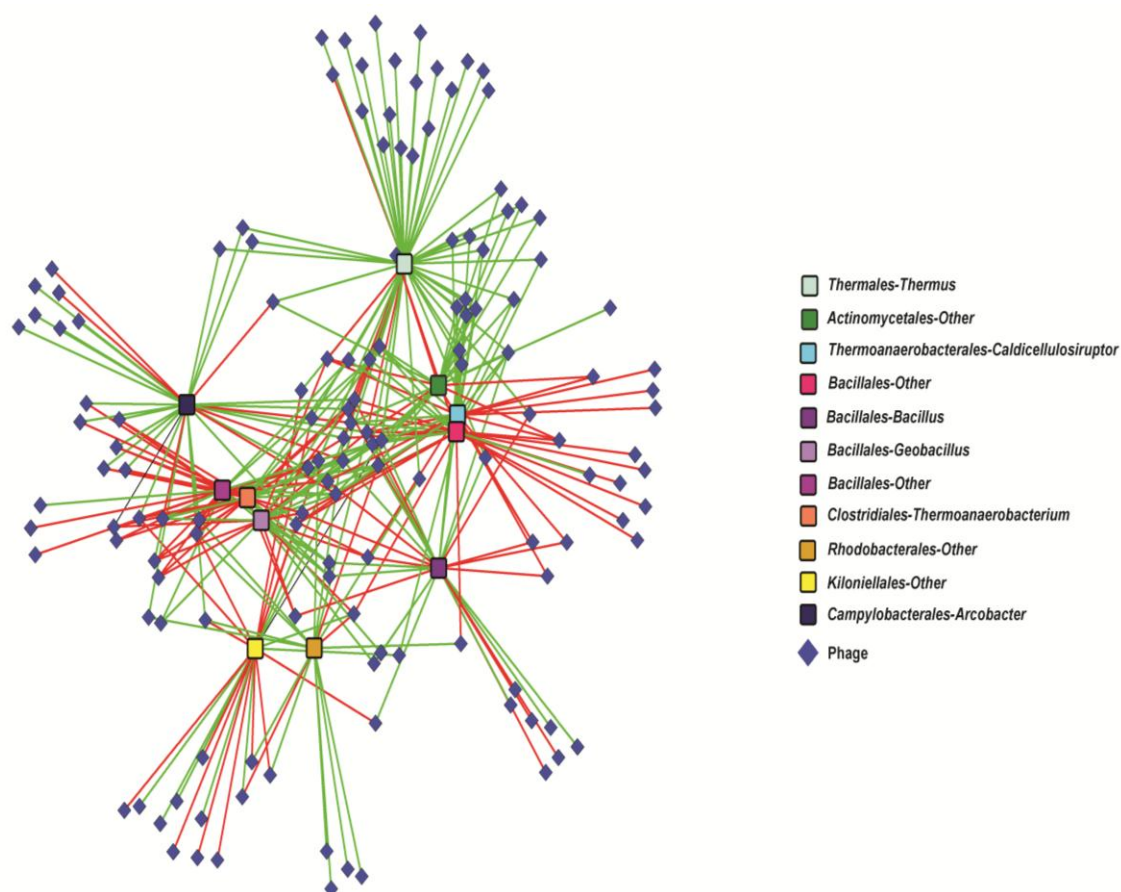
Figure 3.6 Predicted phage-bacteria interaction network. The network was calculated for the 11 bacterial genera contributing to health state community dissimilarity. Squares: bacteria; Diamonds: phage. Bacterial labels are order and genus (separated by a dash). Red lines connecting phage-bacteria pairs indicate significant mutual exclusion patterns, while green lines denote significant co-occurrence patterns ($p \leq 0.05$) as determined by the ReBoot randomization procedure in the CoNet Cytoscape package (Faust et al., 2012). Network layout was calculated using edge-weighted spring embedded layout in Cytoscape (Shannon et al., 2003)
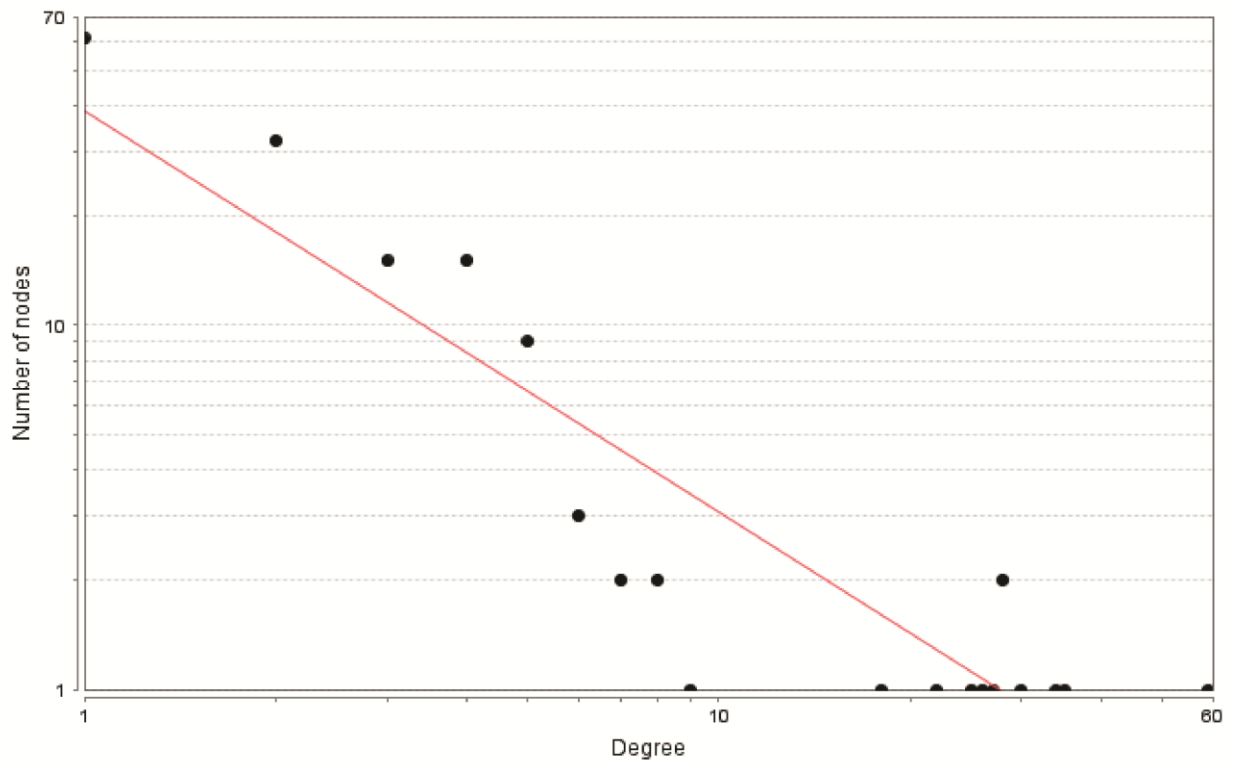
Figure 3.7 Node degree distribution fitted line based on Power law. A Fitted line is based on logarithmic scale and was calculated the NetworkAnalyzer plugin in the format of y= ax^b, where a= 38.526, and b= -1.098.
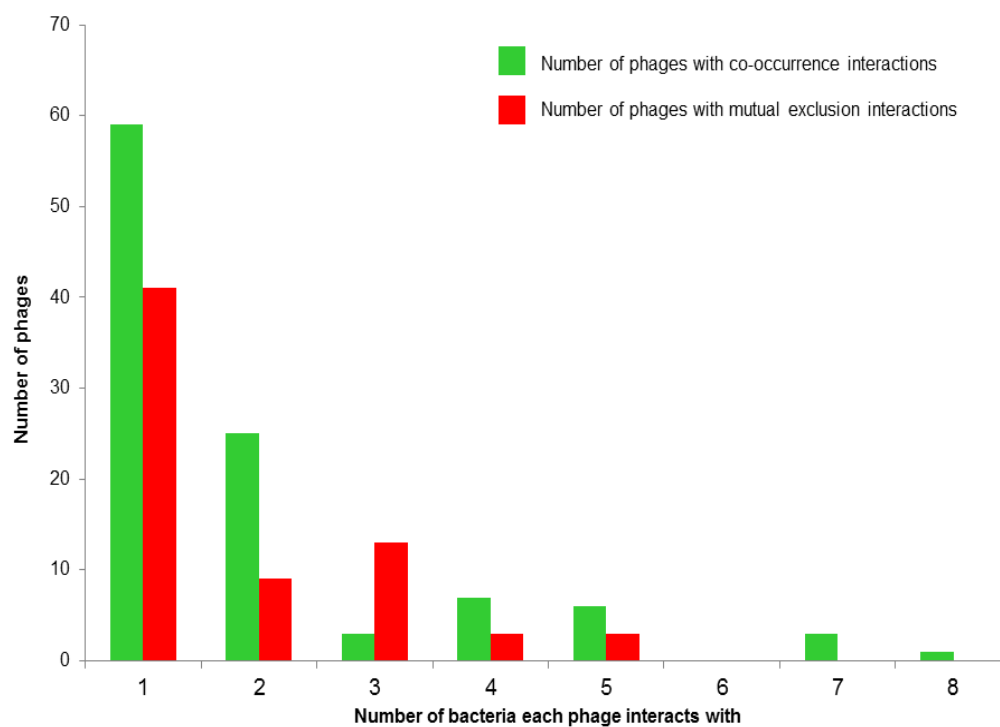
Figure 3.8. Phage specificity based on predicted network. Each bar represents the number of bacterial hosts that a phage was predicted to interact with. Most phages only interacted with one bacterial host.
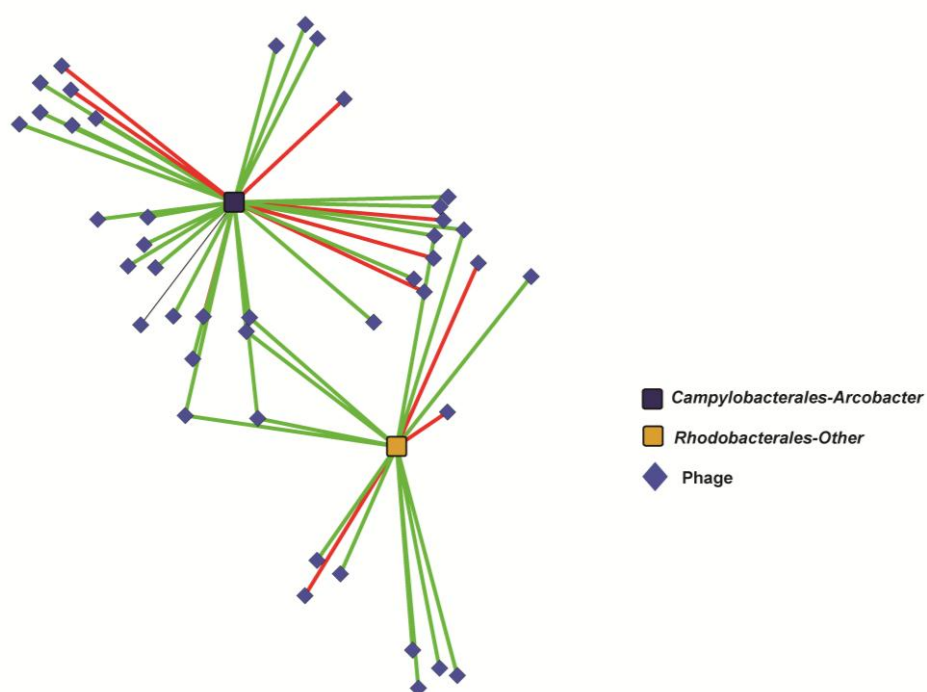
Figure 3.9 Phage bacteria interactions of two bacteria associated with D tissues. Edges and nodes isolated from original network (Fig 3.6).Green lines represent co-occurrence interactions, while red lines represent mutual exclusion interactions.
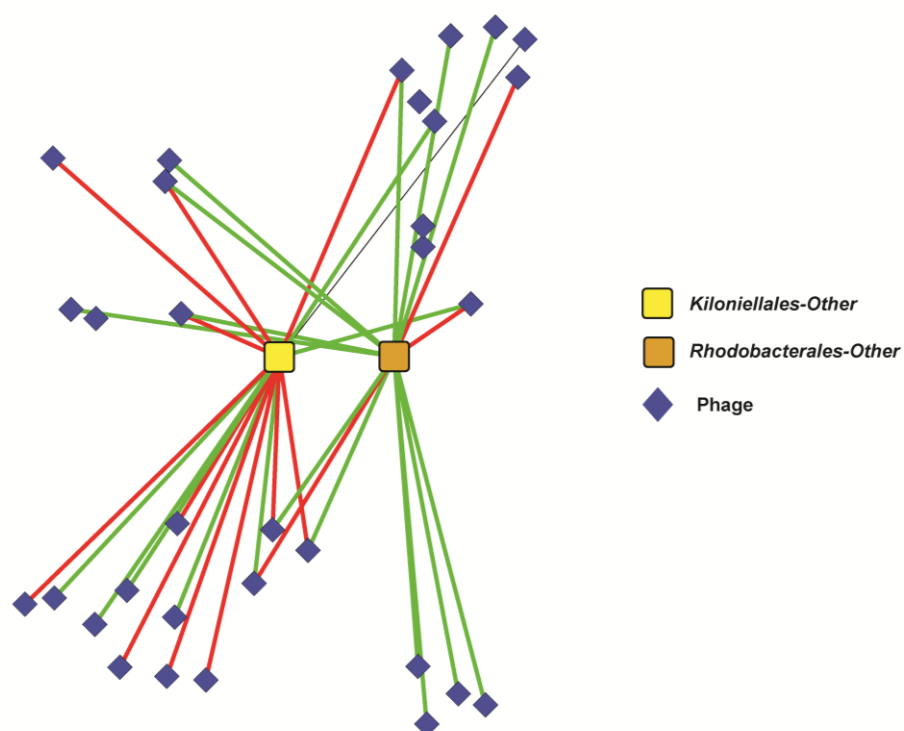
Figure 3.10 Phage-bacteria interactions of *Kiloniellales* and *Rhodobacterales* only. Edges and nodes isolated from original network (Fig 3.6). Green lines represent co-occurrence interactions, while red lines represent mutual exclusion interactions.

Tables

Table 3.1 Phylum relative percent abundance and standard error for each health state. Phyla were assigned in QIIME with UCLUST (97% identity).

Phylum	Healthy	Bleached	Bleached+ Diseased	Diseased
Acidobacteria	0.67±0.67	0.24±0.15	0.31±0.16	0.22±0.21
Actinobacteria	1.06±1.06	1.91±0.43	0.97±0.22	0.19±0.11
AncK6	0±0	0±0	0.02±0.02	0±0
Archaea-Other	0±0	0±0	0±0	0.03±0.03
Bacteria-Other	2±0.18	0.85±0.27	4.67±2.3	4.57±1.32
Bacteroidetes	33.61±22.26	31.38±8.6	24.24±5.4	13.04±5.24
BRC1	0±0	0±0	0±0	0.01±0.01
Chlamydiae	0.08±0.08	0±0	0.05±0.03	0.04±0.02
Chlorobi	0±0	0±0	0.03±0.02	0.46±0.36
Chloroflexi	2.07±2.07	0.24±0.19	0.31±0.28	0.11±0.1
Crenarchaeota	0±0	0±0	0.05±0.05	0±0
Cyanobacteria	1.05±0.97	0.13±0.13	1.11±0.32	0.67±0.35
Deferribacteres	0±0	0±0	0±0	0.61±0.6
Elusimicrobia	0±0	0±0	0±0	0.04±0.04
Euryarchaeota	0±0	0.01±0.01	0.02±0.02	0.05±0.03
Fibrobacteres	0±0	0±0	0±0	0.01±0.01
Firmicutes	5.8±5.8	11.95±10.94	7.92±5.08	2.94±1.26
Fusobacteria	0±0	0.05±0.05	0.01±0.01	0±0
Gemmatimonadetes	0.7±0.7	0.48±0.31	0.21±0.18	0.03±0.02
GN02	0±0	0±0	0±0	0.18±0.06
H-178	0±0	0±0	0±0	0±0
Lentisphaerae	0±0	0±0	0.01±0.01	0.07±0.04
Nitrospirae	0.34±0.34	0±0	0.14±0.12	0±0

OD1	0±0	0±0	0.03±0.03	0±0
OP8	0±0	0±0	0±0	0.23±0.22
PAUC34f	1.37±1.37	0±0	0.1±0.1	0±0
Planctomycetes	0±0	0.15±0.15	1.01±0.6	0.88±0.7
Poribacteria	0±0	0±0	0.02±0.02	0±0
Proteobacteria	50.97±9.13	50.16±9.07	53.68±10.11	73.31±7.27
SAR406	0±0	0±0	0±0	0.23±0.14
SBR1093	0±0	0±0	0.06±0.06	0±0
Spirochaetes	0±0	1.65±0.64	4.87±2.35	1.85±1.2
SR1	0±0	0±0	0±0	0.01±0.01
Thermi	0.04±0.04	0.75±0.26	0.06±0.06	0±0
Thermotogae	0±0	0±0	0±0	0.01±0.01
TM6	0±0	0±0	0±0	0.01±0.01
Unclassified-Other	0.23±0.08	0.06±0.02	0.01±0.01	0.14±0.07
Verrucomicrobia	0±0	0±0	0.05±0.03	0.02±0.02
WS3	0±0	0±0	0.04±0.03	0.03±0.02

Table 3.2 Significantly different bacterial orders. Significance based on Kruskal-Wallis (with Bonferonni *posthoc* pairwise tests).

Bacteria Order	Significant Pairwise Differences	Kruskal-Wallis Statistic	P-value
Campylobacterales	H-D; B-D; BD-D	18.57	P <0.0001
Kiloniellales	H-D; B-D; BD-D	8.57	P<0.04
Rhodobacterales	H-D; BD-D	10.45	P<0.02

Table 3.3 Number of phages interacting with each bacteria. Single partner interactions denote how many phages are exclusively interacting with that particular bacterium.

Bacteria Phylum;class;order;family;genus	co- presence	Mutual exclusion	Total phage interactions	Single partner interactions
Actinobacteria;c--Actinobacteria;o--Actinomycetales;f--Promicromonosporaceae;Other	20	6	26	1
Firmicutes;c--Bacilli;o--Bacillales;f--Bacillaceae;g--Bacillus	17	13	30	11
Firmicutes;c--Bacilli;o--Bacillales;f--Bacillaceae;g--Geobacillus	11	11	22	0
Firmicutes;c--Bacilli;o--Bacillales;f--Bacillaceae;Other	12	16	28	7
Firmicutes;c--Bacilli;o--Bacillales;f--Sporolactobacillaceae;Other	19	16	35	14
Firmicutes;c--Clostridia;o--Clostridiales;f--Clostridiaceae;g--Thermoanaerobacterium	10	18	28	1
Firmicutes;c--Clostridia;o--Thermoanaerobacterales;f--Caldicellulosiruptoraceae;g--Caldicellulosiruptor	14	13	27	6
Proteobacteria;c--Alphaproteobacteria;o--Kiloniellales;f--;g--	9	15	24	19
Proteobacteria;c--Alphaproteobacteria;o--Rhodobacterales;f--Rhodobacteraceae;Other	15	3	18	6
Proteobacteria;c--Epsilonproteobacteria;o--Campylobacterales;f--Campylobacteraceae;g--Arcobacter	26	7	33	15
Thermi;c--Deinococci;o--Thermales;f--Thermaceae;g--Thermus	52	7	59	20

Table 3.4 Number of bacteria that each phage interacts with. Interactions are supported by at least 2 correlation metrics (Pearson, Spearman, Bray-Curtis or Kullback-Liebler) and P<0.05. Phage annotations best on tBLASTx best hit (e-value $\leq 10^{-5}$).

Phage	Co-occurence interactions	Mutual interactions	Total interactions
Acinetobacter-phage-Ac42	2	3	5
Aeromonas-phage-31	1	0	1
Aggregatibacter-phage-S1249	2	0	2
Azospirillum-phage-Cd	1	0	1
Bacillus-phage-250	1	0	1
Bacillus-phage-BCJA1c	4	0	4
Bacillus-phage-Bcp1	0	4	4
Bacillus-phage-G	4	0	4
Bacillus-phage-Gamma	1	0	1
Bacillus-phage-phBC6A51	0	1	1
Bacillus-phage-phBC6A52	2	0	2
Bacillus-phage-phi105	0	1	1
Bacillus-phage-phiNIT1	1	1	2
Bacillus-phage-SPbeta	0	1	1
Bacillus-thuringiensis-phage-MZTP02	0	1	1
Bdellovibrio-phage-phiMH2K	2	5	7
Burkholderia-phage-Bcep176	1	0	1
Burkholderia-phage-Bcep22	2	0	2
Burkholderia-phage-BcepGomr	5	1	6
Burkholderia-phage-BcepIL02	1	0	1
Burkholderia-phage-Bups-phi1	1	0	1
Burkholderia-phage-KS10	2	3	5
Burkholderia-phage-phi644-2	1	1	2
Burkholderia-phage-phiE12-2	1	0	1
Burkholderia-phage-phiE125	5	0	5
Caulobacter-phage-CcrRogue	4	0	4
Chlamydia-phage-3	2	3	5
Chlamydia-phage-4	0	1	1
Chlamydia-phage-Chp1	0	4	4
Chlamydia-phage-Chp2	0	3	3
Chlamydia-phage-CPAR39	1	5	6
Chlamydia-phage-phiCPG1	1	4	5
Clostridium-phage-c-st	1	0	1
Clostridium-phage-phi3626	5	0	5
Clostridium-phage-phiC2	0	2	2
Clostridium-phage-phi-CD119	1	0	1

Clostridium-phage-phiCD6356	1	1	2
Clostridium-phage-phiSM101	0	2	2
Cyanophage-8109-2a	1	2	3
Cyanophage-MED4-213	1	1	2
Deep-sea-thermophilic-phage-D6E	1	3	4
Edwardsiella-phage-eiAU	2	0	2
Edwardsiella-phage-eiDWF	1	0	1
Enterobacteria-phage-BP-4795	1	0	1
Enterobacteria-phage-f1	0	3	3
Enterobacteria-phage-HK97	1	0	1
Enterobacteria-phage-Mu	1	2	3
Enterobacteria-phage-P1	1	0	1
Enterobacteria-phage-phiP27	0	0	0
Enterobacteria-phage-phiX174	1	3	4
Enterobacteria-phage-SfV	0	5	5
Enterobacteria-phage-T1	2	0	2
Enterobacteria-phage-VT1-Sakai	0	1	1
Enterococcus-phage-phiFL3A	0	1	1
Environmental-halophage-1-AAJ-2005	1	0	1
Erwinia-phage-phiEt88	0	1	1
Geobacillus-phage-GBSV1	8	0	8
Klebsiella-phage-phiKO2	2	0	2
Lactobacillus-phage-LF1	1	1	2
Lactobacillus-phage-phiAT3	2	0	2
Lactobacillus-phage-phiFSW	0	2	2
Lactobacillus-prophage-Lj965	2	0	2
Lactococcus-phage-bIL312	1	0	1
Lactococcus-phage-P087	1	0	1
Listeria-phage-A511	1	0	1
Listeria-phage-P100	2	0	2
Listeria-phage-P40	3	0	3
Loktanella-phage-pCB2051-A	0	2	2
Microbacterium-phage-Min1	1	0	1
Microvirus-CA82	0	3	3
Mycobacterium-phage-Cooper	1	0	1
Mycobacterium-phage-D29	2	0	2
Mycobacterium-phage-Giles	4	0	4
Mycobacterium-phage-Myrna	1	0	1
Mycobacterium-phage-Omega	1	3	4
Mycobacterium-phage-Rizal	2	0	2
Mycoplasma-phage-phiMFV1	1	0	1
Oenococcus-phage-fOg30	0	1	1
Paenibacillus-phage-phiBP	1	0	1

Phage-TP	0	1	1
Prochlorococcus-phage-P-HM1	2	0	2
Prochlorococcus-phage-P-HM2	2	1	3
Prochlorococcus-phage-P-SSM2	2	0	2
Prochlorococcus-phage-Syn1	1	2	3
Prochlorococcus-phage-Syn33	0	1	1
Prochlorococcus-phage-Syn33	1	1	2
Pseudoalteromonas-phage-H105-1	1	0	1
Pseudomonas-phage-201phi2-1	5	1	6
Pseudomonas-phage-D3112	5	0	5
Pseudomonas-phage-DVM-2008	0	1	1
Pseudomonas-phage-EL	4	0	4
Pseudomonas-phage-MP38	1	0	1
Pseudomonas-phage-PA1-KOR-2010	1	0	1
Pseudomonas-phage-PaP3	0	2	2
Pseudomonas-phage-Pf3	4	0	4
Pseudomonas-phage-phiCTX	1	0	1
Pseudomonas-phage-PhiPA3	1	0	1
Ralstonia-phage-p12J	0	1	1
Ralstonia-phage-PE226	0	1	1
Ralstonia-phage-RSL1	2	0	2
Ralstonia-phage-RSM3	0	3	3
Rhodococcus-phage-ReqiDocB7	1	0	1
Rhodococcus-phage-ReqiPine5	0	1	1
Rhodovulum-phage-RS1	0	3	3
Roseovarius-sp.-217-phage-1	1	1	2
Shigella-phage-Sf6	0	1	1
Silicibacter-phage-DSS3phi2	0	1	1
Sinorhizobium-phage-PBC5	1	1	2
Sodalis-phage-SO-1	2	0	2
Spiroplasma-phage-4	2	1	3
Staphylococcus-phage-phi-12	1	1	2
Staphylococcus-phage-phi2958PVL	1	3	4
Staphylococcus-phage-phiN315	1	1	2
Staphylococcus-phage-phiSLT	2	0	2
Staphylococcus-phage-SA1	1	0	1
Staphylococcus-phage-tp310-2	0	1	1
Stenotrophomonas-phage-S1	0	1	1
Streptococcus-phage-Dp-1	2	0	2
Streptococcus-phage-PH10	1	0	1
Streptococcus-phage-phi3396	7	0	7
Streptococcus-phage-phi-SsUD.1	0	1	1

Streptococcus-pyogenes-phage-315.1	4	0	4
Synechococcus-phage-S-CAM1	1	3	4
Synechococcus-phage-S-CBM2	0	1	1
Synechococcus-phage-S-CBS4	1	1	2
Synechococcus-phage-S-SKS1	7	1	8
Synechococcus-phage-S-SM2	2	1	3
Synechococcus-phage-S-SSM5	1	0	1
Temperate-phage-phiNIH1.1	1	0	1
Thermus-phage-IN93	1	0	1
Thermus-phage-P23-45	1	0	1
Thermus-phage-P23-77	7	1	8
Thermus-phage-phiYS40	3	0	3
Tsukamurella-phage-TPA2	2	0	2
uncultured-phage	1	0	1
Vibrio-phage-11895-B1	5	0	5
Vibrio-phage-KVP40	1	0	1
Vibrio-phage-VBM1	0	1	1
Vibrio-phage-VP882	3	1	4
Wolbachia-endosymbiont-wVitB-of-Nasonia-vitripennis-phage-WOVitB	1	0	1
Wolbachia-phage-WO	0	1	1

MICROBIAL AND VIRAL ASSEMBLAGES FROM DIFFERENT HEALTH STATES OF THE HAWAIIAN CORAL *PORITES LOBATA*

Nitzan Soffer, Courtney S. Couch, Jesse R. Zaneveld, Drew Harvell, Rebecca Vega Thurber

CHAPTER 4 MICROBIAL AND VIRAL ASSEMBLAGES FROM DIFFERENT HEALTH STATES OF THE HAWAIIAN CORAL *PORITES LOBATA*

4.1 Abstract

Growth anomalies (GAs) are widespread coral diseases in the Indo-Pacific that result in abnormal growths of the skeleton and impaired fitness. GAs are especially common on *Porites* spp. in the Hawaiian archipelago where disease levels are considerably higher than many other regions. Past research has suggested this disease is the result of an infectious agent, however this remains controversial and no pathogen has been identified. Furthermore, water quality has been implicated with the prevalence of this disease. Therefore, we characterized the microbial communities associated with *Porites lobata* GAs at decreasing proximities to a groundwater output (potential source of contaminants). In addition, microbial communities and the viral consortia associated with apparently healthy *P. lobata* colony tissues, GA tissues and tissues from apparently healthy regions of colonies with GAs were compared. We determined that *Oceanspirillales* was the dominant bacterial taxon in all communities, regardless of tissue sample location or health state, suggesting that this hypothesized coral symbiont is resilient to environmental stressors. Although the overall microbial community structure did not differ across location or health state, less abundant taxa increased in GAs. *Vibrionales* and *Verrucomicrobiales* abundance increased significantly in diseased tissue compared to both healthy colonies and sections of healthy coral from diseased colonies. However, members of the *Sphingobacteriales* order were significantly increased in both diseased tissues and healthy colonies compared to healthy portions of the diseased tissues

of the GA. *P. lobata* viromes were dominated by similarities to the bacteriophages in the *Myoviridae* family and included up to 16 types of eukaryotic viruses. However neither viral consortia structure nor any viral taxa changed with health state indicating that viruses are not likely associated with this disease. While it's unclear whether disease is the cause or result of these microbial changes, this study demonstrates overall microbial resilience to environmental stress.

4.2 Introduction

Coral reefs are critical to ocean health, providing infrastructure, habitats and nutrient recycling to the local ecosystem (Modberg and Folke 1999; Veron et al., 2009). In the last four decades, tropical reefs have been under increasing threat from natural and anthropogenic stressors such as extremes in sea surface temperatures, nutrient pollution and overfishing, that often acting synergistically (Harvell et al., 1999; Nystrom et al., 2000; Hughes et al. 2003; Pandolfi, 2005). One hypothesized result of these alterations in coastal habitat conditions is an increase of coral disease. For example, increased levels of ambient inorganic nutrients (nitrogen and phosphorus) has been linked to increased prevalence and severity of coral disease and bleaching (Voss and Richardson, 2006; Bruno et al., 2007; Vega Thurber et al., In press). In addition, multiple coral diseases, such as black band diseases and white syndromes (e.g. white plague), are exacerbated by warm temperatures, leading to greater incidences of disease worldwide with climate change (Burge et al., 2013a; Harvell et al., 2002; Brandt and McManus; Voss and Richardson 2006). Yet, although researchers have identified some extrinsic factors associated with epizootics, infectious agents are also typically involved in disease onset.

Corals harbor a diversity of microbes ranging from viruses, bacteria, archaea, fungi, protists and symbiotic dinoflagellates (Rohwer and Knowlton 2003). These associations can range from commensal to parasitic, and perturbations to these symbioses can result in disease and/or reduced fitness (Ritchie and Smith, 1995; Bourne et al., 2008). One result of the alteration of a coral's microbiome is the introduction of potential opportunist pathogens. Opportunistic pathogens cause disease in stressed or immune compromised hosts and have been linked to several coral diseases (Sutherland, 2004;

Lesser et al., 2007;Burge et al., 2013b). For example, increased temperature has been shown to alter the surface mucus layer bacterial community from one dominated with commensals to one with pathogenic *Vibrio species* (Mao-jones et al., 2010). Yet, since corals are inhabited by hundreds to thousands of bacterial and viral types, differentiating between pathogenic and mutualist/commensal taxa requires careful quantitative evaluation of the communities associated with healthy organisms and their diseased conspecifics.

In recent years there has been a variety of next generation sequencing studies on the disease etiology of corals. For example, there have been multiple studies on the bacterial communities and now viral consortia of some diseases including: white plague (Pantos et al., 2003; Sunagawa et al., 2009; Cardenas et al., 2012; Roder et al., 2013; Garcia et al., 2013;Cook et al., 2013; Soffer et al., 2013), black band disease (reviewed in Miller and Richardson), and white syndromes (Wilson et al., 2012; Sweet and Bythell, 2013; Apprill et al., 2013). These studies concluded that multiple opportunistic pathogens, such as members of *Rhodobacteriales*, *Clostridiales, Vibrionales* and assemblages of cyanobacteria are often associated with these disease states. In addition, viral metagenomic and microscopy studies found that a variety of viruses are associated with corals (for review see Vega & Correa, 2011), including viruses similar to circoviruses that may be involved in white plague disease and nucleocytoplasmic large DNA viruses that may be involved with bleaching (Correa et al., 2012; Soffer et al., 2013).

All these described coral metagenomic studies have focused on acute fast progressing diseases. However corals also suffer from slow, chronic diseases such as the abnormal growths of the coral skeleton called growth anomalies (GAs). Growth anomalies are skeletal deformities found in corals worldwide, and are one of the most common Indo-Pacific coral diseases (Aeby et al., 2011a; Aeby et al., 2011b). In Hawaii, GAs are especially prevalent in the dominant reef building coral genus *Porites*. These Hawaiian species GAs were first reported in Kaneohe Bay in 1990 (Hunter 1999) and their prevalence in human impacted locations are up to 25-fold more prevalent than less impacted sites (Aeby et al., 2011a; Aeby et al., 2011b ; Stimson et al., 2010). GAs cause negative fitness changes to corals including: partial mortality and reduced colony growth, reduced polyp and zooxanthellae abundance, and reduced fecundity (Loya et al., 1984; Coles and Seapy, 1998; Yamashiro et al., 2000; Domart-Coulon et al., 2006; Work et al. 2008; McClanahan et al. 2009). Some GAs display signs of hyperplasia, which is a general response from injury or parasitism, (Domart-Coulon et al., 2006) suggesting that a pathogen may be responsible for some GA formations. Furthermore, viruses have been hypothesized to be associated with this disease due to their presence in GA tissue (Kaczmarksy, 2009) and transformative abilities in tumorigenic diseases in other organisms (Kaczmarsky and Richardson, 2007). Lastly, Breitbart et al., 2005 found both an increase in microbial growth rates and the abundance of culturable *Vibrios* in GA infected corals (both in the GA and healthy appearing tissues) compared to healthy *Porites compressa*. In addition to microbial factors, data suggest that colony size and regional water motion (Couch, 2013) human population densities (Aeby et al., 2011b), light, nutrients, and bleaching status (McClanahan et al., 2009; Aeby et al., 2011a,

Kaczmarsky and Richardson 2010) are all correlated with increased prevalence and severity of *Porites* GAs.

To determine if a bacterial or viral taxa and/or regional abiotic parameters were associated with *Porites lobata* GAs, we created 16S amplicon sequence and viral shotgun metagenomes from healthy (H), GA-diseased (D) and apparently healthy areas of GA-diseased (DH) from multiple sites with pervasive disease located off the Island of Hawaii. We found that *Oceanspirillales* dominated all samples, regardless of site or health state, demonstrating overall microbial resistance to environmental stress. However, low abundance bacteria in the orders *Vibrionales* and *Verrucomicrobiales* were more relatively abundant in D tissues than either DH or H. In addition, bacteria in the order *Sphingobacteriales* was decreased in DH tissues compared to D and H. Lastly, viral consortia across health states did not show any significant differences.

4.3 Methods:

Coral sample collections

Porites lobata fragments and mucus were collected in 2009 and 2011 from two areas in the North Kona District of the island of Hawaii, USA. To determine whether microbial communities changed over an environmental gradient , *P. lobata* samples were collected from 6 sites extending away from an area of high submarine ground water discharge (SGD) in Kailua-Kona Bay, Hawaii, (~8 km from Keauhou) in August 2011 (Fig. 4.1). The SGD is a source of terrestrial derived nutrients, pollutants and anthropogenic contamination (Knee et al., 2010). Samples were collected by abrading a ~ 10 cm^2 patch on the surface of the coral with a sterile, blunt-ended 30 ml Luer Lock syringe and

transported back to shore. Mucus samples (n= 4-5) of apparently healthy *P. lobata*

colonies (H), from the surface of GA tissue (D) and from healthy tissue adjacent to a GA

(DH) within a single colony were collected (Fig. 4.2). The slurry was allowed to settle in

the syringe, transferred to a 2 ml eppendorf tube, frozen at -20ºC, shipped to Cornell

University on dry ice, and stored at -80ºC until DNA extraction.

In October 2009, 2 cm^2 fragments were collected for viral analysis from Keauhou,

(19°34.231 N, 155°58.111 W) using SCUBA by hammer and chisel from 3 apparently

healthy (H) colonies (no visible signs of disease), 2 apparently healthy regions (DH) ~20

cm from a growth anomaly, and 3 growth anomaly regions (D) of ~20-50 cm in diameter

(Fig. 4.2). The GA margin was included to assess the regions of active physiological

change. This size class was chosen because it was the most dominant size class in

sampled population. Each fragment was placed in a separate WhirlPak® and stored in a

cooler with ice until processed for viral isolations

16S library preparation and sequencing

Nucleic acid extractions were conducted using the MOBIO UltraClean Microbial

DNA Isolation Kit according to the manufacture's protocol. Resulting DNA was

amplified using barcoded 16S primers (515F/806R) (Caporaso et al., 2011; Walters et al.,

2011). Amplicons were amplified in triplicate with GoTaq Flexi reagents from Promega

(Madison, WI, USA) using manufactures protocols. Triplicate reactions were pooled and

cleaned using AMPure magnetic beads from Agencourt (Brea, CA, USA). Quantification

of products was conducted with an Invitrogen Qubit HS dsDNA kit (Eugene, OR, USA)

and quality was determined on an Agilent Bioanalzer 2100. Equimolar ratios of the

amplicons were pooled and sequenced on 454 GS FLX machine at the Center for

Genome Research and Biocomputing (CGRB) at OSU.

16S rRNA gene sequence analysis

Amplicon libraries were processed in QIIME (Caporaso et al., 2010). Reads were

parsed and filtered for quality using default parameters (quality score >25, min length =

200, max length = 1000, and no ambigious bases and mismatches allowed). Operational

Taxonomic Units (OTUs) were assigned, and OTU tables were constructed in Uclust

(Edgar, 2010) using 97% similarity. OTUs were annotated based on the Ribosomal

Database Project (RDP) (Wang et al., 2007). Chloroplasts similarities were removed.

Since microbial diversity has previously been reported to be altered in diseased

organisms (Fillion et al., 2004; Dicksved et al., 2008), microbial alpha-diversity across

health states was measured using Shannon's diversity (H') in Primer 6 (Clarke and

Gorley, 2006) and tested for significance using Kruskall-Wallis tests when data failed

tests of normality and equal variance (Analyse-it v2.3). OTU tables for microbial order

("level 4" in the Greengenes/RDP taxonomic hierarchy) were used for all analyses. OTU

tables were either log transformed or absence/presence transformed for further analyses.

Non-metric Multidimensional Scaling (MDS) plots of Bray-Curtis distances were

constructed to visualize potential differences among bacterial communities from each

health state, and site. Because sites varied in proximity to groundwater input, site was

tested as a potential factor influencing bacterial community composition. A 2-way

crossed ANOSIM was used to determine whether microbial communities varied across

health states, site, and the interaction of those two factors. These statistical tests were

repeated for combined diseased tissues (D combined with DH) because although D

tissues are morphologically different than the adjacent apparently healthy tissue,

microbes can potentially be translocated between these tissues.

Similarity Percentage Analysis (SIMPER) was used to rank bacterial orders

according to their contribution to dissimilarities between bacterial communities (if any).

The top 10 most abundant bacterial orders, encompassing all orders identified by

SIMPER, were analyzed for differences across health state, site, and their interaction

using 2-way ANOVAs on rank transformed data with Tukeys-HSD (95% significance)

pairwise post-hoc tests (Sigma-Plot v. 11). Kruskal-Wallis tests were conducted to

compare groups for each factor separately when rank transformed data still failed

Shapiro-Wilk tests after rank transformation. To determine whether any OTUs varied

between sites, OTU relative abundance was regressed against site using Pearson

correlation with Bonferroni or FDR corrections (QIIME).

Bacterial functional analysis using PICRUSt

Previous work has shown that although marker gene analysis may show no

differences in the overall structure of the community the functional capacity of those taxa

can be different (Vega Thurber et al., 2009). Therefore we analyzed the gene functional

pathways of the microbial community associated with the different coral health states and

site locations. Functional analysis of the bacterial community was conducted with

PICRUSt in the Galaxy/Huttenhower lab module (Langille et al., 2013). PICRUSt is a

recently published method that predicts microbial community function from 16S

phylogenies based on a core genes database (Langille et al., 2013). First an OTU table

was made in QIIME using UCLUST at the 94% identity level; higher percentages led to few predicted functional pathways. From this initial OTU table, representative clusters were selected using the recommendations for PICRUSt. The resulting OTU table was then normalized by copy number in the Galaxy PICRUSt module. The normalized table was used to predict metagenomes by selecting "predict metagenome" on the Galaxy/Huttenhower module. Lastly, the predicted metagenomes were organized into KEGG level 3 and level 1 pathway hierarchies. Relative abundance of predicted functional pathways were compared across health state, site and their interactions using a 2-way crossed ANOSIM on log transformed or presence/absence data. To determine whether there were significant functional differences among the health states and/or transect site, an ANOVA with either an FDR or Bonferroni correction was carried out in QIIME for both health states and site.

Virome preparation

Coral tissue cores from the initial sampling (October 2009) were rinsed in viral free seawater then airbrushed into a sterile Tri-cornered beaker. The airbrushed tissue was resuspended in 40 ml of 0.02 μm filtered 1X PBS, transferred to a 50 ml sterile conical tube and preserved with 2 ml reagent grade chloroform. All chloroform-persevered samples were stored at 4°C and shipped overnight to the Vega Thurber lab and kept at 4°C upon arrival.

Twenty-four ml of supernatant were filtered through a 1.0 μm filter using a swin-lock and 10 ml luer lok syringe to remove large cells and debris. Viral particles were concentrated using CsCl density gradient ultracentrifugation as described (Vega Thurber

et al., 2009). Prior to processing all the samples, one sample from each health state (healthy, healthy tissue of GA colonies and the GA itself) was chosen to determine in which densities the virons were distributed. The presence of viral particles at each density was accessed using SYBR Gold staining (Vega Thurber et al., 2009). Viral particles were primarily distributed within the 1.35 mg ml^{-1} and 1.2 mg ml^{-1} densities. The remainders of the samples were then processed and viral particles removed from the 1.35 mg ml^{-1} and 1.2 mg ml^{-1} densities in triplicate. Each resulting sample was filtered through a 0.22 µm Sterivex filter to remove bacteria. The removal of bacterial cells was confirmed using SYBR Gold staining on several samples.

Viral DNA was extracted from each sample using the protocol outlined by Vega Thurber et al. (2009). To confirm that bacterial and eukaryotic contamination was removed during filtration, we PCR amplified 16S and 18S rDNA in the extracted coral samples. Viral DNA underwent multiple displacement amplification in quadruplet using GE Health Sciences Genomphi kit (Pittsburgh, PA, USA).

Virome sequencing, bioinformatics and statistical analyses

Approximately 2 µg of viral DNA was pyrosequenced at Engencore (University South Carolina) on a Roche 454 Titanium machine. Sequence reads first underwent preprocessing to remove sequences that had low quality scores (<20 average), were short (<100 bases), and/or were duplications using Galaxy (Goecks et al., 2010). After quality control processing, human and host reads were removed using DeconSeq (Schmieder and Edwards , 2011); these sequences were then manually confirmed as contamination through NCBI tBLASTx (Altschul et al., 1990). Processed reads were then analyzed

using the tBLASTx algorithm to a boutique viral database that contained all the fully

sequenced and annotated viral genomes at NCBI through Community Cyberinfrastructure

for Advanced Microbial Ecology Research and Analysis (CAMERA)(Sun et al., 2010).

Sequence reads with viral genome similarities of expected values (e-values) $\leq$ to 10^{-5}

were considered. In addition, sequence reads were analyzed for functional hierarchal

analysis using default parameters in MGRAST (normalized, 60% identity, e-values $\leq 10^{-5}$, 15 minimum alignment length), and the SEED database (Meyer et al., 2008). Diseased

(D) and Diseased-Healthy (DH) metagenomes were analyzed as separate health states

and with diseased combined (D and DH) for statistical analysis in MGRAST. P-values

were determined in MGRAST for normalized abundances using an un-paired t-test.

Viral taxonomy results were compared by calculating percentage of tBLASTx

similarities of known viral genomes for 2 categories: "phage and eukaryotic viruses" and

"eukaryotic viruses and unclassified human fecal" for each health states (H, DH, D).

Multidimensional scaling plots (MDS) of log transformed and presence/absence

transformed data were constructed in Primer 6 (Clarke and Gorley, 2006) to elucidate any

viral consortia differences among health states for the different categories

(bacteriophage+ eukaryote; eukaryotes). ANOSIM was used to determine if there were

any statistical differences in the viral consortia among health states. SIMPER analysis

was used to determine if any viral types drove differences among the consortia. Any viral

types that SIMPER determined to be differentially contributing to viral consortia were

statistically analyzed with non- parametric Kruskal-Wallis for each both each health state

separately and combined diseased (D+DH vs H) after failing normality and equal

variance tests.

4.4. Results

Microbial communities from Porites lobata *are similar, except for some rare taxa*

Each of the 85 *P. lobata* 16S libraries, regardless of health state or site, was dominated by similarities to the order *Oceanspirillales* (*Proteobacteria*, γ-*proteobacteria*), with an overall mean relative percentage of 55±2%, (Fig. 4.3). Additionally, there were no significant differences in relative abundance of *Oceanspirillales* when comparing health state, site or their interaction ($p > 0.05$). The next most abundant OTU was an unknown bacterial taxon, whose relative abundance also not significantly different ($p > 0.05$) among the different health states or sites as well (Fig. 4.3).

When analyzing the entire bacterial communities across each health state, site, and their interaction, we found that the majority members of the bacterial communities are stable in *P.lobata.* Regardless of the way the microbial communities were analyzed there were no differences identified among the communities (Fig. 4.4, Table 4.1). In addition, linear regression analysis determined that no OTU was significantly correlated with proximity to ground water input ($p>0.05$). When comparing Shannon diversity metrics there also was no significant difference ($p>0.05$) in diversity across health states, sites or their interaction.

When examining only the rare microbial types, it was found that three bacterial orders were significantly increased among the Diseased and Diseased-Healthy samples. The orders *Sphingobacteriales, Verrucomicrobiales* and *Vibrionales* were elevated (~3.0, 4.5 and ~4.0 fold respectively), although all found at low abundances (Fig. 4.3).

Vibrionales and *Verrucomicrobiales* were also elevated compared to the healthy *P.lobata* microbiomes (~4.0 and ~5.0 fold respectively-Fig. 3). However, surprisingly, the order *Sphingobacteriales* did not differ in relative abundance compared to the healthy *P.lobata* microbiomes (Fig. 4.3). Site and the interaction of site and health state did not significantly affect the relative abundance among these bacterial orders (p>0.05).

Microbial functional pathways are similar across health state and proximity to groundwater input

PICRUSt predicted 213 gene functions (Kegg level 3) associated with these *P.lobata* samples. Fifty percent of the KEGG level 1 pathways were related to metabolism (Fig 4.5). The metabolic pathways include carbohydrate and amino acid metabolism such as galactase, tyrosine or lysine degradation. Approximately 14% of the predictions were to unclassified pathways. Only 1% of the KEGG pathways predicted were related to pathogens (SEED category 'human disease'- Fig. 4.5), such as genes in *Vibrio cholera*. When examining more specific KEGG pathways (level 3), the most relatively abundant pathways for all samples included transporter, "general function prediction" and ABC transporters (Table 4.2. Similar to the structural data, functional aspects of the of bacterial communities were not significantly different for any KEGG functional pathways (Table 4.2) among health states or sites (ANOSIM P>0.05).

 Porites lobata *viromes were dominated by bacteriophages*

Unlike other microbes, viruses do not contain universal genes for phylogenetic comparisons. Therefore we collected tissue samples, isolated viral particles, and shotgun sequenced the DNA to determine if GAs contain unique viruses compared to healthy

corals. Approximately 90% of the sequences in the viral metagenomes had no similarity to any known viral genome (Table 4.3). Bacteriophage similarities dominated all libraries regardless of health state (Fig. 4.6). Similarities to the dsDNA bacteriophage *Myoviridae* were the most relatively abundant, ranging from 57-71% of the libraries, while similarities to other phage families *Microviridae*, *Podoviridae*, *Siphoviridae* and *Inoviridae* also were present (Fig. 4.7). No bacteriophage family was significantly different among the health states (p> 0.05). Bacteriophage to eukaryotic virus ratios also were not significantly different among the different health states (p>0.05). Shannon diversity (H') of the viral families again was not significantly different among health states for any combination of the phages, eukaryotic viruses, or unclassified viruses (p>0.05).

No eukaryotic viral types associated with any disease state

The relative abundances of viral families among individual eukaryotic viral libraries were highly variable (Table 4.4). Many of the eukaryotic viral families were either only represented in only one or a few individuals, such as: *Adenoviridae, Baculoviridae*, satellite DNAs, and REP-encoding eukaryotic viruses such as *Geminiviridae, Nanoviridae, Circoviridae* and *Cycloviridae* (Fig. 4.8). However, the presence of many expected coral viruses such as *Herpesviridae* and *Poxviridae* were found in all health states (Fig. 4.8). Similarities to the viral family *Polydnaviridae* was greater than 20% of the similarities to eukaryotic viruses. Similarities to the family *Iridoviridae*, were found in all but two libraries, and similarities to the viral family *Nimaviridae*, was detected in one diseased library at a relatively high percentage (15%).

No viral family was determined to be statistically different among the different health states.

Virally encoded virulence factors and prophage genes more abundant in diseased corals

Although viral taxonomy did not vary among disease health states, functional analysis determined that diseased corals (combined DH and D) viromes had a significantly higher relative abundance of similarities to virulence, disease, and defense genes than healthy coral viromes ($p<0.05$) (Fig 4.9). Within that subgroup, antibiotics (specifically bacteriocins) and toxic compound resistance genes were elevated in the diseased libraries. In addition, the relative abundance of signature genes in the SEED category defined as "phages/prophages and transposable/elements/plasmids" were statistically more abundant in diseased (D+DH) coral tissues ($p < 0.05$) (Fig. 4.9). Photosynthesis and metabolism associated genes were abundant and equally represented in all libraries.

4.5 Discussion

Oceanspirillales *dominate bacterial community regardless of site and disease state*

Oceanspirillales is a hypothesized cosmopolitan scleractinian coral symbiont (Sharp et al., 2012; McKew et al., 2012; Rodriguez-Lanetty et al., 2013) and was a major bacterial member in these *Porites lobata* microbiomes. Based on the site and disease data it was also found that this symbiotic relationship is stable and persistent even across gradients of environmental stressors such as proximity to the outflow of groundwater. The resiliency and stability of coral-associated microbial communities has also been

demonstrated in *P. cylindrica* exposed to fish farm effluent (Garren et al., 2009). Their

study demonstrated that bacterial communities started returning to their original

composition 22 days after exposure to highly eutrophied effluent. In addition, a study by

Meron et al., 2012, has demonstrated that differences in pH in the natural environment,

much like this study's groundwater gradient, did not alter the microbial communities of

corals. The lack of changes in *Oceanspirillales* relative abundance regardless of

differential exposure to groundwater input demonstrates the strong association between

the bacteria and coral host. Further support for a coral host-*Oceanspirillales* symbiosis is

that D tissues have reduced symbiotic algae (Couch- personal observation), but the

majority of their microbial community consists of *Oceanspirillales*. Therefore this

bacterial type is likely not associated with the algae of the coral, but likely directly

interacts with the coral host. It is also striking that despite clear physiological differences

in D tissue from DH tissues, there is still no change in *Oceanspirillales* dominance,

alluding that this coral-bacteria symbiosis may be obligatory as suggested by (Rodriguez-

Lanetty et al., 2013).

Low abundance bacterial orders Vibrionales *and* Verrucomicrobiales *are increased in GAs*

The abundance of *Vibrionales* and *Verrucomicrobiales* were elevated in D tissue

compared to the healthy portion of diseased corals (DH) and healthy corals (H). This

study corroborates previous findings where more *Vibrios* were cultured from GA tissues

than healthy *P. compressa* (Breitbart et al. 2005). The *Vibrio* order includes known coral

pathogens, such as *Vibrio coralliilyticus,* (Ben-Haim et al., 2003). Conversely, *Vibrios*

can also be secondary opportunists that increase in coral tissues during stress events

(Bourne et al., 2008; Ainsworth et al., 2008). Regardless if these bacterial orders are not the ultimate cause of this disease, they may still have negative effects on the microbial community by outcompeting beneficial antibiotic producing bacteria (Ricthie, 2006). On the other hand, *Verrucomicrobiales* are ubiquitous in marine environments (Freitas et al., 2012) and are found in both shallow and cold-water corals and are thought to be important in carbon cycling (Kellogg et al.,2009; Freitas et al., 2012). Cold water corals lack symbiotic algae, and it is plausible that *Verrucomicrobia* might just grow more efficiently on aposymbiotic corals.

However, we only found low levels of these orders, even in the D portion of GA infected corals, so their role in disease is not clearly discernible. In addition, some GA growth is seasonal, and GAs in our field sites have been shown to increase in partial mortality and area during the winter seasons (Couch, 2013). Thus, if there was a bacterial infection, by the time these GAs were sampled in late summer the bacterial communities could have been recovering and only trace amounts of pathogens detected. Therefore, long term monitoring of *Vibrio* and *Verrucomicrobiales* abundances across D and DH tissues would be useful for elucidating how these bacteria are involved in GA generation and/or progression. Lastly, only infection studies would be able to unequivocally determine whether *Vibrios* and/or *Verrucomicrobiales* cause GAs or are increased as a consequence of GAs physiology.

Sphingobacteriales *is differentially abundant in GA diseased colonies*

The bacterial taxa *Sphingobacteriales* was decreased in DH tissues compared to D and H tissues, suggesting that there is also a local effect of this disease.

Sphingobacteriales are in the phylum *Bacteriodetes* which includes members that

specialize in metabolizing high molecular weight polysaccharides and proteins (reviewed

in Thomas et al., 2011), such as those found in coral mucus (Ducklow and Mitchell 1979,

Brown and Bythell 2005). Therefore, these bacteria might be responding to a shift in

metabolism. A similar paradoxical pattern, where D tissues are more similar to H than

DH was found in a previous study looking at gene expression in growth anomalies of

Montipora capitata (Spies and Takabayshi, 2013). This study determined that *galaxin*, a

calcification protein, is two-fold up-regulated in apparently healthy tissues of GA

affected corals, but not the GA tissue itself (compared to healthy controls). It was

suggested that this was a possible mechanism to compensate or repair the nearby

damaged tissue. Since these tissues from the same animal are physiologically and

metabolically different, it is possible that the growth anomaly produces substrates that

makes certain types of bacteria, like *Sphingobacteriales,* preferentially grow on one of

the tissue types in a GA affected coral over the other.

Bacterial functional predictions do not vary across health states or sites

Functional pathways were consistent among all health states and sites. Even though

some minor bacterial groups were significantly different in DH samples, the functional

properties as predicted by PICRUSt were not altered among any health states. One of the

top contributing pathway (KEGG level 3) was of "general predicted functions" in our

PICRUSt dataset. Half of the pathways were related to metabolism, and some were

similar to those previously found in a shotgun metagenomic study on *Porites asteriodes*

including tyrosine and lysine metabolism (Wegley et al., 2007). In addition, this study

corroborates Langille et al., 2013 findings of galactose metabolic pathways in coral

bacterial communities. Even though *Vibrio* relative abundance was increased in D from

the other health states, KEGG functional pathway predictions identified as *Vibrio*

pathogenic pathways were not different among any of the health states, which was

unexpected. This may indicate that other taxa containing *Vibrio* pathogenic pathways are

found in all health states. In addition, the presence of *Vibrio* pathogenic pathways

PICRUSt annotations are based on conserved genomes of known bacteria, therefore

novel metabolic functions and genes that have been acquired through horizontal gene

transfer, plasmids or have not been characterized yet would evade PICRUSt annotations.

However, PICRUSt provides functional information that would not otherwise be possible

without shotgun sequencing bacterial communities, which is expensive and would have

required isolating bacterial particles from coral mucus/tissue with time consuming

protocols. Overall, this functional analysis provides more evidence that bacterial

communities may not be affected by environmental gradients or GAs.

Eukaryotic viruses are highly variable among and within health states

This is one of a few studies to compare viromes from diseased and healthy corals, and

many types of viruses considered 'typical' of coral viral consortia (e.g., *Herpesviridae,*

Phycodnaviridae, Poxviridae, small circular eukaryotic dsDNA viruses, NCLDVs,

Polydnaviridae and bacteriophages) were found in these libraries (Wegley et al.,2007;

Marhaver et al., 2008;Vega Thurber et al., 2009; Correa et al., 2012; Soffer et al., 2013).

"Unclassified fecal viruses" was the most relatively abundant non-phage group in all

samples but represents a polyphyletic group consisting of a variety of viral types. Human-

associated viruses have been previously found on coral mucus (Futch et al., 2010), and yet their role in coral disease is unknown. *Polydnaviridae* – like sequences were detected in many of the *P. lobata* samples, and have been also found in *Porites compressa* and *Porites asteriodies* (Vega Thurber et al., 2008; Wegeley et al., 2007). This viral family is known to be in symbiosis with wasps, but whether corals have viral symbionts is still unclear.

There was large variability detected in the types of eukaryotic viruses associated with the three different health states. Combining the two diseased tissues (D +DH) also did not show any differences. The lack of any statistical differences in these samples may be attributable to low sample size, database biases, or that viral consortia are not different. Furthermore, since viral replication can be fast (on the order of hours), and since viruses can remain quiescent, the timing of sampling can be extremely important in identify a viral pathogen.

Unlike the eukaryotic viruses, bacteriophage viral consortia of all health states were dominated by similarities to a single family, *Myoviridae*. Given that *Oceanspirillales* is the most abundant bacteria in all libraries, it would be interesting for future studies to explore whether these phages infect *Oceanspirillales,* since it is possible that the most common phages are associated with the most common bacterial member of the coral microbiome.

Corals as reservoirs for marine viral diseases

One diseased viral library contained 15% sequence similarities to (relative eukaryotic viral abundance) *Nimaviridae*, a virus associated with White Spot syndrome in

shrimp which is spread through the water (Munn, 2006). Although *Nimaviridae* is only

known as a crustacean infecting viral family, there may be variants that affect other

marine invertebrates. *Iridoviridae,* another viral family known to be pathogenic to

marine and freshwater fish globally (Hyatt et al., 1999), was found in multiple *P. lobata*

samples. The presence of viral families associated with marine diseases shows that

perhaps corals can either act as reservoirs for disease (Wegley et al., 2007) by allowing

replication of these viruses, or by providing a stable environment, such as UV protection,

and contact with hosts (i.e. when a fish grazes). On the other hand, these viral annotations

are based on closest similarities to known viruses, and may actually be novel viral types

infecting the coral or its associated symbionts.

Increased virulence and defense genes in diseased viromes

Although viral types were not significantly different among the health states, their

functional signatures were different for key gene clusters. Virulence and defense gene

similarities were more relativity abundant in GA corals (combined D and DH tissues)

than in healthy corals. More specifically, some of these increased genes include

bacteriocins which are antibiotics secreted by bacteria to kill closely related bacterial

types (Tagg et al., 1976; Abriouel et al., 2010). Bacteriocins are also morphologically and

genetically similar to *Myoviridae* phage tails (Smarda and Benada, 2005). *Myoviridae*

sequences were common in all libraries, but bacteriocins are only relatively abundant in

diseased samples, therefore it is unlikely that this is a result of annotation error.

Bacteriophages can be detrimental to bacterial growth, but they can also enrich bacterial

survivorship by transferring genetic material, such as antibiotic resistance (Breitbart,

2012). If these phages are encoding bacteriocins they can provide a competitive advantage to the rare bacterial hosts. Alternatively if some phages were to provide a selective advantage to the abundant bacterial types, then perhaps this would contribute to the stability in the microbial community.

 Caveats

Typical for environmental viral metagenomics studies, a majority (over 90%) of our sequences were unknown. In addition, approximately 50% of the bacterial 16S amplicon libraries were unknown. It is possible that a pathogen has been missed because there are no similarities in the databases, although the relative abundance of unknown bacterial types were not significantly different. On the other hand, since GAs develop slowly its possible we missed the window of infection and the presence of virulence genes may be remnants of previous infection.

Lastly, PICRUSt assigns functional pathways to bacterial libraries based on phylogeny, while the viral metagenomic functional analysis was based on shotgun libraries, ie all genetic sequence information is potentially included. Since the viral associated virulence genes were likely from phages, these genes would not be found in the PICRUSt analysis, since plasmids and gene function acquired through horizontal gene transfer is not exclusive to any phylogeny. Therefore, bacteriocins and other phage-encoded genes that could have led to bacteria acquiring virulence factors would not be detected in PICRUSt annotated functional libraries.

4.6 Conclusions

Viral variation among and within health states was dynamic, while bacterial communities remained surprisingly stable across health state, and site. Similarities to dsDNA bacteriophages in the *Myoviridae* family were the majority of all viral metagenomes. Although no viral type was significantly different among the different health states, virulence and defense genes were more relatively abundant in diseased corals. Bacteria in the order *Oceanspirillales* dominated all samples, as well as unknown bacterial types. A low abundance bacterial taxa *Sphingobacteriales* was found in different relative abundances in D samples than DH. Additionally, the rare bacterial taxa *Vibrionales* and *Verrucomicrobiales* relative abundances were increased in D from DH and H samples, suggesting that they may be involved with GAs. However, functional analysis of bacterial communities showed no differences. Therefore, these analyses combined demonstrate that overall *Porites lobata* microbial communities and viral consortia are similar despite environmental stress or health state, with some rare microbial types differentially abundant in GAs.

4.7 Acknowledgments

Figures

Figure 4.1. Satellite map of 6 sites that bacterial communities were sampled from. Site A is located at the mouth of the submarine ground water outflow. The 6 sites where sampling took place are: A,D,3,4,5,6 (in order of closest to farthest to the groundwater respectively).
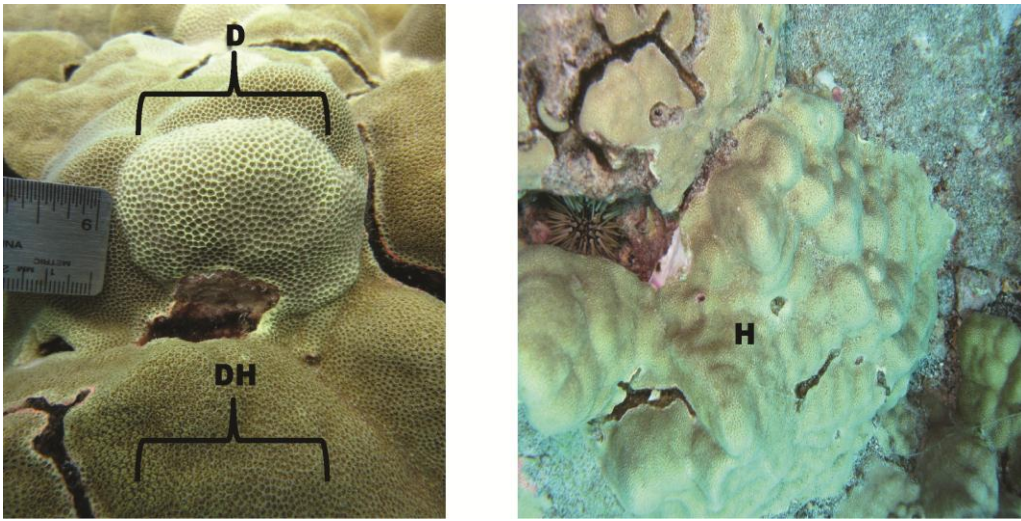
Figure 4.2. Images of healthy tissue (H), healthy tissue on Growth Anomalies infected corals (DH) and Growth Anomalies tissue(D). Bold letters denote tissue health state.
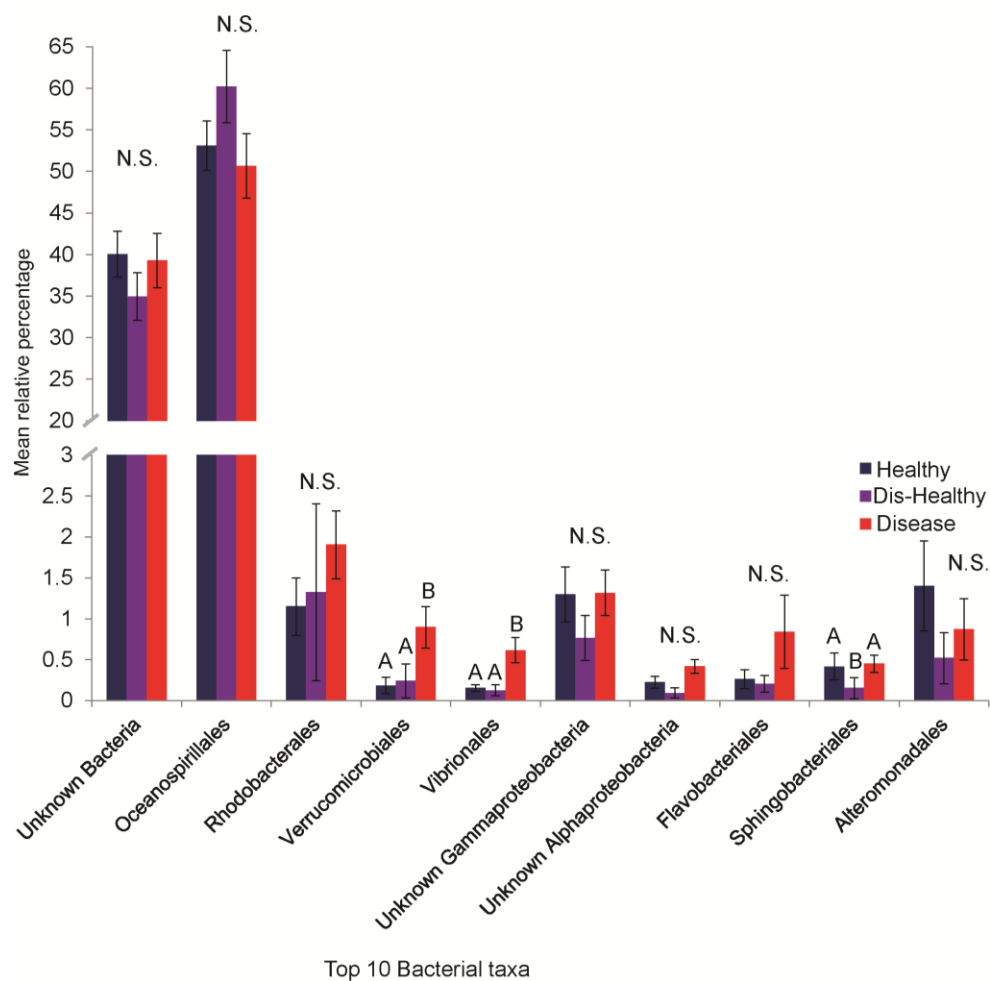
Figure 4.3. Relative mean abundance of the top ten most abundant bacterial orders (or unknown) by health state. Letters denote whether there was significance among health states. N.S. = Not Significant. Significance determined by pairwise *post-hoc* tests are letters A,B.
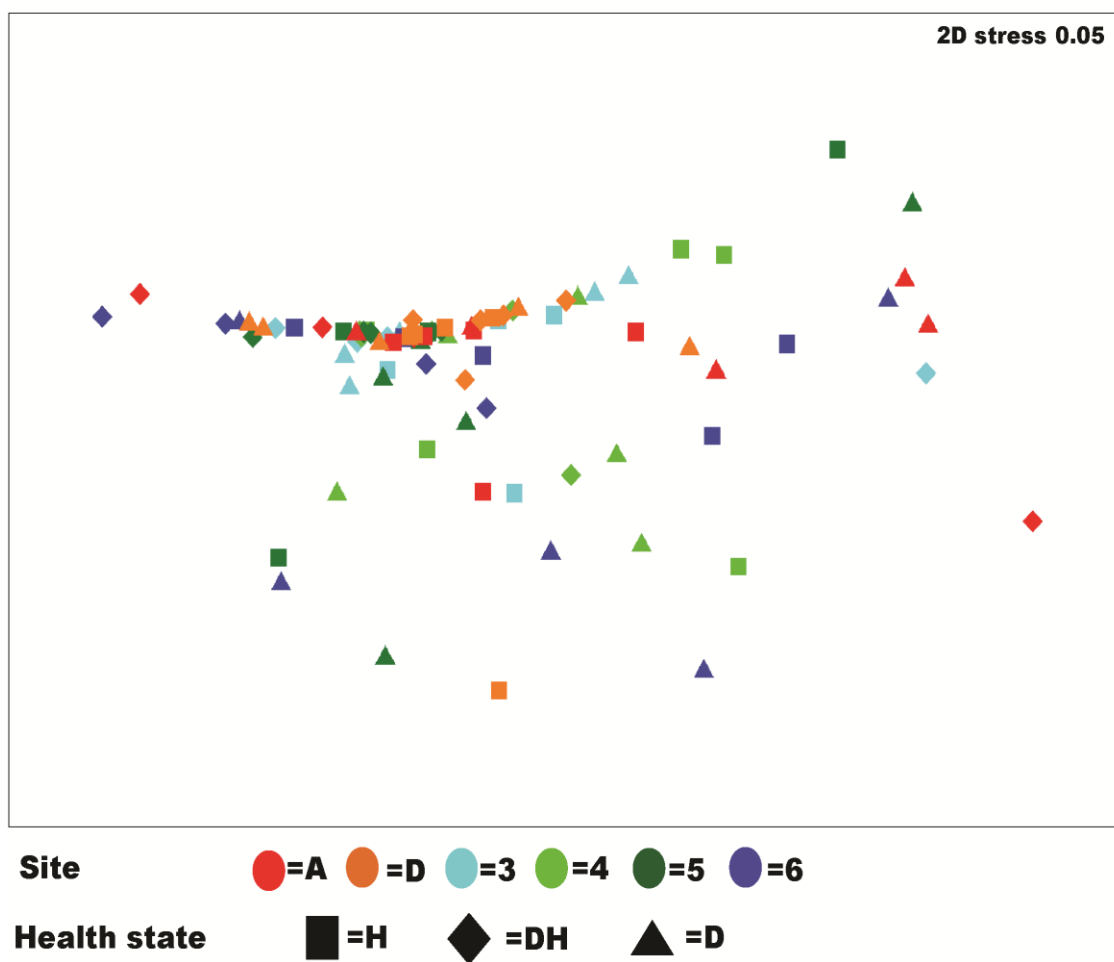
Figure 4.4. Non-metric Multidimensional Scaling plot of bacterial taxa (order level). Colors denote the site location (A,D,3,4,5,6), with A closest to the ground water outflow and 6 the furthest. Shapes denote which tissue health state types (H= healthy; DH= diseased-healthy; D= diseased GA).
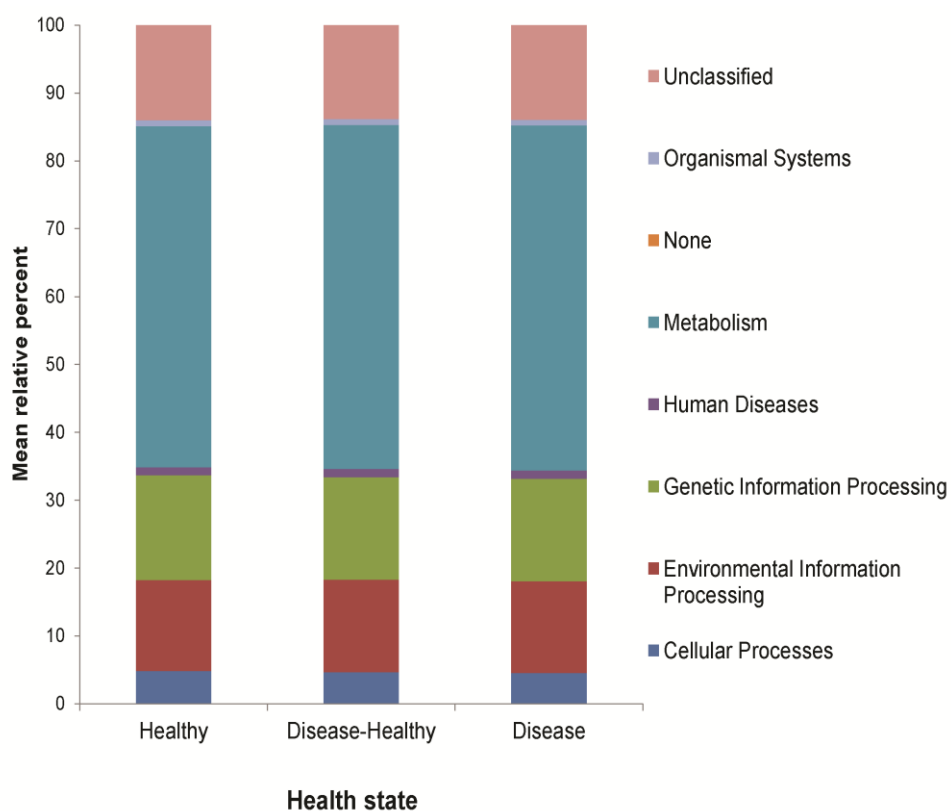
Figure 4.5. General KEGG functional pathway categories (level 1) predicted by PICRUSt. Mean relative percent of pathway abundance for each health state. No significant differences were determined (p>0.05).
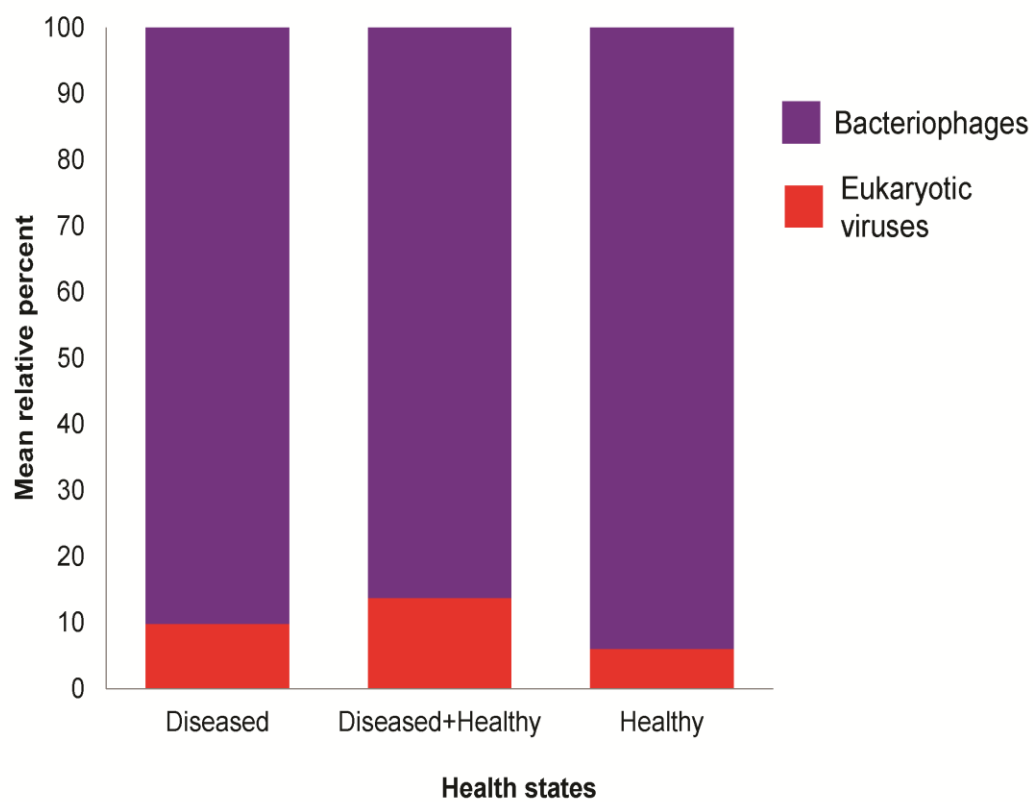
Figure 4.6. Relative mean percent of eukaryotic viruses and bacteriophages among the different health states. No significant differences were determined (p>0.05).
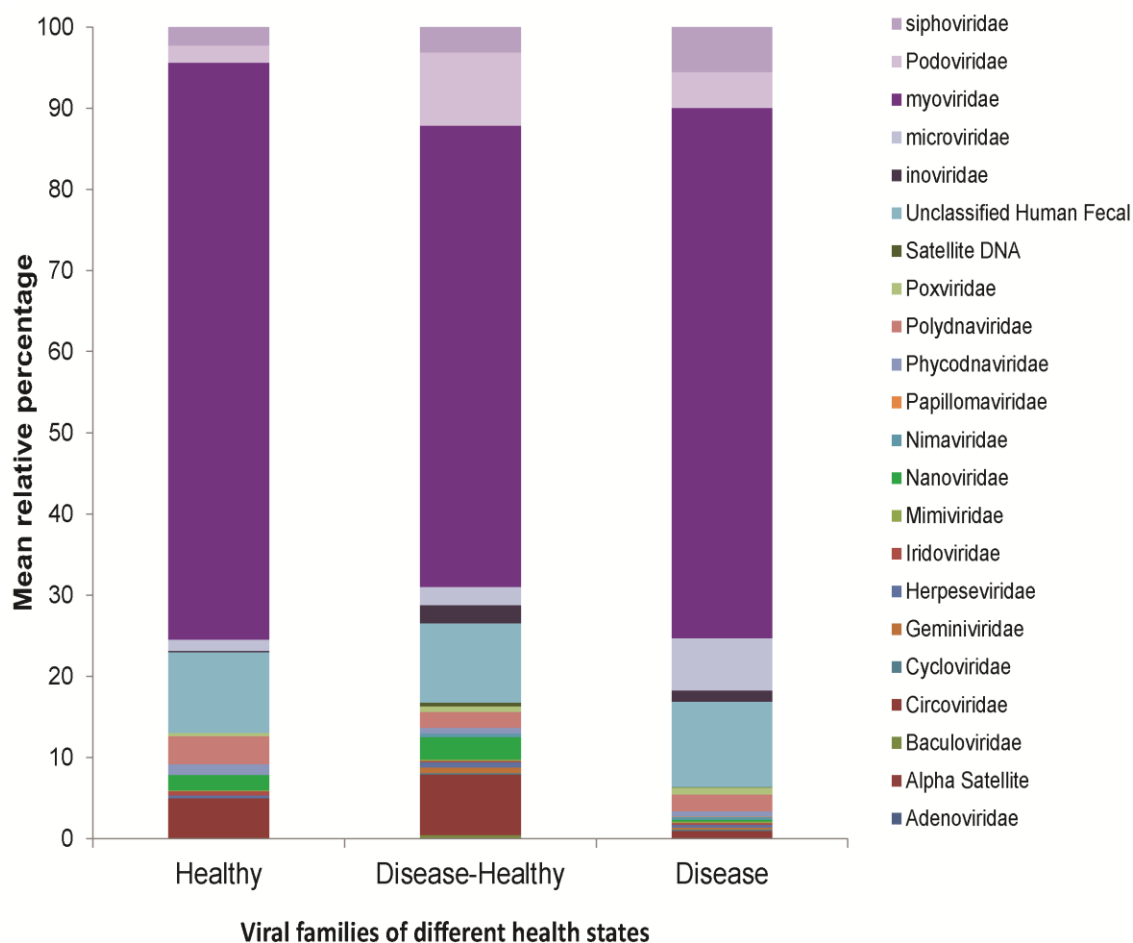
Figure 4.7. Mean relative percentage of viral similarities (family level or unclassified) by health state. No significant differences were determined (p>0.05).
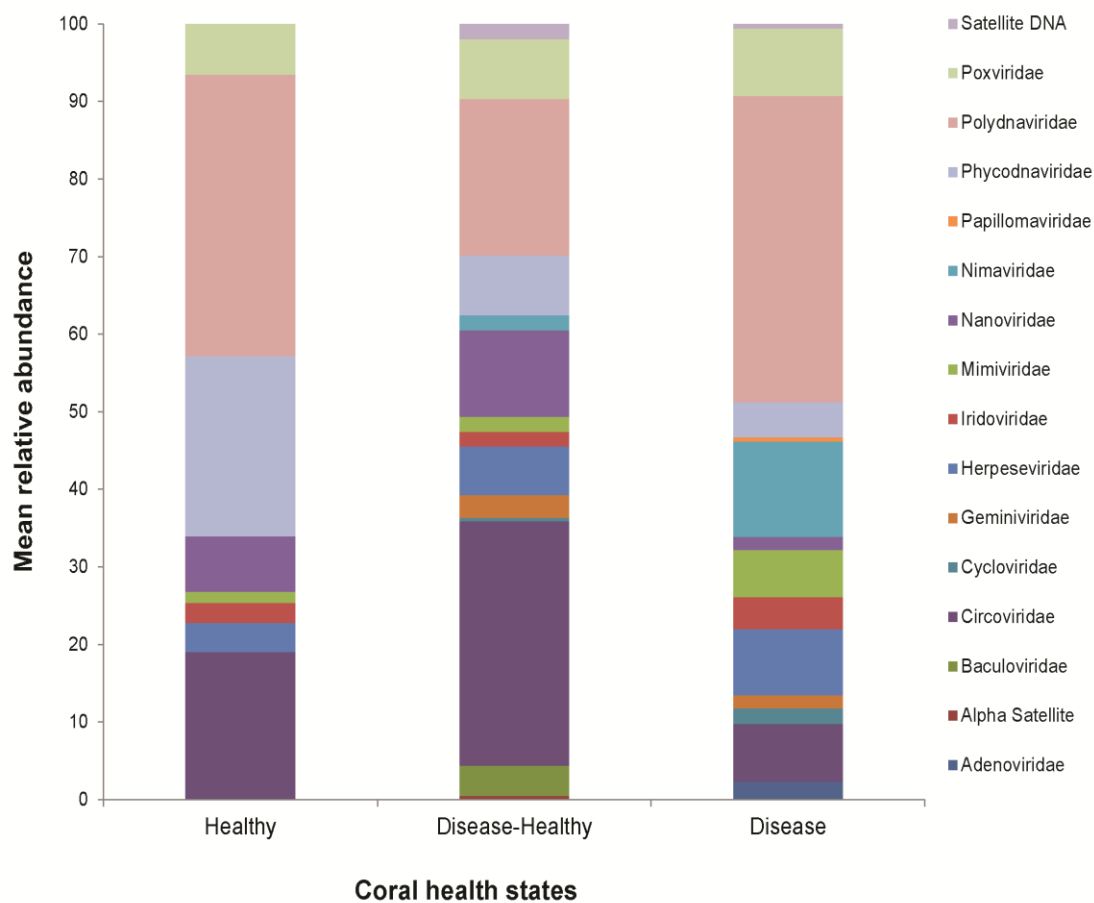
Figure 4.8. Relative mean percent of only eukaryotic viruses among the different health states. No significant differences were determined (p>0.05).
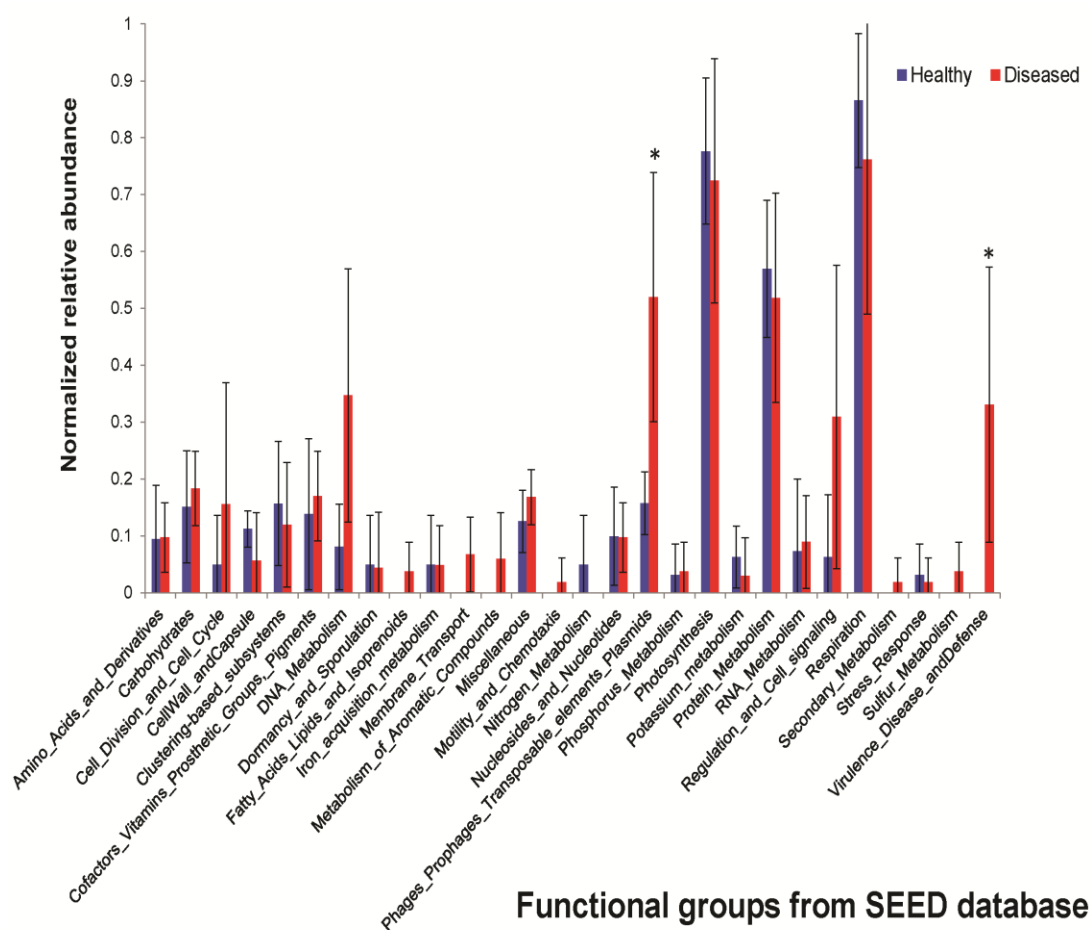
Figure 4.9. Normalized relative abundance of functional groups from combined diseased viral metagenomes and healthy viral metagenomes. Asterisks denotes significant differences (p≤0.05).

Tables

Table 4.1. Comparisons of bacterial communities in both health states and among transect sites. Statistical results of 2-way crossed ANOSIM for either log transformed or absence/presence transformation. Bray Curtis similarities were used for all. The two factors tested were health states and sites.

Transformation	2-way cross ANOSIM	Global R	Percent significance	P-value
Log	Health-state across sites	0.031	22.6	0.22
	Sites across health-state	0.015	32.0	0.32
Absence/Presence	Health-state across sites	-0.038	75.1	0.75
	Sites across health-state	0.01	34.1	0.34

Table 4.2. PICRUSt KEGG level 3 functional pathway gene mean relative percentage with Bonfferoni correction and FDR (P-val).

OTU	Healthy	Healthy-Diseased	Diseased	Bonferroni corrected (P-value)	FDR corrected (P-value)
Transporters	0.0409	0.0399	0.0435	41.42	0.35
General function prediction only	0.0348	0.0350	0.0342	13.40	0.30
ABC transporters	0.0257	0.0250	0.0276	41.89	0.34
Secretion system	0.0270	0.0272	0.0251	32.31	0.31
Two-component system	0.0250	0.0252	0.0239	21.20	0.27
Bacterial motility proteins	0.0238	0.0240	0.0220	26.43	0.29
DNA repair and recombination proteins	0.0208	0.0210	0.0207	68.48	0.43
Function unknown	0.0195	0.0197	0.0189	26.69	0.29
Purine metabolism	0.0183	0.0184	0.0184	213.49	0.86
Ribosome	0.0159	0.0160	0.0158	112.11	0.56
Arginine and proline metabolism	0.0135	0.0135	0.0136	154.09	0.66
Peptidases	0.0135	0.0137	0.0134	40.11	0.35
Transcription factors	0.0129	0.0128	0.0130	84.21	0.50
Ribosome Biogenesis	0.0130	0.0131	0.0125	14.23	0.28
Chromosome	0.0127	0.0128	0.0125	3.37	0.37
Amino acid related enzymes	0.0123	0.0124	0.0121	24.93	0.28
Propanoate metabolism	0.0120	0.0117	0.0121	51.30	0.38
Valine, leucine and isoleucine degradation	0.0119	0.0115	0.0121	35.85	0.33
Pyrimidine metabolism	0.0117	0.0117	0.0119	60.40	0.41

Butanoate metabolism	0.0105	0.0103	0.0109	6.61	0.41
Bacterial secretion system	0.0114	0.0113	0.0107	57.54	0.41
Fatty acid metabolism	0.0106	0.0102	0.0106	46.29	0.36
Pyruvate metabolism	0.0102	0.0102	0.0105	49.08	0.37
Carbon fixation pathways in prokaryotes	0.0103	0.0101	0.0105	9.65	0.32
Oxidative phosphorylation	0.0099	0.0099	0.0104	30.74	0.30
Chaperones and folding catalysts	0.0106	0.0108	0.0101	12.10	0.28
Others	0.0087	0.0088	0.0098	19.12	0.26
Porphyrin and chlorophyll metabolism	0.0092	0.0093	0.0095	153.12	0.66
Energy metabolism	0.0097	0.0097	0.0094	63.39	0.42
Glycine, serine and threonine metabolism	0.0088	0.0087	0.0092	41.26	0.35
Glycolysis / Gluconeogenesis	0.0088	0.0089	0.0090	93.48	0.50
Aminoacyl-tRNA biosynthesis	0.0090	0.0091	0.0090	86.28	0.50
Flagellar assembly	0.0093	0.0092	0.0088	88.94	0.50
Lipid biosynthesis proteins	0.0088	0.0087	0.0087	105.92	0.54
Membrane and intracellular structural molecules	0.0090	0.0089	0.0086	67.03	0.43
Alanine, aspartate and glutamate metabolism	0.0085	0.0086	0.0085	51.71	0.37
Methane metabolism	0.0083	0.0083	0.0084	150.53	0.66
Amino sugar and nucleotide sugar metabolism	0.0084	0.0085	0.0083	30.11	0.30

Translation proteins	0.0085	0.0087	0.0082	14.81	0.27
Tryptophan metabolism	0.0079	0.0077	0.0081	31.12	0.30
Cysteine and methionine metabolism	0.0081	0.0082	0.0080	33.78	0.32
Nitrogen metabolism	0.0080	0.0081	0.0079	9.20	0.35
DNA replication proteins	0.0079	0.0080	0.0079	61.73	0.41
Protein folding and associated processing	0.0076	0.0077	0.0077	143.28	0.65
Other ion-coupled transporters	0.0071	0.0071	0.0075	7.33	0.43
Lysine degradation	0.0073	0.0071	0.0074	51.54	0.38
Bacterial chemotaxis	0.0078	0.0078	0.0073	39.71	0.35
Glyoxylate and dicarboxylate metabolism	0.0068	0.0066	0.0071	9.81	0.32
beta-Alanine metabolism	0.0071	0.0069	0.0071	90.99	0.50
Transcription machinery	0.0071	0.0072	0.0070	100.22	0.53
Phenylalanine, tyrosine and tryptophan biosynthesis	0.0070	0.0071	0.0069	14.06	0.29
Citrate cycle (TCA cycle)	0.0067	0.0066	0.0069	4.38	0.40
Geraniol degradation	0.0070	0.0068	0.0068	145.85	0.65
Replication, recombination and repair proteins	0.0064	0.0066	0.0067	157.51	0.68
Valine, leucine and isoleucine biosynthesis	0.0064	0.0064	0.0066	7.89	0.38
Homologous recombination	0.0062	0.0063	0.0062	93.14	0.50
Limonene and pinene degradation	0.0062	0.0060	0.0062	90.67	0.50
Benzoate degradation	0.0059	0.0056	0.0061	19.69	0.27

Peptidoglycan biosynthesis	0.0060	0.0060	0.0059	24.89	0.29
Histidine metabolism	0.0053	0.0053	0.0055	26.59	0.29
Aminobenzoate degradation	0.0054	0.0053	0.0055	33.37	0.32
Pentose phosphate pathway	0.0053	0.0054	0.0055	65.99	0.43
Mismatch repair	0.0054	0.0055	0.0054	94.91	0.51
Terpenoid backbone biosynthesis	0.0054	0.0054	0.0054	67.79	0.43
Lysine biosynthesis	0.0053	0.0053	0.0054	55.29	0.39
Fatty acid biosynthesis	0.0053	0.0052	0.0053	22.14	0.27
Lipopolysaccharide biosynthesis proteins	0.0056	0.0056	0.0053	47.32	0.36
Pores ion channels	0.0055	0.0055	0.0053	59.85	0.42
Fructose and mannose metabolism	0.0049	0.0050	0.0051	61.31	0.42
Pantothenate and CoA biosynthesis	0.0050	0.0050	0.0051	91.37	0.50
Glutathione metabolism	0.0050	0.0049	0.0050	24.92	0.28
Protein kinases	0.0053	0.0055	0.0050	5.46	0.39
Folate biosynthesis	0.0051	0.0052	0.0049	37.87	0.34
Tyrosine metabolism	0.0047	0.0046	0.0048	47.57	0.36
One carbon pool by folate	0.0048	0.0048	0.0048	242.44	0.97
Glycerophospholipid metabolism	0.0048	0.0048	0.0047	126.83	0.61
Carbon fixation in photosynthetic organisms	0.0047	0.0048	0.0047	180.20	0.74
Protein export	0.0048	0.0048	0.0047	40.05	0.35
Photosynthesis proteins	0.0047	0.0053	0.0047	133.22	0.62
DNA replication	0.0047	0.0047	0.0047	131.34	0.62

RNA degradation	0.0047	0.0048	0.0046	11.00	0.31
Caprolactam degradation	0.0046	0.0044	0.0045	141.14	0.64
Signal transduction mechanisms	0.0046	0.0047	0.0044	11.58	0.28
Sulfur relay system	0.0046	0.0047	0.0044	14.89	0.27
Lipopolysaccharide biosynthesis	0.0045	0.0045	0.0043	67.94	0.43
Nicotinate and nicotinamide metabolism	0.0042	0.0042	0.0042	78.10	0.47
Translation factors	0.0043	0.0043	0.0042	19.69	0.26
Biosynthesis of unsaturated fatty acids	0.0043	0.0043	0.0041	61.59	0.41
Naphthalene degradation	0.0040	0.0039	0.0040	108.80	0.55
Starch and sucrose metabolism	0.0040	0.0041	0.0040	91.02	0.50
Photosynthesis	0.0039	0.0043	0.0039	124.57	0.60
Cell cycle - Caulobacter	0.0037	0.0037	0.0038	7.92	0.36
Thiamine metabolism	0.0039	0.0039	0.0038	16.05	0.24
Base excision repair	0.0038	0.0038	0.0038	54.81	0.39
Ubiquinone and other terpenoid-quinone biosynthesis	0.0038	0.0040	0.0037	14.03	0.29
Prenyltransferases	0.0037	0.0037	0.0035	18.67	0.26
Phenylalanine metabolism	0.0034	0.0033	0.0035	16.09	0.24
Glycosyltransferases	0.0035	0.0036	0.0035	67.45	0.43
Chloroalkane and chloroalkene degradation	0.0033	0.0032	0.0034	77.82	0.47
Sulfur metabolism	0.0032	0.0032	0.0031	29.13	0.30
C5-Branched dibasic acid metabolism	0.0030	0.0029	0.0031	2.52	0.63

Cell motility and secretion	0.0031	0.0031	0.0030	102.16	0.53
Inorganic ion transport and metabolism	0.0028	0.0027	0.0030	16.45	0.24
PPAR signaling pathway	0.0030	0.0030	0.0030	100.64	0.53
Drug metabolism - cytochrome P450	0.0030	0.0029	0.0029	66.48	0.43
Metabolism of xenobiotics by cytochrome P450	0.0029	0.0029	0.0029	70.29	0.44
Glycerolipid metabolism	0.0028	0.0028	0.0028	151.49	0.66
Amino acid metabolism	0.0028	0.0028	0.0028	201.10	0.81
Pentose and glucuronate interconversions	0.0026	0.0025	0.0028	19.82	0.26
Riboflavin metabolism	0.0027	0.0028	0.0027	28.69	0.30
Selenocompound metabolism	0.0026	0.0026	0.0027	28.21	0.29
Other transporters	0.0027	0.0028	0.0026	41.77	0.35
Peroxisome	0.0025	0.0025	0.0025	150.41	0.66
Galactose metabolism	0.0024	0.0024	0.0024	115.77	0.57
Streptomycin biosynthesis	0.0024	0.0024	0.0024	179.20	0.74
Drug metabolism - other enzymes	0.0023	0.0023	0.0023	51.84	0.37
Vibrio cholerae pathogenic cycle	0.0025	0.0026	0.0023	20.62	0.26
Metabolism of cofactors and vitamins	0.0023	0.0023	0.0022	89.91	0.50
Nucleotide excision repair	0.0022	0.0022	0.0022	105.10	0.54
Cyanoamino acid metabolism	0.0018	0.0018	0.0019	113.24	0.56
Bisphenol degradation	0.0018	0.0017	0.0018	24.83	0.29

Cytoskeleton proteins	0.0017	0.0017	0.0017	86.27	0.50
Alzheimer's disease	0.0017	0.0017	0.0017	159.80	0.68
Vitamin B6 metabolism	0.0017	0.0017	0.0017	34.53	0.32
Biotin metabolism	0.0017	0.0018	0.0017	61.45	0.42
Toluene degradation	0.0016	0.0015	0.0017	7.50	0.39
Polycyclic aromatic hydrocarbon degradation	0.0014	0.0014	0.0016	30.58	0.30
Tetracycline biosynthesis	0.0015	0.0015	0.0015	130.17	0.62
Tropane, piperidine and pyridine alkaloid biosynthesis	0.0015	0.0015	0.0015	180.96	0.74
Tuberculosis	0.0014	0.0014	0.0014	136.13	0.63
Inositol phosphate metabolism	0.0013	0.0012	0.0014	8.08	0.35
Plant-pathogen interaction	0.0014	0.0014	0.0014	158.89	0.68
Taurine and hypotaurine metabolism	0.0013	0.0013	0.0013	46.29	0.36
Synthesis and degradation of ketone bodies	0.0012	0.0011	0.0013	5.41	0.42
RNA polymerase	0.0012	0.0012	0.0012	44.82	0.36
Huntington's disease	0.0012	0.0011	0.0012	21.68	0.27
Retinol metabolism	0.0012	0.0012	0.0012	182.64	0.75
D-Glutamine and D-glutamate metabolism	0.0012	0.0012	0.0012	167.00	0.70
Polyketide sugar unit biosynthesis	0.0012	0.0012	0.0012	243.52	0.97
RNA transport	0.0013	0.0013	0.0012	43.60	0.35
Phosphatidylinositol signaling system	0.0012	0.0012	0.0012	29.67	0.30

Ascorbate and aldarate metabolism	0.0010	0.0010	0.0011	24.67	0.29
Styrene degradation	0.0011	0.0011	0.0011	150.46	0.66
Phenylpropanoid biosynthesis	0.0011	0.0011	0.0011	45.09	0.36
Novobiocin biosynthesis	0.0010	0.0010	0.0010	22.98	0.27
Cell division	0.0011	0.0011	0.0010	57.65	0.40
Glutamatergic synapse	0.0010	0.0009	0.0010	85.63	0.50
Ethylbenzene degradation	0.0009	0.0009	0.0009	10.78	0.32
Lipid metabolism	0.0009	0.0009	0.0009	140.06	0.64
Parkinson's disease	0.0009	0.0008	0.0009	62.84	0.42
Restriction enzyme	0.0009	0.0009	0.0009	134.14	0.62
Arachidonic acid metabolism	0.0009	0.0009	0.0008	0.83	0.83
Chlorocyclohexane and chlorobenzene degradation	0.0007	0.0007	0.0008	41.59	0.35
Adipocytokine signaling pathway	0.0008	0.0008	0.0008	150.11	0.66
Carbohydrate metabolism	0.0008	0.0008	0.0008	133.41	0.62
Glycan biosynthesis and metabolism	0.0008	0.0008	0.0008	107.83	0.55
Cardiac muscle contraction	0.0008	0.0008	0.0007	76.82	0.47
Phosphotransferase system (PTS)	0.0006	0.0006	0.0007	19.00	0.26
Linoleic acid metabolism	0.0006	0.0006	0.0007	4.96	0.41
D-Alanine metabolism	0.0006	0.0006	0.0007	13.09	0.30
Pathways in cancer	0.0006	0.0006	0.0007	11.10	0.30

Lipoic acid metabolism	0.0007	0.0007	0.0007	111.33	0.56
Cellular antigens	0.0006	0.0006	0.0006	47.94	0.36
Isoquinoline alkaloid biosynthesis	0.0006	0.0006	0.0006	120.78	0.59
Stilbenoid, diarylheptanoid and gingerol biosynthesis	0.0006	0.0006	0.0006	40.93	0.35
MAPK signaling pathway - yeast	0.0006	0.0006	0.0005	15.25	0.25
Ribosome biogenesis in eukaryotes	0.0006	0.0006	0.0005	3.14	0.39
Primary immunodeficiency	0.0005	0.0006	0.0005	8.21	0.33
alpha-Linolenic acid metabolism	0.0005	0.0005	0.0005	84.28	0.50
Protein processing in endoplasmic reticulum	0.0006	0.0006	0.0005	9.58	0.35
Photosynthesis - antenna proteins	0.0005	0.0006	0.0005	116.18	0.57
Fluorobenzoate degradation	0.0004	0.0004	0.0004	15.36	0.25
Biosynthesis and biodegradation of secondary metabolites	0.0004	0.0004	0.0004	37.66	0.34
Ubiquitin system	0.0005	0.0005	0.0004	11.32	0.29
Phosphonate and phosphinate metabolism	0.0003	0.0003	0.0004	9.64	0.34
Carotenoid biosynthesis	0.0003	0.0003	0.0004	101.87	0.53
Sphingolipid metabolism	0.0003	0.0003	0.0004	10.49	0.33
Meiosis - yeast	0.0004	0.0004	0.0004	182.91	0.75
Insulin signaling pathway	0.0004	0.0004	0.0004	84.96	0.50
Biosynthesis of ansamycins	0.0003	0.0003	0.0004	11.51	0.29

Atrazine degradation	0.0002	0.0002	0.0004	26.52	0.29
Biosynthesis of vancomycin group antibiotics	0.0003	0.0003	0.0004	107.18	0.55
Epithelial cell signaling in Helicobacter pylori infection	0.0003	0.0004	0.0003	137.38	0.63
Lysosome	0.0003	0.0003	0.0003	13.74	0.29
Dioxin degradation	0.0003	0.0003	0.0003	146.45	0.65
Type I diabetes mellitus	0.0003	0.0003	0.0003	131.68	0.62
Other glycan degradation	0.0003	0.0003	0.0003	19.95	0.26
Penicillin and cephalosporin biosynthesis	0.0003	0.0003	0.0003	109.58	0.55
Bacterial toxins	0.0003	0.0003	0.0003	8.20	0.34
Type II diabetes mellitus	0.0003	0.0003	0.0003	159.78	0.68
Proximal tubule bicarbonate reclamation	0.0003	0.0003	0.0003	49.80	0.37
Butirosin and neomycin biosynthesis	0.0003	0.0003	0.0003	59.87	0.41
Nitrotoluene degradation	0.0002	0.0001	0.0003	17.30	0.25
Zeatin biosynthesis	0.0003	0.0003	0.0003	76.33	0.47
Renal cell carcinoma	0.0003	0.0003	0.0003	132.06	0.62
Pertussis	0.0003	0.0003	0.0003	11.25	0.30
Steroid hormone biosynthesis	0.0003	0.0003	0.0003	121.78	0.59
Flavonoid biosynthesis	0.0003	0.0003	0.0003	36.22	0.33
Fatty acid elongation in mitochondria	0.0003	0.0003	0.0003	164.73	0.69
Glycosaminoglycan degradation	0.0003	0.0003	0.0003	160.38	0.67

beta-Lactam resistance	0.0003	0.0003	0.0003	20.05	0.26
Proteasome	0.0003	0.0003	0.0003	33.71	0.32
NOD-like receptor signaling pathway	0.0003	0.0003	0.0003	21.87	0.27
Glycosphingolipid biosynthesis - globo series	0.0003	0.0003	0.0003	210.40	0.85
Antigen processing and presentation	0.0003	0.0003	0.0002	15.99	0.25
Progesterone-mediated oocyte maturation	0.0003	0.0003	0.0002	15.99	0.25
Prostate cancer	0.0003	0.0003	0.0002	15.99	0.24
Bladder cancer	0.0003	0.0003	0.0002	46.15	0.36
Transcription related proteins	0.0002	0.0002	0.0002	86.69	0.50
Primary bile acid biosynthesis	0.0002	0.0002	0.0002	73.02	0.45
Glycosphingolipid biosynthesis - ganglio series	0.0002	0.0002	0.0002	65.28	0.43
Carbohydrate digestion and absorption	0.0002	0.0002	0.0002	34.15	0.32
Vibrio cholerae infection	0.0002	0.0002	0.0002	27.93	0.29

Table 4.3. Virome sequence read processing and quality control

Name	#reads	#reads post QC (Length>100, Q>20)	#reads Post Deconseq	# tBLASTx similarities in Camera
1H	89,304	4,373	4,366	160
4H	111,817	6,651	6,624	465
5H	196,930	8,806	8,783	757
2HD	100,049	7,963	7,963	766
4HD	18,433	3,191	3,186	576
1D	200,170	9,312	9,299	892
2D	168,679	11,685	11,673	765
4D	97,817	12,059	12,049	2,061

Table 4.4. Mean relative percent and variation (SE) of individual viral families

Viral similarity	Healthy	Healthy-Diseased	Diseased
Adenoviridae	0±0	0±0	0.12±0.07
Alpha Satellite	0±0	0.12±0.12	0±0
Baculoviridae	0±0	0.34±0.24	0±0
Circoviridae	4.98±4.98	7.48±4.15	0.81±0.74
Cycloviridae	0±0	0.12±0.12	0.18±0.14
Geminiviridae	0±0	0.72±0.72	0.23±0.23
Herpeseviridae	0.31±0.31	0.63±0.39	0.36±0.06
Iridoviridae	0.56±0.20	0.17±0.17	0.24±0.13
Mimiviridae	0.10±0.01	0.17±0.17	0.17±0.17
Nanoviridae	1.87±1.87	2.76±2.76	0.23±0.23
Nimaviridae	0±0	0.48±0.48	0.33±0.33
Papillomaviridae	0±0	0±0	0.08±0.08
Phycodnaviridae	1.37±1.09	0.68±0.68	0.61±0.61
Polydnaviridae	3.41±1.38	1.94±1.46	2.08±0.82
Poxviridae	0.39±0.26	0.68±0.68	0.85±0.73
Satellite DNA	0±0	0.48±0.48	0.08±0.08
Unclassified Human Fecal	9.96±3.14	9.78±8.58	10.51±5.00
Inoviridae	0.20±0.19	2.21±1.87	1.36±1.14
Microviridae	1.39±0.63	2.26±1.58	6.44±5.98
Myoviridae	71.11±7.23	56.86±12.21	65.37±9.98
Podoviridae	2.10±0.28	9.00±7.30	4.40±1.95
Siphoviridae	2.25±1.17	3.12±3.12	5.56±2.98

5 Chapter 5 – Final discussion

5.1 General conclusions

   Reports of coral diseases have increased over the last three decades from a
handful to over 3 dozen (Harvell et al., 1999; Ward and Lafferty, 2004; Sutherland
et al., 2004; Bourne et al., 2009). Escalation of disease types and prevelence may be
a consequence of more efforts to monitor and detect diseases, but it is also likely
related to increased sea surface temperatures, anthropogenic pollutants and
eutrophication (Harvell, 1999; Wilkinson, 2002; Bruno, 2007). It is estimated that
one third of all coral species are threatened, and disease may be responsible for
future extinctions (Carpenter et al., 2008; Huang, 2012). Diseases affecting corals
have historically reshaped the structure and function of coral reefs, demonstrating
their profound influence on ocean health (Aronson et al.,1998). In the Florida Keys
National Marine Sanctuary alone, there was an average loss of 87% coral cover
caused by a disease that affects just one species, *Acropora palmata* (Miller et al.
2002). Yet, even though disease is the leading cause of mortality in corals, most
diseases have no known etiological agent, and the true number of diseases affecting
corals is still unknown.

       This dissertation is about the tumultuous interactions between corals and
their associated microbes. From the Caribbean Sea to the Pacific Ocean, corals have
been declining for many reasons, disease being one of them. My goal was to
investigate the role of bacteria and viruses in diseased corals with the specific aim of
elucidating an etiological agent. Using primarily metagenomics and to a lesser
extent microscopy, I endeavored to find potential disease agents for the following

cases: White plague (WP) from *Montastraea annularis* US Virgin Islands 2010

outbreak (Chapter 2) and Growth Anomalies (GA) in Hawaiian *Porites lobata*

(Chapter 4). Along this journey, realizing that phage-bacterial dynamics also have

an importance in understanding the disease white plague, I utilized an interaction

network model to make hypotheses of phage influence on bacterial community

shifts (Chapter 3). Together, these studies have demonstrated the functionality of

metagenomic and microscopy tools for determining potential pathogens in non-

model organisms, like corals. In addition, these tools can demonstrate that microbial

pathogens might not always be the disease-causing agent, but can still influence or

be influenced by the coral's health state. Lastly, these studies demonstrate that the

role of viruses should not be overlooked, not only because they may be pathogens of

interest, but viruses (specifically phages) can also influence coral bacterial

communities.

5.2 Not all Eukaryotic viruses in corals are equal

   This dissertation conducted viral metagenomic studies on two coral species, from

two disparate geographic regions to explore the potential role of viruses in diseased

corals. Combined, these two studies increase coral viral primary literature by almost

10%, given that there are ~20 coral virus publications to date (reviewed in Vega and

Correa, 2012; Pub Med search). In chapter 2, I compared viral metagenomes from

healthy, bleached , bleached-WP-diseased and WP-diseased *Montastraea annularis*.

This study had one of the more robust sample sizes in coral virus studies to date,

with replicates ranging from 2-7 individual viromes (as opposed to pooling samples

before sequencing- Wegley et al., 2007; Marhaver et al., 2008; Vega Thuber et al., 2008). This allowed statistical comparisons of different health states. This study determined that there is a strong association of novel ssDNA viruses similar to circo and nano -viruses in white plague infected lesions. Healthy corals did not have any detectable presence of eukaryotic ssDNA virus sequences, but were dominated by herpes-like viruses. Interestingly, the top (bleached) portion of the corals, which did not show signs of WP contained a viral consortia more similar to the bleached corals than the WP diseased. These viral types, the Nucleocytoplasmic large DNA viruses (NCLDVs), have been previously implicated in bleaching (Correa et al., 2012).

NCDLVs were also found abundantly in the *Porites lobata* metagenomes (chapter 4). However, in *P.lobata* there were less definitive patterns among the health states. Herpes-like viruses were not as dominant in any health state. Instead, the major viral group represented was similar to the *Polydnaviridae* family. There were also larger variations among and within health states, potentially due to smaller sample sizes (n=2 to 3) than the WP study. Lastly, small circular ssDNA eukaryotic viruses were found in the *P.lobata,* but they were not associated with any health state and not identified in all samples. Although the *P.lobata* viral study did not lead to the association of viral pathogens with GA, it was important to investigate before moving to alternative hypotheses about the disease-causing agent. A majority of sequences derived from metagenomic data were unknown or unclassified and it is still possible that these unknown sequences may hold the key to the cause of GAs.

Viruses could be involved in some of the other coral diseases with unknown etiological agents, such as white syndromes which show no evidence of bacterial

infection (Ainsworth et al., 2006). Thus, future research efforts should continue to consider viruses as a potential pathogen in coral diseases. Even in the case of the GAs, where a viral pathogen was not implicated, future research can now focus on other causes of disease or disease control efforts. In the case of GAs, Couch et al., (Submitted), has demonstrated coral colony size and water motion is correlated with the disease. By examining the viral consortia and finding no link between a virus and the disease, there is now more evidence that environmental factors are major contributors to this disease. Perhaps efforts towards increasing water flow by avoiding dredging/development will be increased, rather than focusing on pathogen control.

When a potential viral pathogen is identified, the next question that arises is what can be done to prevent further infections. In the case of WP, because the novel viruses were not found to be related to similar viruses in seawater, the source of disease was not confirmed. However, because the viral infection appears to be locally contained near the disease lesion, the disease lesion could be chiseled off, protecting the adjacent healthy tissue from the disease. Also, if this viral group can be traced to either an animal, human, soil or sewage source then these sources can be the target of disease mitigation.

5.3 Bacteriophages and bacteria

Bacteriophages have received less attention than eukaryotic viruses in coral metagenomic studies, mostly because they are not directly interacting with the coral host. However, they are the most dominant viral component in the coral virome,

ranging from 73-93% (chapter 2 and chapter 4). Relative abundances of phage families were not significant across health states from either the GA or WP studies, with the exception of sequences similar to *Inoviridae* which was elevated in both healthy and diseased than bleached in *Montastraea annularis*. In the *Porites lobata* viromes, one of the few consistencies among samples was the predominance of bacteriophage sequences similar to *Myoviridae*. Given that all of the GA bacterial libraries were dominated by the bacteria *Oceanspirillales,* it is plausible that these phages are associated with that bacterial group and future studies should examine this possibility. Phage presence is influenced by their bacterial hosts, and conversely bacterial communities are influenced by phages, thus the two should be studied together when possible.

In chapter 3, I characterized the bacterial community of the *Montastraea annularis* coral samples described in chapter 2. Two bacterial types, hypothesized to be opportunistic colonizers, increased in relative abundance in WP-diseased tissues compared to other health states. These include members of the orders *Rhodobacterales* and *Campylobacterales.* Interestingly, one bacterial order, *Kiloniellales* increased in relative abundance in the healthy compared to the WP-diseased. Bleached corals also had unique bacterial types that increased compared to diseased and healthy, but at a smaller relative percentage from their overall community. Once it was determined which bacterial types were increased in diseased, healthy or bleached corals, bacteriophage strain level consortia were compared, and they displayed similar patterns of clustering to the bacterial genus level. This led to the idea that interactions among bacteria and their phage can be

predicted. Even though there has been no study (until a few days before this dissertation was submitted- Chow et al., 2013), which used models to predict bacteria-phage interactions from metagenomic phage and bacteria data, network interaction models have already been developed and optimized for predicting/visualizing interactions among environmental microbes, such as bacteria-bacteria and bacteria-heterotrophs (Steele et al., 2011; Faust et al., 2012; Faust and Raes, 2012). Adapting these techniques, I was able to determine which phages are predicted to interact (and whether these are negative or positive) with 11 bacteria which had significantly higher abundance in at least one of the health states. This model can then be applied for designing phage-therapy tools, in any system.

5.4 Future directions:

The majority of research focusing on coral microbiomes has been on bacterial communities. Even though 16S amplicon libraries are quick, relatively easy and cheap, this does not validate their almost exclusive dominance in coral-microbe primary literature. There were more than seven 16S bacterial community studies on WP in the Caribbean, yet none had strongly supported correlations to any etiological agent, until the study in Chapter 2 examining potential viral WP disease agents. More than 20 potential agents of coral diseases remain unknown, demonstrating the inefficiency of past and present efforts. Future efforts should focus on both microbial (bacteria, archaea, fungi, protists) and viral communities. In addition, even if bacteria are responsible for coral disease states, bacteriophages are important in regulating bacterial communities, and should thus be studied concomitantly with any bacterial study.

Studying coral viruses is challenging and expensive. Merely mashing up coral tissue and sending it to be sequenced will not yield any quality information on viruses. Producing viral metagenomes requires careful isolation from host/other tissue and remains the largest hurdle in the study of coral infectious diseases. In addition, shotgun sequencing can be expensive, but costs have and continue to decline. Another consideration is that viruses cannot always be preserved or extracted in the field easily (ie ethanol preserved, or extracted directly from host), and thus collaboration between field scientists and molecular/microbiology scientists is key to make sure samples are properly handled. Despite these challenges, there have been about half a dozen coral virus studies to date and there is still much to be discovered in regards to coral viruses (especially compared to coral bacteria), such that the reward of doing novel research supersedes the challenges.

In terms of bacterial community coral research, the field is more advanced, but some areas need further investigation. For example, only one study looked at the heterogeneity of bacterial communities within mucus samples (Daniels et al., 2011), even though there is ongoing debate as how consistent communities are in a colony. Sampling mucus is the preferred choice for bacterial profiling because it is non-invasive and collection permits are more readily given. However, if bacterial communities are uneven across a single coral sample, then perhaps mucus sampling is not the best method. Although it is difficult to obtain permits for tissue collections, these samples allow for both viral and bacterial community analysis.

In addition, because bacterial profiling is relatively cheap, easy and fast (compared to viral metagenomic studies), some studies lack focus and better collaboration would lead to more connected information that can be synthetized together. For example, the studies on WP each examine a different species, different location and different methods (ie phylochip vs 16S libraries). If focus was limited to a few locations and multiple species were sampled over time in a planned experiment with consistent methods, then there might a clearer picture as to what is truly happening with the bacterial communities, rather than random "snapshots". The efforts of the human microbiome projects serve as an example of productive collaboration that coral biologists could benefit from.

Overall, metagenomic analyses have provided basic information in coral biology and have laid the foundation for understanding potential roles of coral associated microbes. In addition the functional complexity and taxonomic diversity of microbes associated with corals is beginning to be understood. However, there should be more focus on culture based studies, and not just on bacterial communities from corals, but also their associated phages. In addition, it would be interesting to monitor corals that recovered from disease and determine how long bacteria/viruses remain post infection, and whether corals can be re-infected, or become resistant. There are still many mysteries in coral virology that should be explored, such as the role of herpes-like viruses, which appear to be found in all coral viral studies. For example, are herpes-viruses sometimes pathogenic? Are they similar across species/ocean basins, are they transmitted horizontally/vertically or both? The fact that they have been found in all coral metagenomic studies thus far is an indication that they are an important member of the coral microbiome.

Lastly, I propose an application of phage-bacteria networks for synthetic phage therapy that is currently premature for the existing technologies. However, the field of synthetic biology has progressed immensely (Cheng and Lu, 2012; Lu et al., 2013) and it is foreseeable that the necessary tools (such as fast and cheap oligonucleotide synthesis) will be developed in the near future. Phage-bacteria networks constructed from metagenomes of diseased and healthy individuals can provide knowledge to generate phage therapies, without the use of serendipitous culturing. One can potentially use a phage-bacteria interaction network for phage therapies using the following steps (constructed from either clinical samples or existing databases): 1. identify phages shown to only interact with detrimental bacteria (the key for safe treatment- and overcomes a major criticism of phage therapy), 2. determine which sequences are associated with these phages, 3. construct a synthetic genome with known sequence features, and 4. validate synthetic phage functionality on cultured bacteria of interest 5. Apply phages in clinical setting. Functional synthetic phages have been successfully constructed (Smith et al., 2003), and these techniques are becoming more efficient and commercialized (Ruder et al., 2011; Baker, 2011). Once these potential treatment phages are constructed and functionality demonstrated on cultures of the specified bacteria (such as the antibiotic resistant Methicillin-resistant Staphylococcus aureus -MRSA), these can be produced in a commercial level.

BIBLIOGRAPHY

Abriouel,H., Franz,C.M. a P., Ben Omar,N., and Gálvez,A. (2011) Diversity and applications of Bacillus bacteriocins. *FEMS Microbiol. Rev.* **35**: 201–32.

Aeby,G.S., Williams,G.J., Franklin,E.C., Haapkyla,J., Harvell,C.D., Neale,S., et al. (2011a) Growth anomalies on the coral genera Acropora and Porites are strongly associated with host density and human population size across the Indo-Pacific. *PLoS One* **6**: e16887.

Aeby,G.S., Williams,G.J., Franklin,E.C., Kenyon,J., Cox,E.F., Coles,S., and Work,T.M. (2011b) Patterns of coral disease across the Hawaiian archipelago: relating disease to environment. *PLoS One* **6**: e20370.

Ainsworth,T.D., Fine,M., Roff,G., and Hoegh-Guldberg,O. (2008) Bacteria are not the primary cause of bleaching in the Mediterranean coral Oculina patagonica. *ISME J.* **2**: 67–73.

Ainsworth,T.D., Kvennefors,E.C., Blackall,L.L., Fine,M., and Hoegh-Guldberg,O. (2007) Disease and cell death in white syndrome of Acroporid corals on the Great Barrier Reef. *Mar. Biol.* **151**: 19–29.

Ainsworth, T. D., Thurber, R. V., Gates, R. D. (2010) The future of coral reefs: a microbial perspective. *TREE* **25:**233-240.

Altschul, S. F., Gish, W., Miller, W., Myers, E. W., & Lipman,D.J. (1990) Basic local alignment search tool. *J. Mol. Biol.* **215**: 403–410.

Angly,F.E., Felts,B., Breitbart,M., Salamon,P., Edwards,R.A., Carlson,C., et al. (2006) The marine viromes of four oceanic regions. *PLoS Biol.* **4**: e368.

Apprill,A., Hughen,K., and Mincer,T. (2013) Major similarities in the bacterial communities associated with lesioned and healthy Fungiidae corals. *Environ. Microbiol.* **15**: 2063–72.

Aronson,R.B., Precht,W.F., and Macintyre,I.G. (1998) Extrinsic control of species replacement on a Holocene reef in Belize: the role of coral disease. *Coral Reefs* **17**: 223–230.

Assenov,Y., Ramírez,F., Schelhorn,S.-E., Lengauer,T., and Albrecht,M. (2008) Computing topological parameters of biological networks. *Bioinformatics* **24**: 282–4.

Baker, M. (2011) The next step for the synthetic genome. *Nature* **473:** 403-408.

Barabási, A. (1999) Emergence of Scaling in Random Networks. *Science* **286**: 509–512.

Barneah,O., Ben-Dov,E., Kramarsky-Winter,E., and Kushmaro,A. (2007) Characterization of black band disease in Red Sea stony corals. *Environ. Microbiol.* **9**: 1995–2006.

Barott,K.L., Rodriguez-Brito,B., Janouškovec,J., Marhaver,K.L., Smith,J.E., Keeling,P., and Rohwer,F.L. (2011) Microbial diversity associated with four functional groups of benthic reef algae and the reef-building coral Montastraea annularis. *Environ. Microbiol.* **13**: 1192–204.

Barr,J.J., Auro,R., Furlan,M., Whiteson,K.L., Erb,M.L., Pogliano,J., et al. (2013) Bacteriophage adhering to mucus provide a non-host-derived immunity. *Proc. Natl. Acad. Sci. U. S. A.* **110**: 10771–6.

Beman, J. M., Roberts, K. J., Wegley, L., Rohwer, F., Francis, C. A. (2007) Distribution and diversity of archaeal ammonia monooxygenase genes associated with corals. *AEM* **73:**5642-5647.

Belák,S., Karlsson,O.E., Blomström,A.-L., Berg,M., and Granberg,F. (2013) New viruses in veterinary medicine, detected by metagenomic approaches. *Vet. Microbiol.* **165**: 95–101.

Bellantuono,A.J., Hoegh-guldberg,O., and Rodriguez-Lanetty,M. (2012) Resistance to thermal stress in corals without changes in symbiont composition. *Proc. Biol. Sci.* **279**: 1100–7.

Ben-Haim,Y. (2003) Vibrio coralliilyticus sp. nov., a temperature-dependent pathogen of the coral Pocillopora damicornis. *Int. J. Syst. Evol. Microbiol.* **53**: 309–315.

Ben-Haim, Y., Rosenberg, E. (2002). Microbial diseases of corals and global warming. *Env. Microbiol.* **4:** 318-326.

Benjamini, Y., Hochberg, Y. (1995) Controlling the false discovery rate: a practical andpowerful approach to multiple testing. *J. of the Royal Stat. Soc.. Ser. B (Methodol.)***57**: 289-300.

Bermingham, a, Chand,M., Brown,C., Aarons,E., Tong,C., Langrish,C., et al. (2012) Severe respiratory illness caused by a novel coronavirus, in a patient transferred to the United Kingdom from the Middle East, September 2012. *Euro Surveill.* **17**: 1–5.

Blomström,A.-L., Widén,F., Hammer,A.-S., Belák,S., and Berg,M. (2010) Detection of a novel astrovirus in brain tissue of mink suffering from shaking mink syndrome by use of viral metagenomics. *J. Clin. Microbiol.* **48**: 4392–6.

Bourne,D., Iida,Y., Uthicke,S., and Smith-Keune,C. (2008) Changes in coral-associated microbial communities during a bleaching event. *ISME J.* **2**: 350–63.

Bourne,D.G., Dennis,P.G., Uthicke,S., Soo,R.M., Tyson,G.W., and Webster,N. (2013) Coral reef invertebrate microbiomes correlate with the presence of photosymbionts. *ISME J.* **7**: 1452–8.

Bourne,D.G., Garren,M., Work,T.M., Rosenberg,E., Smith,G.W., and Harvell,C.D. (2009) Microbial disease and the coral holobiont. *Trends Microbiol.* **17**: 554–62.

Bourne,D.G. and Munn,C.B. (2005) Diversity of bacteria associated with the coral Pocillopora damicornis from the Great Barrier Reef. *Environ. Microbiol.* **7**: 1162–74.

Brandt, M. E., and McManus, J. W. (2009) Disease incidence is related to bleaching extent in reef-building corals. *Ecol.* **90:** 2859-2867.

Breitbart,M. (2012) Marine Viruses: Truth or Dare. *Ann. Rev. Mar. Sci.* **4**: 425–448.

Breitbart,M., Bhagooli,R., Griffin,S., Johnston,I., and Rohwer,F. (2005) Microbial communities associated with skeletal tumors on Porites compressa. *FEMS Microbiol. Lett.* **243**: 431–6.

Breitbart,M., Hewson,I., Felts,B., Mahaffy,J.M., Nulton,J., Salamon,P., and Rohwer,F. (2003) Metagenomic Analyses of an Uncultured Viral Community from Human Feces **185**:6220-6223

Breitbart,M., Salamon,P., Andresen,B., Mahaffy,J.M., Segall,A.M., Mead,D., et al. (2002) Genomic analysis of uncultured marine viral communities. *Proc. Natl. Acad. Sci. U. S. A.* **99**: 14250–5.

Brown,B. and Bythell,J. (2005) Perspectives on mucus secretion in reef corals. *Mar. Ecol. Prog. Ser.* **296**: 291–309.

Brown,B.E. (1997) Coral bleaching : causes and consequences. **2100**: 129–138.

Bruno,J.F., Selig,E.R., Casey,K.S., Page,C.A., Willis,B.L., Harvell,C.D., et al. (2007) Thermal stress and coral cover as drivers of coral disease outbreaks. *PLoS Biol.* **5**: e124.

Brüssow,H., Canchaya,C., Hardt,W., and Bru,H. (2004) Phages and the Evolution of Bacterial Pathogens : from Genomic Rearrangements to Lysogenic Conversion Phages and the Evolution of Bacterial Pathogens **68:**560-602.

Burge,C. a, Eakin,C.M., Friedman,C.S., Froelich,B., Hershberger,P.K., Hofmann,E.E., et al. (2013a) Climate Change Influences on Marine Infectious Diseases: Implications for Management and Society. *Ann. Rev. Mar. Sci.6:1-29.*

Burge, C. A., Kim, C. J., Lyles, J. M., & Harvell, C. D. (2013). Special Issue Oceans and Humans Health: The Ecology of Marine Opportunists. *Microbiol. Ecol.* **65:**869-879.

Caporaso,J.G., Kuczynski,J., Stombaugh,J., Bittinger,K., Bushman,F.D., Costello,E.K., et al. (2010) correspondEnce QIIME allows analysis of high- throughput community sequencing data Intensity normalization improves color calling in SOLiD sequencing. *Nat. Publ. Gr.* 7: 335–336.

Caporaso,J.G., Lauber,C.L., Walters,W. a, Berg-Lyons,D., Lozupone,C. a, Turnbaugh,P.J., et al. (2011) Global patterns of 16S rRNA diversity at a depth of millions of sequences per sample. *Proc. Natl. Acad. Sci. U. S. A.* **108**: 4516–22.

Cárdenas,A., Rodriguez-R,L.M., Pizarro,V., Cadavid,L.F., and Arévalo-Ferro,C. (2012)

Shifts in bacterial communities of two Caribbean reef-building coral species affected by white plague disease. *ISME J.* **6**: 502–12.

Carpenter,K.E., Abrar,M., Aeby,G., Aronson,R.B., Banks,S., Bruckner,A., et al. (2008) One-third of reef-building corals face elevated extinction risk from climate change and local impacts. *Science* **321**: 560–3.

Ceh,J., Raina,J.-B., Soo,R.M., van Keulen,M., and Bourne,D.G. (2012) Coral-bacterial communities before and after a coral mass spawning event on Ningaloo Reef. *PLoS One* **7**: e36920.

Cervino,J.M., Hayes,R.L., Polson,S.W., Polson,S.C., Goreau,T.J., Martinez,R.J., and Smith,G.W. (2004a) Relationship of vibrio species infection and elevated temperature to yellow blotch/band disease in caribbean corals. *Appl. Environ. Microbiol.* **70**: 6855–6864.

Chaffron,S., Rehrauer,H., Pernthaler,J., and von Mering,C. (2010) A global network of coexisting microbes from environmental and whole-genome sequence data. *Genome Res.* **20**: 947–59.

Cheng, A. A., & Lu, T. K. (2012) Synthetic biology: an emerging engineering discipline. *Annu. Rev. Biomed. Eng.* **14:**155-178.

Chimetto,L. a, Brocchi,M., Thompson,C.C., Martins,R.C.R., Ramos,H.R., and Thompson,F.L. (2008) Vibrios dominate as culturable nitrogen-fixing bacteria of the Brazilian coral Mussismilia hispida. *Syst. Appl. Microbiol.* **31**: 312–9.

Chiu,C.Y. (2013) Viral pathogen discovery. *Curr. Opin. Microbiol.* **16**: 468–78.

Chow, C.T., Kim, D.Y., Sachdeva, R., Caron, D.A., Furhman, J.A.(2013) Top-down controls on bacterial community structure: microbial network analysis of bacteria, T4-like viruses and protists. *ISME J* Advance online: doi:10.1038/ismej.2013.199

Clarke, K.R., Gorley,R.N. Primer v6: User Manual/Tutorial.Plymouth, UK.

Clarke, K.R., Warwick,R.M. (2001) Change in marine communities: an approach to statistical analysis and interpretation 2nd edition. Pylmouth, UK.

Cleary,D.F.R., Becking,L.E., de Voogd,N.J., Pires,A.C.C., Polónia,A.R.M., Egas,C., and Gomes,N.C.M. (2013) Habitat- and host-related variation in sponge bacterial symbiont communities in Indonesian waters. *FEMS Microbiol. Ecol.* **85**: 465–82.

Coles,S.L. and Seapy,D.G. (1998) Ultra-violet absorbing compounds and tumorous growths on acroporid corals from Bandar Khayran, Gulf of Oman, Indian Ocean. *Coral Reefs* **17**: 195–198.

Collado, L., and Figueras, M. J. (2011) Taxonomy, epidemiology, and clinical relevanceof the genus Arcobacter. *Clin. Microbiol. Rev.* **24:**174-192.

Cook,G.M., Rothenberger,J.P., Sikaroodi,M., Gillevet,P.M., Peters,E.C., and Jonas,R.B. (2013) A comparison of culture-dependent and culture-independent techniques used to characterize bacterial communities on healthy and white plague-diseased corals of the Montastraea annularis species complex. *Coral Reefs* **32**: 375–388.

Cooney,R.P., Pantos,O., Le Tissier,M.D.A., Barer,M.R., O'Donnell,A.G., and Bythell,J.C. (2002) Characterization of the bacterial consortium associated with black band disease in coral using molecular microbiological techniques. *Environ. Microbiol.* **4**: 401–13.

Correa,A.M.S., Welsh,R.M., and Vega Thurber,R.L. (2012) Unique nucleocytoplasmic dsDNA and +ssRNA viruses are associated with the dinoflagellate endosymbionts of corals. *ISME J.* 1–15.

Cróquer, A., Bastidas, C., & Lipscomb, D. (2006). Folliculinid ciliates: a new threat to Caribbean corals? *Dis. Aquat. Org.* **69**: 75-78.

Daszak,P. (2000) Emerging Infectious Diseases of Wildlife-- Threats to Biodiversity and Human Health. *Science (80-.).* **287**: 443–449.

Dean,F.B., Nelson,J.R., Giesler,T.L., and Lasken,R.S. (2001) Rapid amplification of plasmid and phage DNA using Phi 29 DNA polymerase and multiply-primed rolling circle amplification. *Genome Res.* **11**: 1095–9.

Denner,E.B.M., Smith,G.W., Busse,H.-J., Schumann,P., Narzt,T., Polson,S.W., et al. (2003) Aurantimonas coralicida gen. nov., sp. nov., the causative agent of white plague type II on Caribbean scleractinian corals. *Int. J. Syst. Evol. Microbiol.* **53**: 1115–22.

Dicksved,J., Halfvarson,J., Rosenquist,M., Järnerot,G., Tysk,C., Apajalahti,J., et al. (2008) Molecular analysis of the gut microbiota of identical twins with Crohn's disease. *ISME J.* **2**: 716–27.

Domart-Coulon, I.J., Traylor-knowles,Peters,E., Elbert,D., Downs,C.A., Cox,E., Aeby,G., et al. (2006) Comprehensive characterization of skeletal tissue growth anomalies of the finger coral Porites compressa. 531–543.

Ducklow, H. W., & Mitchell, R. (1979) Composition of mucus released by coral reef coelenterates. *Limnol. Oceanogr*, **24:**706-714.

Dunne,J. a., Williams,R.J., and Martinez,N.D. (2002) Network structure and biodiversity loss in food webs: robustness increases with connectance. *Ecol. Lett.* **5**: 558–567.

Dustan,P. (1999) Coral reefs under stress: sources of mortality in the Florida Keys. *Nat. Resour. Forum* **23:**147-155

Edgar,R.C. (2010a) Search and clustering orders of magnitude faster than BLAST. *Bioinformatics* **26**: 2460–1.

Efrony,R., Atad,I., and Rosenberg,E. (2009) Phage therapy of coral white plague disease: properties of phage BA3. *Curr. Microbiol.* **58**: 139–45.

Efrony,R., Loya,Y., Bacharach,E., and Rosenberg,E. (2007) Phage therapy of coral disease. *Coral Reefs* **26**: 7–13.

Fabricius,K.E. (2005) Effects of terrestrial runoff on the ecology of corals and coral reefs: review and synthesis. *Mar. Pollut. Bull.* **50**: 125–46.

Faust,K. and Raes,J. (2012) Microbial interactions: from networks to models. *Nat. Rev. Microbiol.* **10**: 538–50.

Faust,K., Sathirapongsasuti,J.F., Izard,J., Segata,N., Gevers,D., Raes,J., and Huttenhower,C. (2012) Microbial co-occurrence relationships in the human microbiome. *PLoS Comput. Biol.* **8**: e1002606.

Flores,C.O., Meyer,J.R., Valverde,S., Farr,L., and Weitz,J.S. (2011) Statistical structure of host − phage interactions. *PNAS* **108**:E288-E297

Flores,C.O., Valverde,S., and Weitz,J.S. (2013) Multi-scale structure and geographic drivers of cross-infection within marine bacteria and phages. *ISME J.* 7: 520–32.

Frias-Lopez, J., Zerkle, A. L., Bonheyo, G. T., and Fouke, B. W. (2002) Partitioning of bacterial communities between seawater and healthy, black band diseased, and dead coral surfaces. *App.o and Environ. Microbiol.***68:** 2214-2228.

Freitas,S., Hatosy,S., Fuhrman,J. a, Huse,S.M., Welch,D.B.M., Sogin,M.L., and Martiny,A.C. (2012) Global distribution and diversity of marine Verrucomicrobia. *ISME J.* **6**: 1499–505.

Funk,S., Bogich,T.L., Jones,K.E., Kilpatrick, a M., and Daszak,P. (2013) Quantifying trends in disease impact to produce a consistent and reproducible definition of an emerging infectious disease. *PLoS One* **8**: e69951.

Futch,J.C., Griffin,D.W., Lipp,E.K., and Keys,F. (2010) Human enteric viruses in groundwater indicate offshore transport of human sewage to coral reefs of the Upper Florida Keys. *Environ. Microbiol.* **12**: 964–974.

Gálvez,A., Abriouel,H., López,R.L., and Ben Omar,N. (2007) Bacteriocin-based strategies for food biopreservation. *Int. J. Food Microbiol.* **120**: 51–70.

Garcia,G.D., Gregoracci,G.B., Santos,E.D.O., Meirelles,P.M., Silva,G.G.Z., Edwards,R., et al. (2013) Metagenomic analysis of healthy and white plague-affected Mussismilia braziliensis corals. *Microb. Ecol.* **65**: 1076–86.

Garren,M., Raymundo,L., Guest,J., Harvell,C.D., and Azam,F. (2009) Resilience of coral-associated bacterial communities exposed to fish farm effluent. *PLoS One* **4**: e7319.

Goecks,J., Nekrutenko,A., and Taylor,J. (2010) Galaxy: a comprehensive approach for

supporting accessible, reproducible, and transparent computational research in the life sciences. *Genome Biol.* **11**: R86.

Gómez,P. and Buckling,A. (2011) Bacteria-phage antagonistic coevolution in soil. *Science* **332**: 106–9.

Grard,G., Fair,J.N., Lee,D., Slikas,E., Steffen,I., Muyembe,J.-J., et al. (2012) A novel rhabdovirus associated with acute hemorrhagic fever in central Africa. *PLoS Pathog.* **8**: e1002924.

Green, E P.,B.A.W. (2000) The significance of coral disease epizootiology for coral reef conservation. *Biol. Conserv.* **96**: 347–361.

Handelsman,J. (2004) Metagenomics : Application of Genomics to Uncultured Microorganisms Metagenomics. *Microbiol. Molec Rev.* **68**:669-685

Handelsman,J., Rondon,M.R., Brady,S.F., Clardy,J., and Goodman,R.M. (1998) Molecular biological access to the chemistry of unknown soil microbes: a new frontier for natural products. *Chem. Biol.* **5**: R245–9.

Harvell,C.D., Kim,K., Burkholder,J.M., Colwell,R.R., Epstein,P.R., Grimes,D.J., et al. (1999) Emerging marine diseases--climate links and anthropogenic factors. *Science* **285**: 1505–10.

Harvell,C.D., Mitchell,C.E., Ward,J.R., Altizer,S., Dobson,A.P., Ostfeld,R.S., and Samuel,M.D. (2002) Climate warming and disease risks for terrestrial and marine biota. *Science* **296**: 2158–62.

Hendrix, R. W., Smith, M. C., Burns, R. N., Ford, M. E., & Hatfull, G. F. (1999) Evolutionary relationships among diverse bacteriophages and prophages: all the world's a phage. PNAS 96: 2192-2197.

Ho, H. T., Lipman, L. J., and Gaastra, W. (2006) Arcobacter what is known and unknown about a potential foodborne zoonotic agent!. Vet. Microbiol. 115: 1-13.

Holmfeldt, K., Middelboe, M., Nybroe, O., Riemann, L. (2007).= Large variabilities in host strain susceptibility and phage host range govern interactions between lytic marine phages and their Flavobacterium hosts. *AEM* **73:** 6730-6739.

Huang,D. (2012) Threatened reef corals of the world. *PLoS One* **7**: e34459.

Hughes,T.P., Baird, a H., Bellwood,D.R., Card,M., Connolly,S.R., Folke,C., et al. (2003) Climate change, human impacts, and the resilience of coral reefs. *Science* **301**: 929–33.

Hurwitz,B.L. and Sullivan,M.B. (2013) The Pacific Ocean virome (POV): a marine viral metagenomic dataset and associated protein clusters for quantitative viral ecology. *PLoS One* **8**: e57355.

Hyatt, a D., Gould, a R., Zupanovic,Z., Cunningham, a a, Hengstberger,S.,

Whittington,R.J., et al. (2000) Comparative studies of piscine and amphibian iridoviruses. *Arch. Virol.* **145**: 301–31.

Johnson,P.T.J., Townsend,A.R., Cleveland,C.C., Glibert,P.M., Howarth,R.W., McKenzie,V.J., et al. (2010) Linking environmental nutrient enrichment and disease emergence in humans and wildlife. *Ecol. Appl.* **20**: 16–29.

Johnston,I.S. and Rohwer,F. (2007) Microbial landscapes on the outer tissue surfaces of the reef-building coral Porites compressa. *Coral Reefs* **26**: 375–383.

Kaczmarsky,L. and Richardson,L.L. (2010) Do elevated nutrients and organic carbon on Philippine reefs increase the prevalence of coral disease? *Coral Reefs* **30**: 253–257.

Kaczmarsky,L. and Richardson,L.L. (2007) Transmission of growth anomalies between Indo-Pacific Porites corals. *J. Invertebr. Pathol.* **94**: 218–21.

Kaczmarsky, L.T. (2009) Characterizations of the Major Coral Diseases of the Philippines : Ulcerative White Spot Disease and Novel Growth Anomalies of Porites. Doctoral Dissertation.

Kellogg,C. (2004) Tropical Archaea: diversity associated with the surface microlayer of corals. *Mar. Ecol. Prog. Ser.* **273**: 81–88.

Kellogg,C. , Lisle,J.T., Galkiewicz,J.P. (2009) Culture-independent characterization of bacterial communities associated with the cold-water coral Lophelia pertusa in the northeastern Gulf of Mexico. *Appl. Environ. Microbiol.* **75**: 2294–303.

Kellogg,C. a, Piceno,Y.M., Tom,L.M., DeSantis,T.Z., Zawada,D.G., and Andersen,G.L. (2012) PhyloChip^{TM} microarray comparison of sampling methods used for coral microbial ecology. *J. Microbiol. Methods* **88**: 103–9.

Kim,K.-H. and Bae,J.-W. (2011) Amplification methods bias metagenomic libraries of uncultured single-stranded and double-stranded DNA viruses. *Appl. Environ. Microbiol.* **77**: 7663–8.

Klaus,J.S., Janse,I., Heikoop,J.M., Sanford,R. a, and Fouke,B.W. (2007) Coral microbial communities, zooxanthellae and mucus along gradients of seawater depth and coastal pollution. *Environ. Microbiol.* **9**: 1291–305.

Kline,D., Kuntz,N., Breitbart,M., Knowlton,N., and Rohwer,F. (2006) Role of elevated organic carbon levels and microbial activity in coral mortality. *Mar. Ecol. Prog. Ser.* **314**: 119–125.

Knee,K., Street,J.H., Grossman,E.G., and Paytan,A. (2010) Nutrient inputs to the coastal ocean from submarine groundwater discharge in a groundwater-dominated system: Relation to land use (Kona coast, Hawaii, U.S.A.). *Limnol. Oceanogr.* **55**: 1105–1122.

Knowlton,N. and Rohwer,F. Multispecies Microbial Mutualisms on Coral Reefs: The Host as a Habitat. *Am. Nat.* **162**: S51-S62

Koenig, J. E., Spor, A., Scalfone, N., Fricker, A. D., Stombaugh, J., Knight,et al. (2011) Succession of microbial consortia in the developing infant gut microbiome. *PNAS* **108:**4578–85.

Koop,K., Booth,D., Broadbent, a, Brodie,J., Bucher,D., Capone,D., et al. (2001) ENCORE: the effect of nutrient enrichment on coral reefs. Synthesis of results and conclusions. *Mar. Pollut. Bull.* **42**: 91–120.

Kooperman,N., Ben-Dov,E., Kramarsky-Winter,E., Barak,Z., and Kushmaro,A. (2007) Coral mucus-associated bacterial communities from natural and aquarium environments. *FEMS Microbiol. Lett.* **276**: 106–13.

Krediet,C.J., Ritchie,K.B., Alagely,A., and Teplitski,M. (2013) Members of native coral microbiota inhibit glycosidases and thwart colonization of coral mucus by an opportunistic pathogen. *ISME J.* **7**: 980–90.

Kuntz, N. M., Kline, D. I., Sandin, S. A., & Rohwer, F. (2005) Pathologies and mortality rates caused by organic carbon and nutrient stressors in three Caribbean coral species. *Marine Ecol. Prog. Series* **294:** 173-180.

Kushmaro, a, Banin,E., Loya,Y., Stackebrandt,E., and Rosenberg,E. (2001) Vibrio shiloi sp. nov., the causative agent of bleaching of the coral Oculina patagonica. *Int. J. Syst. Evol. Microbiol.* **51**: 1383–8.

Kvennefors,E.C.E., Sampayo,E., Ridgway,T., Barnes,A.C., and Hoegh-Guldberg,O. (2010) Bacterial communities of two ubiquitous Great Barrier Reef corals reveals both site- and species-specificity of common bacterial associates. *PLoS One* **5**: e10401.

Langille,M.G.I., Zaneveld,J., Caporaso,J.G., McDonald,D., Knights,D., Reyes,J. a, et al. (2013) Predictive functional profiling of microbial communities using 16S rRNA marker gene sequences. *Nat. Biotechnol.* **31**: 814–21.

Lesser,M.P., Bythell,J.C., Gates,R.D., Johnstone,R.W., and Hoegh-Guldberg,O. (2007) Are infectious diseases really killing corals? Alternative interpretations of the experimental and ecological data. *J. Exp. Mar. Bio. Ecol.* **8**:36-44

Lipp,E.K., Futch,J.C., and Griffin,D.W. (2007) Analysis of multiple enteric viral targets as sewage markers in coral reefs. *Mar. Pollut. Bull.* **54**: 1897–902.

Littman,R. a, Bourne,D.G., and Willis,B.L. (2010) Responses of coral-associated bacterial communities to heat stress differ with Symbiodinium type on the same coral host. *Mol. Ecol.* **19**: 1978–90.

Littman,R. a, Willis,B.L., Pfeffer,C., and Bourne,D.G. (2009) Diversities of coral-associated bacteria differ with location, but not species, for three acroporid corals on the Great Barrier Reef. *FEMS Microbiol. Ecol.* **68**: 152–63.

Littman,R., Willis,B.L., and Bourne,D.G. (2011) Metagenomic analysis of the coral holobiont during a natural bleaching event on the Great Barrier Reef. **3**: 651–660.

Loya,Y., Bull,G., and Pichon,M. (1984) Tumor formations in scleractinian corals. *Helgoländer Meeresuntersuchungen* **37**: 99–112.

Lozupone,C., Faust,K., Raes,J., Faith,J.J., Frank,D.N., Zaneveld,J., et al. (2012) Identifying genomic and metabolic features that can underlie early successional and opportunistic lifestyles of human gut symbionts. *Genome Res.* **22**: 1974–84.

Lu, T. K., Bowers, J., Koeris, M. S. (2013) Advancing bacteriophage-based microbial diagnostics with synthetic biology. *Trends in biotech.* In press.

Mao-Jones,J., Ritchie,K.B., Jones,L.E., and Ellner,S.P. (2010) How microbial community composition regulates coral disease development. *PLoS Biol.* **8**: e1000345.

Marhaver,K.L., Edwards,R. a, and Rohwer,F. (2008a) Viral communities associated with healthy and bleaching corals. *Environ. Microbiol.* **10**: 2277−86.

Marhaver,K.L., Edwards,R. a, and Rohwer,F. (2008b) Viral communities associated with healthy and bleaching corals. *Environ. Microbiol.* **10**: 2277−86.

Mcclanahan,T.R., Weil,E., Cortés,J., Baird,A.H., and Ateweberhan,M. (2009) Consequences of Coral Bleaching for Sessile Reef Organisms. 121–138.

McCLANAHAN,T.R., WEIL,E., and MAINA,J. (2009) Strong relationship between coral bleaching and growth anomalies in massive Porites. *Glob. Chang. Biol.* **15**: 1804–1816.

McClung, C. R., Patriquin, D. G., and Davis, R. E. (1983) Campylobacter nitrofigilis sp. nov., a nitrogen-fixing bacterium associated with roots of Spartina alterniflora Loisel. IJSEM **33:** 605-612.

McKew,B. a, Dumbrell, a J., Daud,S.D., Hepburn,L., Thorpe,E., Mogensen,L., and Whitby,C. (2012) Characterization of geographically distinct bacterial communities associated with coral mucus produced by Acropora spp. and Porites spp. *Appl. Environ. Microbiol.* **78**: 5229–37.

Meron,D., Atias,E., Iasur Kruh,L., Elifantz,H., Minz,D., Fine,M., and Banin,E. (2011) The impact of reduced pH on the microbial community of the coral Acropora eurystoma. *ISME J.* **5**: 51–60.

Meyer,F., Paarmann,D., D'Souza,M., Olson,R., Glass,E.M., Kubal,M., et al. (2008) The metagenomics RAST server - a public resource for the automatic phylogenetic and functional analysis of metagenomes. *BMC Bioinformatics* **9**: 386.

Miller,A.W. and Richardson,L.L. (2011) A meta-analysis of 16S rRNA gene clone libraries from the polymicrobial black band disease of corals. *FEMS Microbiol. Ecol.* **75**: 231–41.

Miller,J., Muller,E., Rogers,C., Waara,R., Atkinson, a., Whelan,K.R.T., et al. (2009) Coral disease following massive bleaching in 2005 causes 60% decline in coral cover on

reefs in the US Virgin Islands. *Coral Reefs* **28**: 925–937.

Miller, MW, Baums IB, Williams DE,S.A. (2002) NOAA Technical Memorandum NMFS-SEFSC-479 STATUS OF CANDIDATE CORAL,. *Fish. Sci.* 1998–2001.

Moberg,F. and Folke,C. (1999) Ecological goods and services of coral reef ecosystems. *Ecol. Econ.* **29**: 215–233.

Modi, S. R., Lee, H. H., Spina, C. S., and Collins, J. J. (2013) Antibiotic treatment expands the resistance reservoir and ecological network of the phage metagenome. *Nature 499:* 219–22.

Mokili,J.L., Rohwer,F., and Dutilh,B.E. (2012b) Metagenomics and future perspectives in virus discovery. *Curr. Opin. Virol.* **2**: 63–77.

Monot,M., Honoré,N., Garnier,T., Araoz,R., Coppée,J.-Y., Lacroix,C., et al. (2005) On the origin of leprosy. *Science* **308**: 1040–2.

Montoya,J.M., Pimm,S.L., and Solé,R. V (2006) Ecological networks and their fragility. *Nature* **442**: 259–64.

Mouchka,M.E., Hewson,I., and Harvell,C.D. (2010) Coral-associated bacterial assemblages: current knowledge and the potential for climate-driven impacts. *Integr. Comp. Biol.* **50**: 662–74.

Munn,C.B. (2006) Viruses as pathogens of marine organismsö from bacteria to whales. *J. Mar. Biol. Assoc. United Kingdom* **86**: 453–467.

Mydlarz,L.D., McGinty,E.S., and Harvell,C.D. (2010) What are the physiological and immunological responses of coral to climate warming and disease? *J. Exp. Biol.* **213**: 934–45.

Nelson,C.E., Alldredge,A.L., McCliment,E., Amaral-Zettler,L., and Carlson,C. (2011) Depleted dissolved organic carbon and distinct bacterial communities in the water column of a rapid-flushing coral reef ecosystem. *ISME J.* **5**: 1374–87.

Ng,T.F.F., Manire,C., Borrowman,K., Langer,T., Ehrhart,L., and Breitbart,M. (2009) Discovery of a novel single-stranded DNA virus from a sea turtle fibropapilloma by using viral metagenomics. *J. Virol.* **83**: 2500–9.

Nyström,M., Folke,C., and Moberg,F. (2000) Coral reef disturbance and resilience in a human-dominated environment. *Trends Ecol. Evol.* **15**: 413–417.

Oceanologique,O., Saint-martin,A., and Gtophysiques,F. (1999) Photosynthesis and Calcification at Cellular , Organismal and Community Levels in Coral Reefs : A Review on Interactions and Control by Carbonate. **183**: 160–183.

Olesen,J.M., Bascompte,J., Dupont,Y.L., and Jordano,P. (2006) The smallest of all worlds: pollination networks. *J. Theor. Biol.* **240**: 270–6.

Olsen,C.W. (2002) The emergence of novel swine influenza viruses in North America. *Virus Res.* **85**: 199–210.

Pandolfi,J.M., Connolly,S.R., Marshall,D.J., and Cohen,A.L. (2011) Projecting coral reef futures under global warming and ocean acidification. *Science* **333**: 418–22.

Pandolfi,J.M., Jackson,J.B.C., Baron,N., Bradbury,R.H., Guzman,H.M., Hughes,T.P., et al. (2005) Are U . S . Coral Reefs on. **307**:

Pantos,O., Cooney,R.P., Tissier,M.D.A. Le, Barer,M.R., Donnell,A.G.O., and Bythell,J.C. (2003) The bacterial ecology of a plague-like disease affecting the Caribbean coral Montastrea annularis. **5**: 370–382.

Pantos,O., Cooney,R.P., Le Tissier,M.D.A., Barer,M.R., O'Donnell,A.G., and Bythell,J.C. (2003) The bacterial ecology of a plague-like disease affecting the Caribbean coral Montastrea annularis. *Environ. Microbiol.* **5**: 370–82.

Paramasivam,N., Ben-Dov,E., Arotsker,L., Kramarsky-Winter,E., Zvuloni,A., Loya,Y., and Kushmaro,A. (2013) Bacterial consortium of Millepora dichotoma exhibiting unusual multifocal lesion event in the Gulf of Eilat, Red Sea. *Microb. Ecol.* **65**: 50–9.

Pascual,M. and Bouma,M.J. (2009) Do rising temperatures matter? *Ecology* **90**: 906–12.

Pollock,F.J., Morris,P.J., Willis,B.L., and Bourne,D.G. (2011) The urgent need for robust coral disease diagnostics. *PLoS Pathog.* **7:** e1002183.

Radford,A.D., Chapman,D., Dixon,L., Chantrey,J., Darby,A.C., and Hall,N. (2012) Application of next-generation sequencing technologies in virology. *J. Gen. Virol.* **93**: 1853–68.

Raina,J.-B., Dinsdale,E. a, Willis,B.L., and Bourne,D.G. (2010) Do the organic sulfur compounds DMSP and DMS drive coral microbial associations? *Trends Microbiol.* **18**: 101–8.

Raina,J.-B., Tapiolas,D., Willis,B.L., and Bourne,D.G. (2009) Coral-associated bacteria and their role in the biogeochemical cycling of sulfur. *Appl. Environ. Microbiol.* **75**: 3492–501.

Rappé,M.S. and Giovannoni,S.J. (2003) The uncultured microbial majority. *Annu. Rev. Microbiol.* **57**: 369–94.

Ravasz,E., Somera, a L., Mongru,D. a, Oltvai,Z.N., and Barabási, a L. (2002) Hierarchical organization of modularity in metabolic networks. *Science* **297**: 1551–5.

Richardson,L. (1998) Coral diseases: what is really known? *Trends Ecol. Evol.* **13**: 438–443.

Richardson,L., Goldberg,W., and Kuta,K. (1998) Florida's mystery coral-killer identified. *Nature* 392:557-558

Ritchie,K.B. (2006) Regulation of microbial populations by coral surface mucus and mucus-associated bacteria. **322**: 1–14.

Ritchie,K.B. and Smith,G.W. (2004) Microbial Communities of Coral Surface Mucopolysaccharide Layers. In Coral health and disease (pp. 259-264). Springer Berlin Heidelberg.

Roder,C., Arif,C., Bayer,T., Aranda,M., Daniels,C., Shibl,A., et al. (2013) Bacterial profiling of White Plague Disease in a comparative coral species framework. *ISME J.* 1–9.

Rodriguez-lanetty,M. and Granados-cifuentes,C. (2013) Ecological Inferences from a deep screening of the Complex Bacterial Consortia associated with the coral , Porites astreoides. Mol. Ecol. **22:** 4349–4362.

Rohwer, F. (2003) Global phage diversity. *Cell* **113:**141.

Rohwer, F and Edwards, R.A.. (2005) Viral metagenomics. *Nat. Rev. Microbiol.* **3**: 801–805.

Rohwer,F. and VegaThurber,R. (2009) Viruses manipulate the marine environment. *Nature* **459**: 207–12.

Rohwer,F., Seguritan,V., Azam,F., and Knowlton,N. (2002) Diversity and distribution of coral-associated bacteria. *Mar. Ecol. Prog. Ser.* **243**: 1–10.

Rohwer, M.,B., J.,J., F.,A., and N.,K. (2001) Diversity of bacteria associated with the Caribbean coral Montastraea franksi. *Coral Reefs* **20**: 85–91.

Rosenberg,E. and Falkovitz,L. (2004) The Vibrio shiloi/Oculina patagonica model system of coral bleaching. *Annu. Rev. Microbiol.* **58**: 143–59.

Rosenberg,E., Koren,O., Reshef,L., Efrony,R., and Zilberrosenberg,I. (2007) The role of microorganisms in coral health, disease and evolution. *Nat Rev Microbiol* **5**: 355–362.

Rosenberg,E. and Kushmaro,A. (2011) Microbial disease of corals:pathology and ecology. In Coral Reefs: An Ecosystem in Transition, pp. 451-464.

Rota,P. a, Oberste,M.S., Monroe,S.S., Nix,W.A., Campagnoli,R., Icenogle,J.P., et al. (2003) Characterization of a novel coronavirus associated with severe acute respiratory syndrome. *Science* **300**: 1394–9.

Rowan,R. and Powers,D. (1991) Molecular genetic identification of symbiotic dinoflagellates (zooxanthellae). *Mar. Ecol. Prog. Ser.* **71**: 65–73.

Ruder, W. C., Lu, T., Collins, J. J. (2011) Synthetic biology moving into the clinic. *Science* **333:**1248-1252.

Sarkar,S.K. and Chang,C.-K. (1997) The Simes Method for Multiple Hypothesis Testing with Positively Dependent Test Statistics. *J. Am. Stat. Assoc.* **92**: 1601–1608.

Sato,Y., Willis,B.L., and Bourne,D.G. (2013) Pyrosequencing-based profiling of archaeal and bacterial 16S rRNA genes identifies a novel archaeon associated with black band disease in corals. *Environ. Microbiol.* **15:** 2994-3007.

Sato,Y., Willis,B.L., and Bourne,D.G. (2010) Successional changes in bacterial communities during the development of black band disease on the reef coral, Montipora hispida. *ISME J.* **4**: 203–14.

Schmieder,R. and Edwards,R. (2011) Fast Identification and Removal of Sequence Contamination from Genomic and Metagenomic Datasets. *PLoS One* **6**: e17288.

Sekar,R., Kaczmarsky,L., and Richardson,L. (2008) Microbial community composition of black band disease on the coral host Siderastrea . *Mar. Ecol. Prog. Ser.* **362:** 85-*98.*

Shade, A., Peter, H., Allison, S. D., Baho, D. L., Berga, M., Bürgmann, H., … Handelsman, J. (2012) Fundamentals of microbial community resistance and resilience. *Frontiers in Microbiol*. **3:** 417.

Shannon,P., Markiel,A., Ozier,O., Baliga,N.S., Wang,J.T., Ramage,D., et al. (2003) Cytoscape: a software environment for integrated models of biomolecular interaction networks. *Genome Res.* **13**: 2498–504.

Sharp,K.H., Distel,D., and Paul,V.J. (2012) Diversity and dynamics of bacterial communities in early life stages of the Caribbean coral Porites astreoides. *ISME J.* **6**: 790–801.

Smarda,J. and Benada,O. (2005) Bacteriocins of Budvicia aquatica and Pragia fontium (Enterobacteriaceae) Phage Tail-Like (High-Molecular-Weight) Bacteriocins of Budvicia aquatica and Pragia fontium (Enterobacteriaceae). **71**: 8970-8973.

Smith, H. O., Hutchison, C. A., Pfannkoch, C., Venter, J. C. (2003) Generating a synthetic genome by whole genome assembly: φX174 bacteriophage from synthetic oligonucleotides.*PNAS* **100:**15440-15445

Soffer,N., Brandt,M.E., Correa,A.M., Smith,T.B., and Thurber,R.V. (2013) Potential role of viruses in white plague coral disease. *ISME J.* **2005**: 1–13.

Sokolow,S.H., Foley,P., Foley,J.E., Hastings,A., and Richardson,L.L. (2009) Editor's choice: Disease dynamics in marine metapopulations: modelling infectious diseases on coral reefs. *J. Appl. Ecol.* **46**: 621–631.

Spies,N.P. and Takabayashi,M. (2013) Expression of galaxin and oncogene homologs in growth anomaly in the coral Montipora capitata. *Dis. Aquat. Organ.* **104**: 249–56.

Steele,J. a, Countway,P.D., Xia,L., Vigil,P.D., Beman,J.M., Kim,D.Y., et al. (2011) Marine bacterial, archaeal and protistan association networks reveal ecological linkages. *ISME J.* **5**: 1414–25.

Stimson,J. (2010) Ecological characterization of coral growth anomalies on Porites

compressa in Hawaiʻi. *Coral Reefs* **30**: 133–142.

Sun,S., Chen,J., Li,W., Altintas,I., Lin,A., Peltier,S., et al. (2011) Community cyberinfrastructure for Advanced Microbial Ecology Research and Analysis: the CAMERA resource. *Nucleic Acids Res.* **39**: D546–51.

Sunagawa,Shinichi, Desantis,T.Z., Piceno,Y.M., Brodie,E.L., Desalvo,M.K., Voolstra,C.R., et al. (2009) Bacterial diversity and White Plague Disease-associated community changes in the Caribbean coral Montastraea faveolata. *ISME J.* **3:**512–521.

Sussman,M., Willis,B.L., Victor,S., and Bourne,D.G. (2008) Coral Pathogens Identified for White Syndrome (WS) Epizootics in the Indo-Pacific. **3**: E2393.

Sutherland,K., Porter,J., and Torres,C. (2004) Disease and immunity in Caribbean and Indo-Pacific zooxanthellate corals. *Mar. Ecol. Prog. Ser.* **266**: 273–302.

Sutherland,K.P., Shaban,S., Joyner,J.L., Porter,J.W., and Lipp,E.K. (2011) Human Pathogen Shown to Cause Disease in the Threatened Eklhorn Coral Acropora palmata. *PLoS One* **6**: e23468.

Suttle,C. a (2007) Marine viruses--major players in the global ecosystem. *Nat. Rev. Microbiol.* **5**: 801–12.

Sweet,M. and Bythell,J. (2012) Ciliate and bacterial communities associated with White Syndrome and Brown Band Disease in reef-building corals. *Environ. Microbiol.* **14**: 2184–99.

Tagg,J.R., Dajani, a S., and Wannamaker,L.W. (1976) Bacteriocins of gram-positive bacteria. *Bacteriol. Rev.* **40**: 722–56.

Thomas,F., Hehemann,J.-H., Rebuffet,E., Czjzek,M., and Michel,G. (2011) Environmental and gut bacteroidetes: the food connection. *Front. Microbiol.* **2**: 93.

Tolleter,D., Seneca,F.O., Denofrio,J.C., Krediet,C.J., Palumbi,S.R., Pringle,J.R., and Grossman,A.R. (2013) Coral Bleaching Independent of Photosynthetic Activity. *Curr. Biol.* 1782–1786.

Tucker, K. P., Parsons, R., Symonds, E. M., Breitbart, M. (2010) Diversity and distribution of single-stranded DNA phages in the North Atlantic Ocean. *ISME J* **5:**822-830.

Van Oppen, M. J. H., Leong, J.-A., & Gates, R. D. (2009) Coral-virus interactions: A double-edged sword? *Symbiosis* **47:** 1–8.

Vartoukian,S.R., Palmer,R.M., and Wade,W.G. (2010) Strategies for culture of "unculturable" bacteria. *FEMS Microbiol. Lett.* **309**: 1–7.

Vega Thurber,R.L., Barott,K.L., Hall,D., Liu,H., Rodriguez-Mueller,B., Desnues,C., et al. (2008a) Metagenomic analysis indicates that stressors induce production of herpes-

like viruses in the coral Porites compressa. *Proc. Natl. Acad. Sci. U. S. A.* **105**: 18413–8.

Vega Thurber,R.L., Burkepile,D.E., Fuchs,C., Shantz,A.A., Ryan,M., and Zaneveld,J.R. (2013) Chronic Nutrient Enrichment Increases Prevalence and Severity of Coral Disease and Bleaching. *Glob. Chang. Biol.* **Accepted**

Vega Thurber,R., Haynes,M., Breitbart,M., Wegley,L., and Rohwer,F. (2009) Laboratory procedures to generate viral metagenomes. *Nat. Protoc.* **4**: 470–83.

Vega Thurber,R.L. and Correa,A.M.S. (2011a) Viruses of reef-building scleractinian corals. *J. Exp. Mar. Bio. Ecol.* **408**: 102–113.

Vega Thurber,R.L. and Correa,A.M.S. (2011b) Viruses of reef-building scleractinian corals. *J. Exp. Mar. Bio. Ecol.* **408**: 102–113.

Vega Thurber,R., Willner-hall,D., Rodriguez-mueller,B., Desnues,C., Edwards,R.A., Angly,F., et al. (2009) Metagenomic analysis of stressed coral holobionts. *Environ. Microbiol.* **11**: 2148–2163.

Vercelli,D. (2004) Genetics, epigenetics, and the environment: switching, buffering, releasing. *J. Allergy Clin. Immunol.* **113**: 381–6; quiz 387.

Veron,J.E.N., Hoegh-Guldberg,O., Lenton,T.M., Lough,J.M., Obura,D.O., Pearce-Kelly,P., et al. (2009) The coral reef crisis: the critical importance of<350 ppm CO2. *Mar. Pollut. Bull.* **58**: 1428–36.

Voss,J.D. and Richardson,L.L. (2006) Nutrient enrichment enhances black band disease progression in corals. *Coral Reefs* **25**: 569–576.

Walters,W. a, Caporaso,J.G., Lauber,C.L., Berg-Lyons,D., Fierer,N., and Knight,R. (2011) PrimerProspector: de novo design and taxonomic analysis of barcoded polymerase chain reaction primers. *Bioinformatics* **27**: 1159–61.

Wang,Q., Garrity,G.M., Tiedje,J.M., and Cole,J.R. (2007a) Naive Bayesian classifier for rapid assignment of rRNA sequences into the new bacterial taxonomy. *Appl. Environ. Microbiol.* **73**: 5261–7.

Wang,Q., Garrity,G.M., Tiedje,J.M., and Cole,J.R. (2007b) Naive Bayesian classifier for rapid assignment of rRNA sequences into the new bacterial taxonomy. *Appl. Environ. Microbiol.* **73**: 5261–7.

Ward,J.R. and Lafferty,K.D. (2004) The elusive baseline of marine disease: are diseases in ocean ecosystems increasing? *PLoS Biol.* **2**: E120.

Webster,N.S., Negri, a P., Flores,F., Humphrey,C., Soo,R., Botté,E.S., et al. (2013) Near-future ocean acidification causes differences in microbial associations within diverse coral reef taxa. *Environ. Microbiol. Rep.* **5**: 243–51.

Wegley,L., Edwards,R., Rodriguez-Brito,B., Liu,H., and Rohwer,F. (2007) Metagenomic

analysis of the microbial community associated with the coral Porites astreoides. *Environ. Microbiol.* **9**: 2707–19.

Wegley, L., Yu, Y., Breitbart, M., Casas, V., Kline, D. I., Rohwer, F. (2004) Coral-associated archaea. *MEPS* **273:** 89-96.

Weil,E., Smith,G., and Gil-agudelo,D.L. (2006) Status and progress in coral reef disease research. *Dis Aquat Organ* **69**: 1–7.

Weis,V.M. (2008) Cellular mechanisms of Cnidarian bleaching: stress causes the collapse of symbiosis. *J. Exp. Biol.* **211**: 3059–66.

Weitz,J.S., Poisot,T., Meyer,J.R., Flores,C.O., Valverde,S., Sullivan,M.B., and Hochberg,M.E. (2013) Phage-bacteria infection networks. *Trends Microbiol.* **21**: 82–91.

Weitz,J.S. and Wilhelm,S.W. (2012) Ocean viruses and their effects on microbial communities and biogeochemical cycles. *F1000 Biol. Rep.* **4**: 17.

Wiese,J., Thiel,V., Gärtner,A., Schmaljohann,R., and Imhoff,J.F. (2009) Kiloniella laminariae gen. nov., sp. nov., an alphaproteobacterium from the marine macroalga Laminaria saccharina. *Int. J. Syst. Evol. Microbiol.* **59**: 350–6.

Williams, W. M., Viner, A. B., Broughton, W. J. (1987) Nitrogen fixation (acetylene reduction) associated with the living coral Acropora variabilis. *Mar. Biol.* **94:** 531-535.

Wilson,B., Aeby,G.S., Work,T.M., and Bourne,D.G. (2012) Bacterial communities associated with healthy and Acropora white syndrome-affected corals from American Samoa. *FEMS Microbiol. Ecol.* **80**: 509–20.

Work,T.M. and Aeby,G.S. (2006) Systematically describing gross lesions in corals. *Dis. Aquat. Organ.* **70**: 155–60.

Work,T.M., Aeby,G.S., and Coles,S.L. (2008) Distribution and morphology of growth anomalies in Acropora from the Indo-Pacific. *Dis. Aquat. Organ.* **78**: 255–64.

Xing,M., Hou,Z., Yuan,J., Liu,Y., Qu,Y., and Liu,B. (2013) Taxonomic and functional metagenomic profiling of gastrointestinal tract microbiome of the farmed adult turbot (Scophthalmus maximus). *FEMS Microbiol. Ecol.* **1**: 1–12.

Yamashirol,H., Yamamoto,M., and Van,R. (2000) Tumor formation on.

Yilmaz,S., Allgaier,M., and Hugenholtz,P. (2010) Multiple displacement amplification compromises quantitative analysis of metagenomes. *Nat. Methods* **7**: 943–4.

Zhou,J., Deng,Y., Luo,F., Molecular,F., Networks,E., This,S., et al. (2010) Functional Molecular Ecological Networks. *MBio* **1**:169-179.